

DISTRESS AND FAILURE OF PAVEMENT SYSTEMS

BY

JOHN FAYI ELLIOTT

B.C.E. Ohio State University

(1966)

M.Sc. Ohio State University

(1966)

Submitted in partial fulfillment
of the requirements for the degree of
Doctor of Philosophy
at the
Massachusetts Institute of Technology
September 1969

Signature of Author.....
Department of Civil Engineering, September 1969

Certified by.....
Thesis Supervisor

Accepted by.....
Chairman, Departmental Committee on Graduate Students

ABSTRACT

DISTRESS AND FAILURE OF PAVEMENT STRUCTURES

by

JOHN FAYI ELLIOTT

Submitted to the Department of Civil Engineering on September 19, 1969 in partial fulfillment of the requirements for the degree of Doctor of Philosophy.

A highway pavement structure is considered as part of a system made up of different interacting socio-economic and structural parts. To effectively analyze the behavior of such a system, each phase of its socio-economic and structural parts has to be separately examined and later meaningfully integrated through the use of models so as to get a realistic picture of performance in an operational environment. This study uses the above systems approach as a basic framework within which the structural aspects of the problem are considered. The performance of a pavement structure in an operational environment is examined from the primary and ultimate response behaviors. Two mechanistic models are developed to predict the distress and eventual failure of the structure in a given load and temperature environment.

The first model treats the structure as a three-layer linear viscoelastic system in which the mechanical properties of the materials in the layers are represented by linear hereditary integral operators of the creep type. The sensitivity of this model to rate effects is established by considering its response to a stationary, repeated and moving load.

The second model establishes the link between the primary and ultimate responses by associating through the use of time-dependent memory functions the developed stresses and deformations to the degree of damage accumulated in a given period of time.

A simple illustration of the use of the models to predict the progression of damage in a pavement structure under repeated loading is presented.

Thesis Supervisor: Professor Fred Moavenzadeh

Title: Associate Professor of Civil Engineering

ACKNOWLEDGEMENTS

The author wishes to express his sincere appreciation to his thesis advisor, Professor F. Moavenzadeh, for his many hours of helpful discussion, advice, and encouragement throughout the course of this research.

Appreciation is also extended to the thesis committee members, Professor F. J. McGarry and Professor T. W. Lambe for their interest and advice.

The helpful comments of Mr. Joseph Soussou are also gratefully acknowledged. Many thanks to Mr. Masaharu Ushiyama and Mr. Hani Findakly for their help in running the computer programs.

Appreciation is extended to the Bureau of Public Roads for the financial assistance which made this research possible.

To his wife, Seraphina, the author wishes to express deep gratitude for her encouragement and many hours of typing during the development and preparation of this thesis.

TABLE OF CONTENTS

	Page
Title Page	1
Abstract	2
Acknowledgement	4
Table of Contents	5
I. Introduction	7
1. The Structural Integrity of the Pavement	11
II. Failure of Engineering Materials	16
III. Classification of Pavements Based on Mechanical Response and Identification of the Parameters of Damage	38
1. Pavement Models for Primary Response	47
2. Model on Ultimate Response Mode	52
IV. The Primary Model	61
V. The General Cumulative Damage Theory	85
VI. Applications of Developed Models	101
1. Dimensionless System Parameters	104
2. Primary Response Model	111
3. The Damage Model	130
VII. Conclusions	184
VIII. Suggestions for Future Work.	186
IX. Bibliography and References	189

	Page
X. Biography	197
XI. Appendices	
A. Definitions of Symbols	199
B. Definitions of Special Terms	201
C. List of Figures	203
D. Derivation of the Moving Load Solution	206

I. INTRODUCTION

A pavement's function as a highway component is manifold. It is designed and constructed to provide safe, durable, smooth and economical highway surfaces which would make possible the swift and convenient transportation of the individual and his commerce. The present design of such facilities is based largely on experience expressed in the form of correlations between soil type, traffic, base course character, and thickness. Although these methods have met with reasonable success in the past, the rapid increases in the number of heavy axle loads and in the variety of subgrades that must support them have outrun past experience. Therefore, a design method that combines theory with empiricism to a lesser degree is needed.

The development of a rational method ^{of} analysis of any system must include certain procedures of which the selection and analysis of a model (or prototype) for realistic input parameters constitute a major part. From the results of such an analysis, an intelligent comparison of the predicted and observed output parameters can be made. The degree of discrepancy between these will then result in the determination of the extent of modification to be made on the originally selected model. After a sufficient number of executions of these comparison cycles, the results predicted by the model and those observed from the prototype should ideally converge.

To provide such a prototype for design, it is necessary that the pavement be first rationally analyzed; knowledge of the design functions and failure mechanisms of the pavement must be secured. This study considers the failure aspect of the problem with a view to identifying the pertinent failure mechanisms.

An initial review of current knowledge in this area, has revealed that the performance of a pavement structure in a given traffic and climatic environment may be defined as its ability to provide an acceptable level of Serviceability*, with a specified degree of Reliability* for an assumed level of Maintainability*. The impairment or loss in the ability to provide the necessary services in a given locale may then be considered as the 'failure' of the pavement. When viewed in this light, 'failure' becomes a loss in performance; it is the extent to which the pavement has failed to render itself serviceable, (i.e., the serviceability level has decreased by a critical amount from an initially acceptable state); it results from an accumulation of damage over a given time period.

Since the response of the structure to imposed loads is not only time, but also temperature dependent, 'physical failure' excluding slipperiness, can be considered as occurring over a range of stress-strain-time - and temperature conditions. The failure age of the pavement within such a context is then, the time

* Defined in Appendix (B). 8

You cannot have
this in the thesis

during which performance deteriorates to an unacceptable level as determined by the users.

Society's perceptions as regards to how well a pavement is performing its stated functions are determined by the users of the highway, and the highway engineers. The user assesses or evaluates the performance of the pavement from factors such as operational costs, comfort, convenience and safety. These factors are intangible or difficult to quantify, because a person's judgment as to the type of service he is receiving from a highway is highly subjective. It depends on the one hand on the vehicle and its physical requirements and on the other by the individual using the vehicle, his physical and psychological needs. For example, the conclusions arrived at (as regards the adequacy of the structure) from someone driving a jeep would not be the same as that for the same person or someone else driving a heavily-loaded intercity truck, nor for an intercity traveler and a man visiting his neighbor on the next block.

The relative importance would also be different for a person who has been accustomed all his life to muddy-rural roads and one who has been accustomed to paved city-streets. Therefore, it will be impossible in such a framework to define failure precisely and a performance evaluation, if any, may be expected to be highly subjective.

From the engineers' viewpoint, other and more significant factors have to be considered in the evaluation of pavement adequacy. They have to evaluate performance from a careful consideration of the objective physical parameters that affect the response behavior of the facility.

In this respect, factors such as the frictional characteristics, the type of geometric design, the mechanical properties of materials in the layers, the extent of deformation and cracking, etc., of the pavement under load and environment are pertinent. It is therefore apparent that a system of correlation is needed to translate the subjective conclusions of the users to the physically objective manifestations of such conclusions. From such a mechanism, the performance history of a pavement in a given environment can be obtained and realistic maintainability assessments can be made. Since there may be many combinations of variables that can satisfy certain performance requirements, the most suitable can be chosen after the optimization of the Serviceability-Reliability-Maintainability characteristics of the problems at hand.

This brief discussion of failure shows that failure is a many-sided problem. It is the result of a series of interacting complex processes none of which is clearly understood. Therefore, in order to present an integrated comprehensive picture of failure, each of its components has to be studied in detail. From such studies,

methods may be developed for analyzing the effect that each component has on the behavior of the structure.

Finally, all of these methods may be grouped together in a meaningful way so that for any given environment, the performance history of a pavement can be predicted. In such a framework, the failure of a pavement may be considered as a function of its rideability, safety, and structural integrity. This study investigates 'failure' from the "Structural Integrity" viewpoint and it must be emphasized that this is only one aspect of the 'failure' problem.

1. The Structural Integrity of the Pavement

The structural integrity of a pavement may be defined as its ability to resist destruction and functional impairment in a particular traffic and climatic environment. Indicators or measures of structural integrity may therefore be expressed in the primary and ultimate response modes of the structure using Hudson et al.'s characterization (Figure 1). In the primary response regime, one can use factors like the magnitude of developed stress, deflection, strain and permanent deformation, whereas in the ultimate response mode, the extent of rupture, disintegration and distortion can be utilized.

Since it is known that parameters like the speed of loading, temperature, position of the load, previous subgrade type, etc., affect the response behavior of the facility, it should be equally obvious that these factors

will also affect its structural integrity as defined above.

In other words, the indicators of structural inadequacy are the manifestations of the physical failure of the facility, in the particular load, temperature and material property environment. It is therefore pertinent to ask whether analytical modes, mathematical or otherwise could be found to account for the manner in which a particular load-temperature-material property-environment would affect the performance of the layered structure. To the writer's knowledge, no such all-inclusive model is in existence at the present time (1969).

This study attempts to analyze the progression of failure within a pavement structure by linking its primary and ultimate response behavior through the use of two mathematical models of the prototype - a primary response model and a cumulative damage model.

It has been observed in the field that deflection accumulates with the number of load repetitions and the magnitude of this variable also changes depending on area of interest, on speed of loading and temperature. The response behavior of these models must therefore be time- and-temperature dependent. To represent such behavior, the structure is assumed to be composed of three layers, each of which may possess time and temperature dependent properties.

In the primary response mode, therefore, cumulative effects can be accounted for and the permanent

7

deformation can be predicted. The model is capable of reflecting the influences of the rate of loading, the magnitude of the applied loading, material properties and changes in the depth of the layers on the indicators of structural integrity, for arbitrarily selected load boundary conditions. The conditions investigated in this study are:

- a) a stationary load,
- b) a repeated load, and
- c) a moving load.

The influence of the rate of loading, its magnitude and number of repetitions is also presented and discussed.

Under the combined destructive action of the traffic and the weather, several distress mechanisms develop within the structure and propagate either independently of each other or through interacting complex processes to produce eventually any or all of these broad groups of distress:

- a) disintegration,
- b) distortion, and
- c) fracture (rupture).

In order to trace the path of such mechanisms from the time of initiation, through propagation to that of global manifestation, a simple but general cumulative damage model is developed. This model is directly related to the primary response model with which it must be combined

so as to predict the conditions under which ultimate distress is most likely to occur. In other words, the accumulation of damage within the structure over a given time period is assumed to be commensurate with a particular internal load, energy, stress or strain state to be determined from the load boundary conditions on the primary model.

Although it is realized that field behavior results from a series of interacting complex processes, and that all failure mechanisms must be analyzed in order to present not only a realistic but also a totally comprehensive picture of failure behavior, only the distress occurring as a consequence of the growth of fatigue cracks has been investigated. The motivation for doing this stems from the fact that an extensive amount of work has been done experimentally on the fatigue behavior of paving materials. This makes it possible, to a certain extent, to adopt certain assumptions as to the manner of damage propagation in this mode of loading. The damage model is, however, flexible enough to allow for the influence of the other failure mechanisms provided that the pertinent failure parameters are identified. For these reasons, the work presented in this thesis must be considered only as a necessary and significant initial step in the area of failure. It is not all-inclusive.

The study is presented in five broad sections. The discussion begins with a close study of the conditions

governing the initiation, propagation and attainment of critical size of the defect area in engineering materials under arbitrary loading histories. It provides the background work necessary for the development of the cumulative damage model.

Having established the conditions governing the physical failure of engineering materials in general, the pavement system is investigated with a view to identifying the variables which affect its performance and subsequently bring about ultimate distress in a given environment. On the basis of the conclusions arrived at, the primary and cumulative damage models are developed.

In the section following this development, the sensitivity of the primary model to pertinent variables is established; an example is then presented of the use of the damage-model in predicting the fatigue life of the asphaltic concrete in the surface layer of a pavement structure. The subsequent sections discuss the advantages and disadvantages of the developed models and suggestions are made for future work.

II. FAILURE OF ENGINEERING MATERIALS

The intensive interest that has developed over the past several years concerning the accumulation of damage in engineering materials and structures has its roots in the following questions:

- a) the problem of the life prediction of an engineering material or structure under an arbitrary load history in a given environment,
- b) the amount and distribution of damage in the material or structure under the arbitrary loading spectrum mentioned above and,
- c) the manner and rate of accumulation of damage

In order to determine the conditions governing the failure of a pavement structure in a rational manner, the physics of failure must be known for the materials which are preconditioned and prestressed from heavy rolling to establish definite density and strength requirements for each layer. This chapter presents a concept of damage by examining the processes of fracture and flow in solid materials. It describes what the damage is, how it manifests itself and which parameters can be employed to describe it.

Several observations are made about the distribution and propagation of damage within a material that is under an arbitrary loading history. Some well known theories and criteria which have been postulated for the

failure of engineering materials are discussed. The damage of materials in a repeated loading environment is closely examined.

Concept of Damage

Damage may be defined as a structure-sensitive property of all solid materials; structure sensitivity is imparted to it through the influence of defects in the form of microscopic and macroscopic cracks, dislocations and voids which may have been artificially or naturally introduced into the material, thereby rendering it inhomogenous. Characteristically, structure sensitive phenomena involve processes which grow gradually and accelerate rapidly once an internal irregularity or defect size exceeds a certain limit. Damage may therefore, be said to occur in a similar fashion.

The progression of damage in an engineering material or engineering structure may occur under the application of uniaxial or multiaxial stationary or repeated loads. The damage progression has been categorized by two different conditions: ductile and brittle. The ductile condition is operative if a material has undergone considerable plastic deformation or flow before rupture. The brittle condition, on the other hand, occurs if localized stress and energy concentrations cause a separation of atomic bonds before the occurrence of any appreciable plastic flow. Note here that no mention is made of a ductile or a brittle material per se. According to von Karman (2), this implies

that failure is not in itself a single physical phenomenon, but rather a condition brought about by several different processes that may lead to the disintegration of a body by the action of mechanical forces. Damage may therefore progress within a material under the different mechanisms of fracture and flow depending on the environmental stress, strain and temperature conditions. For instance, low carbon steel exhibits fibrous and shear types of fracture at room temperature, below -80°C brittle fracture occurs and intergranular creep fracture is dominant in slow straining at 600°C and above (3). A material may, therefore, have several characteristic strength values, when several fracture mechanisms operate at different critical levels of the stress or strain components.

Though the mechanisms of damage initiation and propagation in both failure modes* are different, they have three major points in common:

- a) a particular combination of stress or strain concentration is required to create a defect nucleus,
- b) a different combination of stress or strain quantities is then required for the propagation

* In the brittle mode localized stress and energy concentrations create cracks which grow within the material and upon becoming of significant size propagate rapidly. In ductile materials however, the defects are dislocations, which move slowly until a critical velocity is attained; then plastic flow results.

of the defect and,

- c) a critical combination of stress and strain concentrations is required for the transition from relatively slow to fast propagation to catastrophic failure.

The distribution and progression of damage in solid material is in itself a random process which is both spatial and temporal. Hirata (4) working on glass panes, and Joffe (5) on pyrex-glass filaments concluded that the distribution of internal cracks must be spatial by demonstrating considerable variability in the breaking strength values of these materials. Yokobori (6) in his investigation of the creep fracture of copper under a uniaxial load, demonstrated a considerable scatter in the values of time to fracture of a group of specimens taken from the same stock. Further evidence of these random processes is to be found in the works of Yokobori on fatigue fracture (6), creep fracture and ductile fracture (7) (8), brittle fracture (9) and yielding in steel (9).

The above concepts of damage progression to failure suggest that an engineering material or structure can fail under a given system of external loadings when either of the following two criteria is satisfied:

The distribution of internal flaws is such that;

- 1) excessive deformation is attained (usually for ductile behavior), or

- 2) a fracture threshold is reached under an arbitrary loading history (usually for brittle behavior).

From the foregoing discussion, it should be evident that the fracture of an engineering material is a statistical process brought about by the interaction of several complex mechanisms.

Accordingly, over the years several reasons have been advanced as explanations for the observed behavior of 'damage' in an engineering material, and based on such explanations several theories have emerged. Researchers have approached the problem both deterministically and statistically from the molecular and macroscopic levels. On the molecular basis, the differences between the fracture mechanisms involved are emphasized, since at this level, the material is essentially discontinuous.

On the macro level, the criteria for fracture are basically similar, and utilize the concepts of continuum mechanics. The fracture laws are generally based on either local or global energy, stress or strain concentrations within the material.

Theories like the Eyring rate process (10) developed for viscous materials, Gnauss theory (11) for viscoelastic materials and Weibull's theory (12) for brittle materials have attempted to explain on the basis of a statistical model some of the phenomena observed when materials like metals, textiles, concrete and others fracture under

applied stress. The basic assumption is that an assembly of unit damage processes grows in a probabilistic way to yield an observed macroscopic effect with temperature fluctuations and activation energy distributions playing a significant role.

Weibull (12) studied the manner that probabilistic postulations about the size of the specimen would affect the fracture strength of a material that fails in a brittle manner. He assumed that the probability of failure $P(\sigma_c)$ of a unit volume as a function of applied stress σ_c is given by

$$P(\sigma_c) = 1 - \exp[-\sigma_c/\sigma_0]^m \quad (1)$$

where σ_0 and m are constants dependent on material characteristics.

σ_0 relates to some inherent ultimate strength

m relates to material inhomogeneity.

Using this approach he showed that the strength of a specimen of volume V is proportional to $\sigma_0 V^{-1/m}$.

Though this result has met with some success, Frenkel and Kontorova (13) claim that Weibull's approach is devoid of physical reasoning because of his assumption for $P(\sigma_c)$. They assumed that the specimen had flaws distributed in it in a Gaussian manner and obtained;

$$P(\sigma_c) = \frac{1}{\sqrt{2\pi}} \exp[-(\sigma_c - \bar{\mu})^2/2\sigma^2] \quad (2)$$

where $\bar{\mu}$ = mean strength of specimen of volume, V .

v = strength variance of specimen of volume, V .
 From the above equation for $P(\sigma_c)$ they determined that the strengths of specimens with volume V (with many flaws) is given to a first approximation by

$$\text{Strength} = \bar{\mu} - (2v)^{\frac{1}{2}} \sqrt{(\log \bar{n}V - 2VH)} \quad (3)$$

where \bar{n} = number of flaws/cubic centimeter.

Such statistical theories have a significant advantage over deterministic concepts, because they account for the role of chance in the behavior of materials. The Griffith theory (14) for instance, which states that the reason for the difference between the observed and calculated strengths is the presence of internal flaws predicts the tensile strength of materials that fracture in a brittle manner under uniaxial and biaxial loading conditions in terms of single-crack length, a surface energy and a set of elastic constants. However, if the distribution of flaws is random, then the formulation of the problem is necessarily statistical.

Despite its shortcomings, the Griffith theory has been used quite successfully to predict the occurrence of brittle fracture in many materials among which are glass, cast iron, rocks, asphalts, and polymers. One suspects that one reason for this may be the balancing of experimental errors.

Continuing in the deterministic domain, Nadai (15) has demonstrated that previous experience with glass,

metals and concrete for instance indicates the existence of no universal criterion to mark the end of damage progression in the form of fracture and flow. The failure theories demonstrate that the degree of success of a given criterion depends upon the material with which it is associated. While it may work well for a particular class of materials, it may fail often quite hopelessly to predict conditions of failure for another class.

An example of this is evident in the use of the maximum shear stress theory, (15) distortional theory, (15) the octahedral shear stress theory, (15) all of which work very well for metals and can be justified on an atomic scale because of the mode of crystal slip in a polycrystal. However, their applications to the failure of materials such as sand, gravel and clay are questionable because the shear stress necessary for slip in such materials depends also on hydrostatic pressure. For these materials, the more densely packed the particles, the harder it is to cause them to slide over one another. Coulomb treated this as a simple frictional resistance that is proportional to pressure. He postulated that plastic deformation will start on a slip plane through the material when the normal stress on the plane produces a frictional component which when coupled with the molecular cohesive strength of the material results in the shear resistance of the plane. The outcome of this was the Mohr-Coulomb theory (16), which has met with

reasonable success in soil mechanics. Although, the criterion neglects the influence of the intermediate principal stress on failure, Bishop (17) and others have deemed it a satisfactory first approximation for three-dimensional situations as well.

Parameters of Damage in the Repeated Loading Mode

In many materials, the initiation, progression and ultimate manifestation of distress in the form of fracturing under a repeated load occurs under the action of two separate processes: crack initiation and crack growth which are governed by different criteria. In metals, this behavior has been attributed to localized slip and plastic deformation (18), and to the cyclic motion of dislocations. In commercial alloys, the presence of inclusions, flaws, cracks, and stress raisers creates cracks. In polymers and asphaltic mixtures, the cracks initiate from air holes, inhomogeneities and probably molecular chain orientations and molecular density distributions (20).

Regardless of the process of crack initiation, the mechanism of crack propagation has been explained by many researchers from a consideration of the energy balance at the crack tip which deforms as cycling progresses. The total input energy can be divided into that which is stored, that which is responsible for creating new surfaces and that required to deform molecular segments plastically. The rate of crack propagation is therefore a function of the energy balance. The propagation is slow

when a considerable amount of plastic deformation occurs at the crack tip which as a result of this becomes "blunted". It is fast when the released portion of the stored energy exceeds the energy demand for creating new surfaces.

In polymeric and metallic materials the crack tip is cyclically "blunted" and resharpened during the cyclic deformation (18)(31). For metals several investigators have assessed the rate of damage progression by measuring crack length as a function of number of cycles (21)(22).

For SAE 1020 steel, Forest (23) has shown that the progression of damage is exponential in character (Figure 2). When the stress level is high, the damage propagation is rapid, but as lower stress levels are approached, the crack grows slowly with the number of cycles of load, and crack acceleration precedes subsequent failure of the specimen. It was also observed that when the stress level is below the endurance limit, the cracks either did not form or had their growth arrested.

Erickson and Work (21) discovered that the history of load application had a significant influence on the progression of damage. On the application of a high pre-stress followed by a low stress the degree of damage created was greater than when the application was vice versa. The authors explained this occurrence by suggesting that on the first few cycles of load application, a certain number and distribution of crack sites form depending on the stress level, and the application of subsequent loads

merely causes propagation from these sites.

In order to handle the problem of life prediction for any material in a given repeated load environment, several phenomenological and molecular theories have appeared in the literature.

In some of the molecular theories developed the statistical mechanics principles and kinetic reaction rates concept have been utilized. Coleman (24) and Machlin (25) employed the Eyring rate process theory to study respectively the fatigue characteristics of nylon fibers and metals. The general expression obtained by Coleman for fatigue life is of the following form (24):

$$t_{\beta}(P,q) = \frac{\epsilon_{\beta} \operatorname{cosech} \beta P}{A J_0(\beta i q)} \quad (4)$$

ϵ_{β} = constant strain level at fracture

t_{β} = time to failure

A, β = constants related to energy

$J_0(\beta i q)$ = Zeroeth order hyperbolic bessel function

loading function = $\sigma(t) = P + q \sin wt$. $P > q$

The theory implies that for every material a constant strain level exists at which fracture will occur, but a variety of experimental results shows that this is not the case. Moreover, it does not account for progressive internal damage as only failure conditions are represented. Mott (26) and Orowan (3) have presented fatigue theories for metals which take into account the fact that plastic deformation and strain-hardening occurs during fatigue.

Mott's theory attributes the formation of microcracks to the occurrence of dislocation within the material. Orowan's assumes the presence of a plastic zone within which a crack forms and propagates. Both these theories have given good agreement with experimental results at times. The discrepancy observed is mainly due to the fact that damage is a stochastic phenomenon while the theories are deterministic in nature. To increase their accuracy a statistical approach is needed.

Despite the fact that several molecular mechanisms have been shown to be operative during fatigue growth in a material, one suspects that the process itself may not be that fundamental in nature. Therefore, instead of searching for molecular theories, a possible coherent picture can be found from the continuum mechanics approach (with certain reservations).

This has been the motivation behind several phenomenological theories of cumulative damage - the Miner theory (27), Corten and Dolan's (22), and Valluri's (28) to name a few. The underlying concept in these theories can be illustrated by the work of Newmark (29).

In this approach, it is assumed that when a material is in a given load and climatic environment the degree or percentage of internal damage D_i is at any time commensurate with the appropriate number of load repetitions- N_i . (i.e., for $0 < D_i < 1$, $0 < N_i < N_f$). With this assumption, a damage curve exists for every constant stress or strain repeated mode

of loading. Since damage in effect implies that a loss in original capacity can result from either the creation and growth of plastic zone or the initiation and propagation of cracks, the strain developed in the material under load, the crack length, and the rate of crack growth can all be used as damage determinants.

The above reasoning is currently utilised in constant amplitude stress or strain fatigue tests. If a constant stress amplitude test is taken as an example, the resulting percentage of damage (D_1) vs. the number of load repetitions (N_1) curves for various stress amplitudes may be plotted up as shown in Figure 3.

The higher the stress level, the fewer the number of load application to failure. When cycle ratios ($\frac{n}{N}$) are utilised in place of number of cycles (N) as abscissa, two different plots of damage (D_1) vs. cycle ratios ($\frac{n}{N}$) may result depending upon the constitution of the material.

The damage law operative in Figure 4 is interaction-free, i.e., the fraction of damage instituted in the material, at all levels of stress is the same for a given cycle ratio. Figure 5, however, illustrates the direct opposite of such a law. In this figure, the damage law is not dependent on a given cycle ratio, the fraction of damage varies directly with the stress level. Several damage theories fall into one or the other mode of damage accumulation depending on the constitution of the material.

Generally speaking, the combined effects of damage and recovery processes resulting from microstructural changes imply that the damage curve should have different forms for different stress levels and loading histories. Some damage theories, such as those of Miner and Williams, assume a unique degree of damage caused by a stress cycle-ratio ($\frac{n}{N}$) applied at any time. Williams' theory (30) makes a similar assumption but with respect to time-ratios ($\frac{t}{T_f}$), where t = elapsed time from start of experiment, and T_f is time to failure. In both theories a linear summation of the ratios results, at failure, with the following expressions:

$$\text{i.e. } \sum_{i=1}^n \left(\frac{n_i}{N_i} \right) = 1 \text{ (Miner) and} \quad (5)$$

$$\sum_{i=1}^n \left(\frac{t_i}{T_{fi}} \right) = 1 \text{ (Williams).} \quad (6)$$

with

n_i = number of cycles applied at stress level- S_i

N_i = number of cycles to failure at stress level- S_i

t_i = elapsed time of application of strain rate level- R_i

T_{fi} = elapsed time to failure at strain rate level- R_i

Both theories have a major shortcoming in that prior history and sequence of events cannot be accounted for. Despite this shortcoming, Miner's theory has been successful when applied to rate-insensitive materials. Williams' theory had similar success when used for rate-sensitive materials. In Corten and Dolan's theory (22) the damaging effect under a stress cycle is considered dependent on the state of damage at any instant, and the expression for damage is

$$D_i = mrN^a \quad (7)$$

where

N = number of cycles

r = coefficient of damage propagation which is a function of stress level

a = damage rate at a given stress level which increases with number of cycles

m = number of damage nuclei

The Corten and Dolan approach is a rational attempt to modify Miner's theory. The determination of the significant parameters 'm' and 'r', however, requires the performance of a considerable number of experiments. In the simplest case, where the loading history can be characterized by two sinusoidal stress conditions, the parameters 'r' and 'm' may take on many different values depending upon the absolute magnitudes of the two sinusoids and their relative relationships. In addition, rate effects cannot be adequately accounted for. Consequently in terms of

usefulness over a wide class of materials and circumstance, the Miner theory is preferable.

Several researchers (31)(32)(33) have related the rate of crack growth to the localized energy and elastic stress conditions existing at the crack tip. The expression obtained when this fracture mechanics approach is used can be given in general form, as

$$\frac{dc}{dN} = A c^k \sigma^\ell \quad (8)$$

where

A, k, ℓ are constants and

c = crack length,

σ = stress at tip of crack,

N = number of load cycles.

The constants k, ℓ , are dependent on the properties of the material tested, and on the boundary conditions of the problem in question (31)(32)(33). Lin (34) noted that when $\ell=2.0$ and $k=1.0$; the plastic zone-size ahead of the crack tip is small in comparison with the crack length and specimen thickness. Paris and Erdogan (32) found that the use of values 2.0 and 4.0 for K and ℓ respectively yielded good agreement with experimental results. Paris (78) by considering the energy dissipated per cycle of load application as being proportional to the plastic zone-size ahead of the crack tip found

$$\frac{dc}{dN} \sim \frac{dW}{dN} \quad (9)$$

where

$$\frac{dW}{dN} = A_1 (\Delta K)^4 = A_1 c^2 \sigma^4$$

W = energy dissipated

A_1 = constant

c = crack length

σ = stress at crack tip

K = stress-intensity factor = $\sqrt{\sigma^2 c \Pi}$

It is evident that these analyses have attempted to take rate effects into account in an indirect manner. When conditions of fracture are brittle in nature, then these analyses are accurate. However, in the presence of tearing action, the property of the material changes with time and thereby affects the corresponding response behavior to application of load, and such analyses cannot account for this kind of behavior. Despite these shortcomings, analyses of this type are attractive in the sense that the fatigue process has been linked to microphenomena on a phenomenological basis.

In order to take rate effects, order effects and prior history effects into account Dong (35) postulated a cumulative damage theory to predict the life of a material under any arbitrary loading history. His assumptions were:

- 1) the material is undergoing an arbitrary loading history
- 2) life has full value at zero history and zero

value at failure,

- 3) temperature conditions are isothermal, and
- 4) damage and recovery processes can be accounted for.

The mathematical expression obtained is

$$l(t) = f[\gamma_{ij}(\tau)]_{\tau=-\infty}^{\tau=t} \quad (10)$$

where

$l(t)$ = life remaining in the material at time t , after damage has accumulated during $-\infty \leq \tau \leq t$,

τ = generic time,

t = present time,

γ_{ij} = any set of variables that can be used to describe loading history,

$f[]$ = damage functional.

This theory can account for the effect of prior history and sequence of events in damage behavior because the damage functional represents an infinite series expansion of hereditary integrals of the linear and non-linear type.

$$l(t) = L + \int_{-\infty}^t \beta_1(t, \tau) \gamma_{ij}(\tau) d\tau$$

$$+ \int_{-\infty}^t \int_{-\infty}^t \beta_{ijkl}(t, \tau_1, \tau_2) \gamma_{ij}(\tau_1) \gamma_{kl}(\tau_2) d\tau_1 d\tau_2$$

$$+ \dots + \dots$$

(11)

where

L = life at zero history,

t_f = time to failure,

β_1 = linear damage kernel,

β_i = non-linear damage kernels for $i > 1$, and

the rest of the expression represents cumulative damage which is zero for $t=0$ and equal to one at failure, when $t=t_f$.

The damage behavior of any rate-dependent or rate-independent material can be predicted under any arbitrary loading history using this approach. In the fatigue loading mode however, it can be shown that when a special form is chosen for the linear kernel β_1 , the Miner and Williams theories are recoverable (35). This shows that the inability of Miner and Williams's theories to demonstrate the influence of prior history and sequence of events on failure is due to the restrictive form of their damage kernels.

The above discussion on the damage created within a material in the repeated loading mode lends much credence to the general proposition that its manner of accumulation is a consequence of the fact that engineering materials and structures are inhomogeneous. Under load, various regions of stress concentration exist within the material, and because of its inhomogeneous nature, a distribution of strengths is created such that some regions are weaker than others. When the strength of a weak region is exceeded it is quite possible that a crack may initiate and cause

a redistribution of stresses with attendant crack formation in other regions. As the load is repeatedly applied they propagate and grow to a size which eventually renders the material or structure unserviceable. When this event occurs, fatigue damage is completed.

In light of the several important observations that have been made in regard to cumulative damage in the repeated loading mode, there are a few substantial points to remember in the course of developing a cumulative damage theory for any material or structure:

- a) Damage is a function of the inherent inhomogeneity of materials and structures; its initiation, progression, and attainment of a critical magnitude are therefore stochastic processes.
- b) For a given temperature, damage sites are nucleated under unique stress or strain conditions within the material. They propagate under stress or strain states different from initial conditions until a critical state is reached.
- c) The state of damage at any time is a function of the material property and load history. i.e., damage is not unique, it is a function of stress level and microstructural changes within the material.

d) Assumptions have to be made regarding the manner in which damage propagates, and regarding the parameters utilized to delineate its progression. The damage surface is essentially exponential in most materials, but the characteristics of the surface have to be determined from the stress and microstructural conditions existing in the material under load. For instance, if stress, strain, time and temperature conditions within the material are such that brittle fracture is warranted, then the rate of damage accumulation is one of fast growth to failure. If a tearing kind of fracture is warranted, gradual accumulation of damage is experienced.

The next question that arises in view of the basic premise of this investigation is the possibility of developing a cumulative theory of damage for pavement structures composed of different engineering materials, utilizing the basic concepts of damage progression presented above. Such a theory may be able to bridge the rather wide gap between states of loading in the field and the relatively simple experiments on a mathematical model of the structure. The ability of the structure to adjust itself to these loadings should yield in symbolic terms, with some degree of reliability, the relationships between the external loadings

and the physical constants which measure the competence of the system. To do this, it will be necessary to know how a pavement fails in practice. The information thus collected must be interpreted in the light of the failure mechanisms governing the performance of the materials comprising the pavement. When this is done, an adequate failure theory will begin to emerge. To this end the performance of a pavement structure in a repeated loading environment is examined in the next chapter within the context of internal damage development.

III. CLASSIFICATION OF PAVEMENTS BASED ON MECHANICAL RESPONSE AND IDENTIFICATION OF THE PARAMETERS OF DAMAGE

The response of a pavement structure in a given load and climatic environment has been divided for the purposes of analysis, into the primary response and ultimate response modes. (See Chapter I). This approach allows the categorization of pavement systems according to their manner of resisting structural impairment in the given environment. It further helps to identify and clarify the parameters responsible for internal damage progression. The classification consists of three separate categories of pavement systems: the frictional type, the flexural type and the frictional-flexural type. Before discussing the delineation of the mechanics of such a categorization, it is necessary that the concept of damage be first presented.

Figure 6 is a simplified two dimensional simulation of the variation in the performance level of a pavement structure with increasing time or number of load repetitions in a given environment. The figure simply demonstrates that the performance level of the structure diminishes in some manner until extensive repair is needed (1).

The curve indicates that under the combined stochastic action of traffic and the weather, pockets of

local distress are created within the system - the primary response. These propagate in a manner which depends upon the composition of the materials in the layers, and bring about a loss in structural integrity with the passage of time. The base level B_L represents an unacceptable level of performance as determined by users of the facility and characterises the time at which the extent of rupture and disintegration become intolerable -- the ultimate response. At any instant of time t_i , P_i represents a level of performance, and associated with it is the degree of damage D_i which has developed within the structure over the period of time $t = 0$ to $t = t_i$.

Using the base line B_L as a base of operations for the facility, the figure demonstrates that at zero time, or zero history of load applications, P_i and D_i have values equal to 1.0 and 0.0, respectively. This means that initially the life remaining in the facility is one hundred percent of its full value. At anytime t_i under the combined destructive action of the traffic and the weather, internal damage develops and the remaining life is less than the initial value.

The integrity level of the structure at any instant t_i is therefore 1.0 minus the amount of damage accumulated within that time.

i.e. $P_i(t_i) = 1 - D_i(t_i)$

or $1 = P_i(t_i) + D_i(t_i)$ (12)

In view of the discussion on damage in Chapter II, the concepts of serviceability, reliability, and maintainability discussed in Chapter I, and the observations of the properties of paving materials (36), it is obvious that the quantities P_i and D_i are probabilistic in nature. Thus, depending on the temporal and spatial distributions of damage within the structure the real instantaneous performance level will be on, below, or above the drawn curve. This means that each point on the curve has a probability of occurrence and a frequency distribution of values associated with it and this fact must always be acknowledged.

The preceding discussion was conducted in the two-dimensional domain, with the intent of illustrating precisely and clearly in a simple mathematical way, the manner in which damage accumulates in a pavement structure in a given traffic and climatic environment. The real picture is, however, more complex. The observed response of the structure depends on rate effects (36)(37), the position and magnitude of the applied load (38), climate (39), materials type (38), previous traffic history (38),

temperature (38), and constructional variables (41).

It can therefore be linear or non-linear depending upon the manner in which these variables combine. If the system behavior can be characterised as linearly or non-linearly elastic, plastic or viscoelastic, the response will have similar characteristics. Then at any point t_j in time a 'performance surface' which is a function of these variables exists such that its inverse is a 'damage surface'.

$$\text{i.e. } P_j(R_j, X_j, Y_j, M, H_j, T, C \dots) = 1 - D_j(R_j, X_j, Y_j, M, H_j, T, C \dots)$$

where P_j = portion of surface utilized by time t_j

R_j = rate effects

X_j, Y_j = coordinates of load

M = material properties

H_j = previous traffic history

C = constructional variables

D_j = portion of damage surface utilized by time t_j

Within this context, at any instant, and at some point on the surface, a prediction of the percentage of total life already used and that remaining within the structure can be made. Therefore, the damage surface as well as the performance surface is n-dimensional with

construction, maintenance, load and environmental parameters playing a significant role in its determination. The development of such a surface is not immediately possible. This, however, does not mean that the problem is intractable, because the possibility of reducing 'n' may exist. In fact such a technique is used in the development of yield surfaces for metals. The yield surface is postulated to be a function of the stress tensor, its derivatives, and a work hardening term (42). However, because of the difficulty experienced in developing the surface certain approximations are made and the yield surface is expressed only as a function of either a stress or strain tensor. The pavement area does not preclude the application of a similar technique, and the initial stages in the development of such an approach to the damage problem is discussed in this thesis.

All the significant factors that have a role to play in internal damage progression can be generally accounted for, providing that they are translated, through the properties of the layer materials and the response behavior of the pavement structure for a given quality of construction and maintenance operations, into stress and strain quantities. In other words, the magnitude and type of the stress and strain concentration (tensile or shear) within the pavement structure is a function of

not only the characteristics of the applied load but also of the spatial distribution of layer material properties and local defects. A knowledge of the material properties yields information on the kind of structural response to expect. From such information postulations can be made about the manner of internal damage progression. This technique takes into consideration the two most significant structural properties - material properties and response behavior - which reflect the influence of all the others. It can therefore be used to classify pavements into three broad groups - the frictional group, the flexural group and the frictional-flexural group - so that the stress-strain parameters of damage progression in each group can be identified.

The frictional-type pavement is composed of granular materials in which load transfer occurs at interparticle contact points by purely frictional action. The deformation that takes place under load is purely of the shear or flow type, and for each application of the load a permanent deformation results. Such pavement structures, generally require a thin type of wearing course which can deflect conveniently with the rest of the structure under repeated loading. In order to protect the underlying materials, the wearing course should possess good ductile properties as opposed to brittle properties

since toughness in this case is more important than tensile strength. However, when the deformation becomes excessive, cracks may appear in the surface due to the randomly distributed cumulative shear action in the subgrade. Therefore, in a frictional-type pavement, damage can be considered to develop as a result of shear action. Consequently the damage parameter must somehow be associated with shear stresses and shear strains.

In a flexural-type pavement, the materials in the layers are capable of resisting the applied load through the action of tensile stresses which develop as a result of the flexing action. This implies that bending is the only mode of deformation and upon the repeated application of load, repeated flexing results. In such a pavement, fatigue action is very important, and though the overall shear support of the components is adequate, cracks develop very early due to the accumulation of tensile strains. These propagate slowly or rapidly in a random manner depending on the properties of the layer materials and the rate of the repeated flexing action. The fatigue properties of the materials in the layers are therefore a prime concern during the design stage of such facilities. Damage in such pavements is propagated in the fatigue loading mode under the action of tensile stresses and tensile strains.

The third type of pavement possesses both frictional and flexural materials. Its structural integrity under repeated load is impaired by the destructive tensile and shear action that is manifested within the layer-components. It is conceivable that if one action tensile or shear should dominate in creating damage within the structure, the failure would occur in that mode. On the other hand, it is also possible that both actions may play a significant role during the life of the facility depending upon the environmental conditions. The damage parameter is, therefore, associated with both tensile and shear stresses and strains.

The above classification of pavements accounts for all types of pavements currently in existence (40). It also makes possible the tractability of the damage progression within such structures. One can generally say that the damage 'build-up' occurs in three different modes. When the behavior of the pavement structure is completely frictional, damage initiates and progresses by plastic or shear flow until the appearance of surface cracks terminates or aggravates the situation. When flexural behavior is pertinent the damage, initiation and progression occur by the development and growth of internal cracks, under the action of tensile stresses and strains. However,

in the frictional-flexural type of pavement, the damage initiates and progresses by shear flow and/or by crack growth. Consequently a pavement structure may show signs of distress either from the independent action of excessive deformations, the isolated action of 'fatigue', or from both failure mechanisms working together. This indicates that in order to analyze the response behavior of a pavement structure and predict the failure behavior, a number of models which would account for such behavior in a given traffic and climatic environment should be developed.

At the present time, three such models seem to be appropriate:

- a) A model is needed for the representation of the linear and non-linear behavior of paving materials,
- b) The pavement system must be modeled in terms of the geometrics of the applied load and the structure so that the utilization of the former model within such a framework will aid in the prediction of the developed stresses and strains in a given environment and,
- c) A model that must be capable of handling linear and non-linear damage behavior.

Finally, in order to achieve realistic predictions, it is essential to combine these models in a probabilistic manner, since the progression of damage as has been demonstrated is stochastic in nature.

In this study, only the linear and deterministic aspects of pavement behavior are investigated as a first approximation. Two models are developed: the first accounts for the primary structural response as defined in Chapter I by using models 'a' and 'b' above to predict the magnitude of the developed stresses and displacements under stated boundary conditions; the second establishes the link between the primary and ultimate response behaviors through the use of model 'c'. Although model 'c' - the cumulative damage model - is general enough to treat failure in any mode, the example presented considers only failure in fatigue. This failure mechanism is used because of the availability of experimental data in the literature.

1. Pavement Models for Primary response.

All models that have been developed for the analysis of stresses and displacements of pavement structures fall into two principal categories: those concerned with the elastic analysis of a half space and those concerned with the viscoelastic analysis. These analyses, in general, have been based on the assumption that the half space

is composed of

- a) a linear elastic, homogeneous, and isotropic material of semi-infinite depth, and,
- b) a system of layers, each of which may be linear elastic or viscoelastic, homogeneous, isotropic and in general weightless.

It has been assumed on occasion that either continuity of displacements (free friction) or absence of shear stresses exist at the interfaces of the layers.

The simplest model, the homogeneous half-space, is one in which no change in material properties occurs with depth or with horizontal extent. Boussinesq (43) initially solved the problem of a point load on a homogeneous half-space in 1885. His work was subsequently modified by various authors (44) (45), until Alvin and Ulery (46) presented a comprehensive table for the stresses and displacement at any arbitrary point in a half-space under a uniformly distributed circular load, for arbitrary Poisson's Ratio.

The homogeneous half-space has, since that time, been used extensively by several investigators as that representing a layered pavement structure. The shortcomings of such an assumption are readily obvious. Though the model is relatively simple to use, it lacks the capability of

accounting for the thickness of the layers and the quality of the materials employed in the construction of a real pavement structure. In order to account for these variables in the mathematical model, semi-infinite bodies composed of distinctly different materials in layered form are used and the distribution of the stresses and displacement induced in them by a variety of load and displacement boundary conditions are analyzed.

The analyses of layered half-space systems can be categorized in two groups; those involving rigorous elastic theory, and those involving plate behavior of the top layer. These two analyses are significantly different as result of the dissimilarity of the boundary conditions used.

Westergaard (47) developed the initial solutions for an elastic plate resting on an elastic subgrade which could undergo only vertical displacements or provide vertical reactions (a Winkler foundation). Since then, several modified forms of his method have appeared in the literature.

The first solution for both a two-layer and a three-layer system using the elastic theory was given by Burmister (48). He obtained his solution by assuming the existence of a stress function involving Bessel functions and exponentials from which he was able to develop and

present the general equations and solution for both two and three-layered systems, with the constants for the top-layer also evaluated.

The use of a layered elastic system as a mathematical model for a pavement structure has been quite extensive, and several of the presently available design methods for flexible pavements are indeed based upon such analyses (49). This model takes care of the shortcomings of the homogeneous half-space. The thickness of the layers and the properties of the materials from which the layers are made are shown to be significant in the calculation of the developed stresses and displacements.

The model is based upon the assumption that each layer is composed of a linear elastic material, and the elastic constants of the linear elastic material, and the elastic constants of the layers are the only properties that enter into the analysis. This has resulted in several discrepancies when models of this type are used either to predict the performance of a real pavement or to evaluate the suitability of different materials for use in the pavement structure. Among these are the incapability of the model to account for rate effects, and the accumulation of deflection.

It has been shown that the majority of conventional paving materials are not purely elastic, and their

mechanical response is generally time dependent (36) (38). This indicates that the response of such materials depends upon their entire loading history. To account for this time dependency, use is made of the theories of linear viscoelasticity for both the characterization of the paving materials and the development of mathematical model for stress analysis in pavement structures (50) (51) (52).

The viscoelastic models for the analysis of stress and displacement in a pavement structure differ from those of layered elastic systems only in the material characterization used for each layer. The geometry, boundary conditions and loading functions are exactly similar in the two models. Such similarities between the models have resulted in the development of a technique, known as the correspondence principle, whereby the solutions to the elastic problems can be used to obtain the viscoelastic solutions of the same problem.

The technique of solution presented in the initial parts of the primary model development in this thesis is that of Ashton and Moavenzadeh (54). Parts of their work have therefore been used intact to keep the necessary continuity of the presentation. The analysis of the stresses and displacement in a three-layer system is

44

formulated following Burmister's approach. The formulations are first presented for elastic systems and then for viscoelastic systems for the stated boundary conditions. A detailed description of the model is given in Chapter IV.

2. Model on Ultimate Response Mode.

The pavements discussed in this section belong to the frictional-flexural group and are therefore representative of many current pavement sections. In this type of structure 'fatigue' damage occurs in the surface layer which by our classification, behaves in a flexural manner. The culmination of this kind of action is the appearance of alligator crack patterns randomly distributed on the surface of the structure. This subsequently leads to the rapid deterioration of the entire pavement structure due to either the resulting relatively large increase in the transmitted stresses or the penetration of water into the underlying materials.

The occurrence of fatigue in pavements has been observed or noted for a considerably long period of time. Porter (55) in 1942 observed that pavements do in fact undergo fatigue. In 1953, Nijboer and Van der Poel (56) related fatigue cracks to the bending stresses caused by moving wheel loads. Hveem (57) also correlated the

47

performance of flexible pavements with deflections under various repeated axle loads. The AASHO & WASHO tests (39) confirmed these observations by relating the cracking and initial failure of pavements to repeated loading of the type discussed by Seed et. al. (58)

The field observations of this kind of behavior led to the laboratory investigation. Many researchers have conducted laboratory experiments so as to determine the fatigue properties of paving materials and to investigate the possibility of extrapolating laboratory results to existing field conditions. To this end, Hennes & Chen (59) conducted tests on asphalt beams resting on steel springs and subjected to sinusoidal deformation with a variety of constant amplitude magnitudes. They discovered that as the frequency of applications is increased, the creep-rupture compliance of the material decreases. On the conduction of similar tests by Hveem (57), on beams cut from actual pavements the same results were obtained.

Monismith (60) in his tests on asphalt beams supported on flexible diaphragms mounted on springs under constant stress amplitudes discovered that increases in the stiffness of the material resulted in corresponding increases in fatigue life. Saal and Pell (61) conducted similar tests from which the tensile strain to failure

(ϵ_T) versus the number of cycles to failure, or fatigue life (N_f) relation, was found to be $N_f = 1.44 \times 10^{-16} (1/\epsilon_T)^6$. They further found that this expression does not vary with temperature, rate of loading and type of asphalt. These results are not surprising since one should expect such factors to affect the developed stresses and not the strains through the stiffness of the material. For the mixtures tested, no endurance limit was observed up to 10^8 applications, as is to be expected, since the mode of failure is one of crack initiation and propagation to failure at each stress level. The general conclusion arrived at by several authors from such tests indicate that the fatigue life of an asphaltic paving material is a function of several variables - the tensile strain level Fig.7 (62) to which the specimen is subjected, the amount of asphalt, the age of the mixture, temperature, the stiffness of the mixture, its density and void ratio.

Mode of Loading: Another important factor in such tests is the mode of loading. In controlled-stress tests for example, fatigue life increases not only as the stiffness of the sample increases, but also as the temperature decreases. However, in strain-controlled tests, the fatigue life decreases as stiffness increases; for this test, at low

temperatures no change is observed in fatigue life and as temperature increases the fatigue life increases as well (63) (64) (65). Controlled stress and strain behavior can be explained from a consideration of either the time-temperature superposition principle or the amount of energy stored in the sample when such tests are performed. In controlled stress tests the minimum energy stored per load repetition can be achieved by minimizing deflection and causing a resultant increase in fatigue life. In controlled strain tests the reverse is true. This implies that for a specimen of a given initial stiffness and initial strain, failure under a controlled stress mode of loading will occur sooner. Therefore, when extrapolating laboratory results to field conditions such considerations have a significant role to play. In other words, what is the mode of loading in the field? Is it controlled stress, controlled strain or a mode between the two extremes? Answers to such questions have been obtained by Monismith (67) who through the use of a mode factor suggested that for surface layers less than 2" thick, the controlled strain mode of loading results, while for those layers 6" thick or greater, the controlled stress mode of loading is applicable. For thickness between these, an intermediate mode of loading is appropriate.

Tests have also been performed on granular and other paving materials so as to determine the significant characteristics of their behavior under repeated loading--(Fig. 8) (58) (66). The results of such tests generally indicate the importance of the duration of stress application and rate of deformation, the frequency of load application (67), the type of aggregate and percentage of material passing the number 200 sieve (58), the void ratio (58), degree of saturation and confining pressure and stress level on the response behavior of the soil when measured by a quantity called the resilient modulus (the resilient modulus is defined as the deviatoric stress divided by the recoverable strain).

For untreated granular materials, Monismith et al. (58) suggested an expression to define the influence of stress conditions on the modulus of resilient deformation.

$$M_r = \frac{\sigma_d}{\epsilon_r} = K\sigma_3^n \text{ or } K(\theta)^{n'} \quad (13)$$

where

M_r = Resilient Modulus

K = constant

$\theta = \sigma_1 + \sigma_2 + \sigma_3$ (principal stresses)

→ $n, n' = \text{constants}$

σ_d = repeated axial deviator stress

ϵ_r = resilient axial strain corresponding to a specific number of load applications.

Although this is an empirical expression it, however, points up the important fact that the response of granular and treated materials in pavement sections depends upon the characteristics of the applied loading, the material and the existing confining stress. Since the stresses due to load vary in both the vertical and horizontal directions in a pavement section, the influence of stress on resilience must be properly accounted for to adequately predict the deformation characteristics of the pavement section. The model or method used for the determination of the developed stresses in the pavement must account for this observed behavior.

It would appear, therefore, from the foregoing review that one would first determine the fatigue properties of the pertinent layer materials under conditions representative of moving traffic and environmental conditions before using a cumulative damage theory.

Several authors have used the elastic theory as a first approximation to predict the observed behavior of asphaltic, granular, and the untreated granular material in a moving traffic environment. The results have not been successful because of time and temperature dependent

behavior of paving materials. The viscoelastic analysis discussed in the following section would provide a better means of evaluating the stresses in the pavement sections.

Another important development from the laboratory results is the attempt to make use of the experimental results to predict the occurrence of fatigue damage in a real pavement structure. To this end, the fracture in the field has been attributed to tensile action in the bottom of the pavement Fig. 9 (67), and the damage-determinant has been labelled as the tensile strain level. In general, the results of controlled-strain tests have been represented, after statistical analysis, as:

$$N = K(1/\epsilon)^n \quad (14)$$

N = service life (number of load applications to reach a particular level of damage).

ϵ = magnitude of the tensile strain repeatedly applied.

n = constant

K = constant dependent on:

- a) temperature
- b) asphalt stiffness
- c) asphalt source
- d) aggregate characteristics

This result was, however, obtained from simple loading tests in which the load condition remains unchanged throughout the life of the specimen. Since the real loading condition represents a spectrum of load magnitudes repetitively applied in a random fashion, compound loading considerations must be made. Deacon and Monismith (69), suggested a modification of the usual Miner's theory of linear summation of cycle ratios. They point out that such an approach has the desirable features of procedural simplicity, a wide range of applicability to different types of compound loading, minimum data requirements, preferably of a simple loading nature, a theoretical basis and predictive accuracy. Their analysis, however, is rather difficult to interpret. Also, the sequence of events and prior history cannot be accounted for in such an approach as was indicated in Chapter II.

To summarize the foregoing discussion, it would appear that if the tensile strain level in the surface layer is the damage determinant, then a mechanism of ascertaining the strain under various wheel load magnitudes is desired. Using this model and a cumulative damage theory in which the fatigue characteristics have been represented, the prediction of the probable service life can be made by determining the time or the number of load repetitions

at which the degree of damage in the surface layer reaches unity. The models developed to do this are presented and discussed in the next two chapters.

IV. THE PRIMARY MODEL

Statement of the Problem and the Method of Solution

The geometrical model that was selected as representative of the pavement for this investigation is a multi-layered, semi-infinite half space consisting of three distinct layers as shown in Figure 10. It is assumed that each layer has distinct material properties which can be characterized as linear elastic - or linear visco-elastic depending on the problem that is being considered. The variables of interest are the components of the stress tensor and the displacement vector at any point in the system. The load is considered to be uniform, normal to the surface, and acting over a circular area. The following load conditions are considered,

1. A stationary load is applied and maintained at the same region of the surface for an infinite period of time.
2. The same load of step 1 is then repeatedly applied with a specified frequency to the same area on the surface of the pavement.
3. The single wheel load of step 1 is made to travel at a constant velocity V along a straight path on the surface of the system (Figure 11).

For each of these loading conditions, the components of the stress tensor and the displacement vector induced at any point in the system can be determined. The expressions so obtained for the normal vertical deflection

are presented in detail for loading conditions 2 and 3.*

Those determined for the other components of the stress tensor and displacement vector under loading condition 1 - are also presented in detail. This is in keeping with the assumption that these variables can be utilized as indicators of structural integrity in the Primary Response Mode of the system.

The problem in general, excluding the stationary loading case, is a dynamic problem and the inertial terms, if significant should be added to the equations of motion. The effects of the inertial terms, however, become of significant importance when the velocity V of the motion is of the order of magnitude of the distortional or the dilational wave velocity of the medium. For linear viscoelastic materials (70) the distortional velocity is $v = (G\{0\}/\rho)^{1/2}$ where $G\{0\}$ and ρ are respectively the initial value of the shear relaxation modulus and the density of the material. When $V/v \ll 1$, the inertial terms are negligible and the analysis can be conducted in a quasi-static condition. This condition is assumed applicable to the problem discussed in this study.

*This does not in any way detract from the generality of the method to be presented, as the other stress and deflection variables can be determined in the same manner.

57

In order to obtain the viscoelastic solution for the stresses and displacements for the various loading conditions considered, the correspondence principle is utilized. This principle states that if the elastic constants in the elastic solutions to a given boundary problem are replaced by operator forms of the stress-strain relations, then the viscoelastic solution will be obtained.

The above principle was used by Ashton and Moavenzadeh (54) to obtain the viscoelastic solution for the stresses and displacements induced in a three layer viscoelastic system subjected to a stationary load. It was then subsequently modified, in this work by using the principles of the response of initially relaxed linear systems to imposed excitations to obtain the solutions for the moving and repeated load history conditions.

This method of analysis has been selected largely because the viscoelastic behavior of the system materials can be realistically represented by stress-strain relations of the linear and non-aging type, such as hereditary integrals. The steps involved in its application to a boundary value problem as the one considered in this thesis can be concisely stated as follows:

1. The elastic solution for the surface deflection of the system due to a stationary applied load is first obtained (54).
2. The "correspondence principle" is applied to the above solution in the form of hereditary integrals for the stress-strain relations, to obtain the viscoelastic solutions (54).
3. The expressions for the surface deflection due to the repeated and moving loads are then developed through the use of Duhamel's superposition integral for linear systems (71).

Elastic Formulation

The elastic analysis for layered systems has been formulated by several authors using basically Burmister's approach. An explicit statement of the constants involved is presented in reference (72) for the three-layer system.

In the following analysis, Poisson's ratio has been taken equal to $1/2$ in each layer (bulk modulus infinite). This assumption has been made because of the simplifications that result in the numerical computation.

Assuming an axi-symmetric load distribution, the solution to the equations of stress-strain relationships, equilibrium, compatibility, strain-displacement for a general incompressible symmetrical elastic body can be written in terms of a stress function ϕ in the following form.

Stress Components:

$$\sigma_z = \frac{\partial}{\partial z} \left[1.5 \nabla^2 \phi - \frac{\partial^2 \phi}{\partial z^2} \right] \quad (\text{vertical stress}) \quad (15)$$

$$\sigma_r = \frac{\partial}{\partial z} \left[.5 \nabla^2 \phi - \frac{\partial^2 \phi}{\partial r^2} \right] \quad (\text{radial stress}) \quad (16)$$

$$\sigma_\theta = \frac{\partial}{\partial z} \left[.5 \nabla^2 \phi - \frac{1}{r} \frac{\partial \phi}{\partial r} \right] \quad (\text{circumferential stress}) \quad (17)$$

$$\tau_{rz} = \frac{\partial}{\partial r} \left[.5 \nabla^2 \phi - \frac{\partial^2 \phi}{\partial z^2} \right] \quad (\text{shear stress}) \quad (18)$$

Displacement Components:

$$w = \frac{1.5}{E} \left[\frac{\partial^2 \phi}{\partial r^2} + \frac{1}{r} \frac{\partial \phi}{\partial r} \right] \quad (\text{vertical displacement}) \quad (19)$$

$$u = - \frac{1.5}{E} \frac{\partial^2 \phi}{\partial r \partial z} \quad (\text{radial displacement}) \quad (20)$$

where

$$\nabla^2 = \frac{\partial^2}{\partial r^2} + \frac{1}{r} \frac{\partial}{\partial r} + \frac{\partial^2}{\partial z^2}$$

If the stress function ϕ is chosen in the following form

$$\phi = J_0(mr) [Ae^{mz} - Be^{-mz} + Cze^{mz} - Dze^{-mz}] \quad (21)$$

the compatibility equation $\nabla^2 \phi = 0$ is identically satisfied.

The expressions for stresses and displacements can be found by substituting equation (21) into equations (15) through (20).

Boundary Conditions

The boundary conditions for the lower layer are that all stresses and displacements go to zero when z becomes infinite. This results in $A = C = 0$, for this layer as is evidenced by the form of ϕ . At the surface, the boundary conditions are that the shearing stress must be zero

$$\tau_{rz} \Big|_{z=-H_1} = 0 \quad (22)$$

and that the normal stress is given, for a uniform circular load of magnitude q and radius a as

$$\sigma_z \Big|_{z=-H_1} = -qa \int_0^\infty J_0(mr) J_1(ma) dm \quad (23)$$

It will be convenient to use an incremental load

$$\sigma'_z \Big|_{z=-H_1} = -J_0(mr)J_1(ma) \quad (24)$$

and then integrate the final expressions from 0 to ∞ with respect to m , and multiply this result by qa , which will then yield the same result.

The remaining boundary conditions involve the continuity at the interfaces between the layers. At each interface four conditions must be imposed. Assuming continuity of the displacements, vertical stress, and shear stress across an interface, the boundary conditions between layers i and $i + 1$ are

$$w_i = w_{i+1} \quad (\text{vertical displacement}) \quad (25)$$

$$u_i = u_{i+1} \quad (\text{radial displacement}) \quad (26)$$

$$\sigma_{z_i} = \sigma_{z_{i+1}} \quad (\text{vertical stress}) \quad (27)$$

$$\tau_{rz_i} = \tau_{rz_{i+1}} \quad (\text{shear stress}) \quad (28)$$

* σ'_z is not a real stress since it does not have dimensions of stress. However, its use in this context is obvious.

For an n - layer system, equations (25) to (28) yield $4n-4$ equations. In addition, the two equations (22) and (23) are available for the surface layer, and the two constants in the bottom layer are zero. Thus a total of $4n-2$ equations in $4n-2$ unknowns must be solved. For a three-layer system this will be ten equations in ten unknowns.

The values of these constants can then be substituted into the expressions for the stresses and displacements. These expressions can be rewritten in terms of geometry and the elastic constants in the following simplified form for each layer.

$$\sigma'_{z_i} = J_0(mr)J_1(ma) \frac{\sum_{j=1}^{18} \phi_{1,i,j} \alpha_{i,j}}{\sum_{j=1}^9 \theta_j \alpha_{i,j}} \quad (29)$$

$$\tau'_{rz_i} = J_1(mr)J_1(ma) \frac{\sum_{j=1}^{18} \phi_{2,i,j} \alpha_{i,j}}{\sum_{j=1}^9 \theta_j \alpha_{i,j}} \quad (30)$$

$$\sigma'_{r_i} = J_0(mr)J_1(ma) \frac{\sum_{j=1}^{18} \phi_{3,i,j} \alpha_{i,j}}{9} + \frac{\sum_{j=1}^{18} \theta_j \alpha_{i,j}}{9}$$

$$\frac{J_1(mr)J_1(ma)}{mr} \frac{\sum_{j=1}^{18} \phi_{4,i,j} \alpha_{i,j}}{9} + \frac{\sum_{j=1}^{18} \theta_j \alpha_{i,j}}{9} \quad (31)$$

$$w'_i = \frac{J_0(mr)J_1(ma)}{m} \frac{\sum_{j=1}^{18} \phi_{5,i,j} \alpha_{i,j} / E_i}{9} + \frac{\sum_{j=1}^{18} \theta_j \alpha_{i,j}}{9} \quad (32)$$

$$u'_i = \frac{J_1(mr)J_1(ma)}{m} \frac{\sum_{j=1}^{18} \phi_{6,i,j} \alpha_{i,j} / E_i}{9} + \frac{\sum_{j=1}^{18} \theta_j \alpha_{i,j}}{9} \quad (33)$$

where

$$\phi_{m,i,j} = \sum_{k=1}^4 q_{k,i,j} \lambda_{m,k} \quad \begin{matrix} m=1\dots6 \\ i=1\dots3 \\ j=1\dots18 \end{matrix} \quad (34)$$

$$\alpha_{3,j} = \alpha_{2,j} \quad j=1\dots18 \quad (35)$$

$$\alpha_{1,j} = 0 \quad j = 10 \dots 18 \quad (36)$$

and the $\lambda_{m,k}$'s are defined in Table 1. (72)

To obtain the elastic solution under a uniform circular load, the above stresses and displacements must be integrated from zero to infinity with respect to m , and multiplied by qa . For example, the normal stress at any off-set r is given, for a uniform circular load of radius a and intensity q , as follows.

$$\sigma_{z_1} = qa \int_0^{\infty} J_0(mr) J_1(ma) \frac{\sum_{j=1}^{18} \phi_{1,i,j} \alpha_{i,j}}{\sum_{j=1} \theta_j \alpha_{i,j}} dm \quad (37)$$

Viscoelastic Formulation

For the viscoelastic case, the time variation of the loading must be specified. In this case, the normal stress boundary condition will be taken as

$$\sigma_z \Big|_{z=-H_1} = qa \int_0^{\infty} J_0(mr) J_1(ma) dm H(t) \quad (38)$$

where $H(t)$ is the Heaviside step function such that

$$H(t) = 1 \quad t \geq 0$$

$$H(t) = 0 \quad t < 0$$

Again the incremental load

$$\sigma'_z \Big|_{z=-H_1} = J_0(mr) J_1(ma) H(t) \quad (39)$$

will be considered, and then the final result will be integrated from 0 to ∞ with respect to m , and then multiplied by qa , to yield the viscoelastic solution under a uniform load.

Since in the elastic solutions, equations (29) to (37), the Bessel functions appear as multipliers to the summation-over-summation terms, and since these Bessel functions vary only with m for a given geometry, it will be useful to treat the elastic solutions in the following forms.

Define:

$$\psi_{k,i}(m,t) = \frac{\sum_{j=1}^{18} \phi_{k,i,j} \beta_{i,j} H(t)}{\sum_{j=1} \theta_j \alpha_{i,j}} \quad (40)$$

where

$$\beta_{i,j} = \alpha_{i,j} \quad k \leq 4 \quad (41)$$

$$\beta_{i,j} = \alpha_{i,j}/E_i \quad k > 4 \quad (42)$$

$$\textcircled{H}_1(m) = J_0(mr)J_1(ma) \quad (43)$$

$$\textcircled{H}_1(m) = J_1(mr)J_1(ma) \quad (44)$$

Then the time-varying elastic solutions are given as follows:

$$\sigma_{z_i}(t) = qa \int_0^\infty \textcircled{H}_1(m) \psi_{1,i}(t,m) dm \quad (45)$$

$$\tau_{rz_i}(t) = qa \int_0^\infty \textcircled{H}_1(m) \psi_{2,i}(t,m) dm \quad (46)$$

$$\sigma_{r_i}(t) = qa \int_0^\infty \left[\textcircled{H}_1(m) \psi_{3,i}(t,m) + \frac{\textcircled{H}_2(m)}{mr} \psi_{4,i}(t,m) \right] dm \quad (47)$$

$$w_i(t) = qa \int_0^\infty \frac{\textcircled{H}_1(m)}{m} \psi_{5,i}(t,m) dm \quad (48)$$

$$u_i(t) = qa \int_0^\infty \frac{\textcircled{H}_2(m)}{m} \psi_{6,i}(t,m) dm \quad (49)$$

The Application of the Correspondence Principle: In order to obtain the viscoelastic solution, all that is needed is to obtain the corresponding $\psi_{k,i}(t,m)$ for the viscoelastic case, since the $(H)_j(m)$ terms do not vary in time. But the $\psi_{k,i}(t,m)$ terms for the elastic case are in a form which permits the formulation of an integral equation for the viscoelastic solution as a function of time for a given value of m . From the solution of this equation for appropriate m , the total solution can be obtained by numerical integration of the equations (45) to (49).

Since each layer of the system is assumed to be incompressible, then one constitutive relationship is sufficient to define the viscoelastic equation of state of each layer. This constitutive equation is assumed in terms of a viscoelastic equivalent to the elastic compliance. That is, for the i th layer.

$$\frac{1}{E_i} \text{ (equiv.)} = [D_{r_i}(0) - \int_0^{t-} \left(\frac{\partial D_{r_i}}{\partial \tau} (t-\tau) \right) d\tau] \quad (50)$$

In the following, $D_{r_i}(t)$ will be denoted simply by $D_i(t)$ since it is clear from the context what is implied.

By substituting the above operator expressions for each elastic constant, the integral equation for $\psi_{k,i}(t,m)$ for the viscoelastic case can be written as

$$\begin{aligned} \sum_{j=1}^9 \theta_j(m) & \left[\int_{0+}^t \psi_{k,i}(m,t-\tau) \frac{\partial \alpha_{i,j}(\tau)}{\partial \tau} d\tau + \psi_{k,i}(m,t) \alpha_{i,j}(0) \right] \\ & = \sum_{j=1}^{18} \phi_{k,i,j}(m) \beta_{i,j}(t) \end{aligned} \quad (51)$$

in which $\alpha_{i,j}(t)$ is a three-fold convolution integral of the following form [for $\alpha_{i,j} = 1/E_s E_t E_u E_v$] in the elastic case]

$$\begin{aligned} \alpha_{i,j}(t) & = \int_{0+}^t D_s(t-\tau) \frac{\partial}{\partial \tau} \int_{0+}^{\tau} D_t(t-\lambda) \frac{\partial}{\partial \lambda} \int_{0+}^{\lambda} D_u(\lambda-\rho) \frac{\partial D_v(\rho)}{\partial \rho} d\rho \\ & + D_u(\lambda) D_v(0) d\lambda + D_t(\tau) D_u(0) D_v(0) d\tau \\ & + D_s(t) D_t(0) D_u(0) D_v(0) \end{aligned} \quad (52)$$

and

$$\alpha_{3,j}(t) = \alpha_{2,j}(t) = \int_{0+}^t D_w(t-\xi) \frac{\partial \alpha_{i,1}(\xi)}{\partial \xi} d\xi + D_w(t) \alpha_{i,1}(0) \quad (53)$$

with $D_w(t) = D_2(t)$ and $l=j$ for $j \leq 9$, and $D_w(t) = D_1(t)$ and $l = j-9$ for $j > 9$.

$$\beta_{i,j}(t) = \alpha_{i,j}(t) \quad \text{for } k \leq 4$$

$$\beta_{i,j}(t) = \int_{0^+}^t D_i(t-\xi) \frac{\partial \alpha_{i,j}(\xi)}{\partial \xi} d\xi + D_i(t) \alpha_{i,j}(0) \quad \text{for } k > 4 \quad (54)$$

The solution of the integral equation (51) is fully described in Appendix I (71). In order to formulate solutions for the repeated and moving loads, it will be necessary to introduce the principle of the response of linear systems to imposed excitations.

The response of linear systems to imposed excitations

A linear system may be defined as one whose mechanical behavior can be adequately described by a set of linear differential or linear integral equations. Physically, this means that the response of the system is directly proportional to the magnitude of the agent causing it. A purely linear elastic material is considered a linear system, because its response is directly proportional to the input function. The 'constant' of proportionality, between the input and output (response) functions of the system, is defined as a material property "variable" or a "system function". This function is a property of all linear systems, and when input functions of known geometrical and time configurations are coupled with it, the desired

system responses are subsequently obtained.

Linear Systems: Considering the input function to a linear system to be given by $I(t)$, and the output function by $O(t)$, with the additional assumption that the system is initially relaxed (i.e., there is no initial stored energy), the system function $h(t)$, can be defined using linear integral operators like the Laplace or the Fourier transform (73). Besides the use of integral operators differential operators may also be used. When integral operators such as the Laplace transform are used, the relationship between the input function and the output function is given by

$$h(s) = \frac{O(s)}{I(s)} \tag{55}$$

$$h'(s) = \frac{I(s)}{O(s)} \tag{56}$$

where from equations (55) and (56)

$$[h(s)][h'(s)] = 1$$

- $h(s)$ is the s-multiplied transform of $h(t)$,
- $O(s)$ is the Laplace transform of $O(t)$,
- $I(s)$ is the Laplace transform of $I(t)$
- S is the Laplace transform parameter

The relaxation function of a linear viscoelastic material is an example of a system function. It may be determined from a uniaxial relaxation test in which a constant strain, $\epsilon(t) = \epsilon_0 H(t)$, is applied to a cylindrically shaped specimen of the linear material and the time variation of the stress $\sigma(t)$ is measured. The relaxation function, $E_r(t)$, is defined as $E_r(t) = \frac{\sigma(t)}{\epsilon_0 H(t)}$

The input function for this example is the constant strain, $\epsilon(t) = \epsilon_0 H(t)$, and the output function is the time varying stress, $\sigma(t)$. In the Laplace domain the relationship between $E_r(t)$, $\sigma(t)$, and $\epsilon(t)$ is given by

$$E'_r(s) = \frac{\sigma(s)}{\epsilon(s)} \quad (57)$$

where $E'_r(s) = s$ -multiplied transform of $E_r(t)$.

$\sigma(s) =$ Laplace transform of $\sigma(t)$ and

$\epsilon(s) =$ Laplace transform of $\epsilon(t)$.

The equations (55) to (57) illustrate that when the input function is a unit step function (i.e. $I(t)$ or $\epsilon(t) = H(t)$), the response function is the same as the system function.

When a specimen of this material is subjected to general time varying strain, $\epsilon(t)$, the system function

$E_r(t)$, can be used to obtain the time varying stress response $\sigma(t)$.

In the Laplace domain,

$$\sigma(s) = E'_r(s) \quad \epsilon(s) = s E_r(s) \epsilon(s) \dots \quad (58)$$

which once inverted into the time domain, results in the well-known Duhamel Integral (74).

$$\sigma(t) = \int_{-\infty}^t E_r(t-\tau) \frac{\partial \epsilon(\tau)}{\partial \tau} d\tau \quad (59)$$

This expression could be obtained directly in the time domain by using the Boltzman superposition principle (74).

The above operations therefore disclose the significant fact that the system function can be used to obtain the response function of a linear viscoelastic material, when the input function is any time varying load. These same techniques can be used, but with a slight modification, for the response analysis of structures composed of linear viscoelastic materials.

The System Function for Linear Structures

In most cases, linear materials are used in structures in such a way that the resulting equations describing

13

the response of the structure to mechanical excitations are linear. In such cases, the structure can be considered as a linear system and its response to a general time-varying load may be evaluated from its response to a step loading. To elaborate on this point a little further, one can within this framework define two important functions which play a major role in the response mode of the linear system.

The first of these may be called the Response Function of the structure. It is the response of the system to a step loading (i.e., a load whose magnitude is constant with respect to time) of magnitude other than unity. When the step load has unit magnitude, then the response of the structure may be called a System Function, which is dependent on the material properties as well as the geometric features and boundary conditions of the structure or system.

Consider an initially relaxed linear structure with a step response $SR(t)$ (i.e., the response to a load whose magnitude is a constant with respect to time). According to the definitions given above, $SR(t)$ is a system function for a unit load input $UF(t) = H(t)$, and a Response Function for a load of any other magnitude, $UF(t) = UF_0 H(t)$. The response $P_s(t)$ of this structure to any other time-varying

load $P(t)$ with a time configuration other than that of a step load, can be obtained by superposition through the use of the Boltzmann principle as follows:

$$\text{if } SR(t) = L_2^S [UF(\tau)]_{\tau = -\infty}^{\tau = t} = L_2^S UF^* \quad (60)$$

where $SR(t) =$ system function $= L_2^S$ when,

$UF(t) = H(t)$ and a response function when

$UF(t) = UF_0 H(t)$.

then,

$$P_s(t) = \int_{0^-}^t SR(t-\tau) \frac{\partial P(\tau)}{\partial \tau} d\tau \quad (61)$$

where $P_s(t) =$ response of system to load $P(t)$, with time configuration different from that of a step load, with $SR(t)$ defined as above whichever is appropriate.

$P_s(t)$ becomes a Characteristic System Function, L_2^{CS} under any mode of loading (repeated, moving, or otherwise), when $SR(t)$ in equation (61) is the same as the System Function $-L_2^S$. There are, therefore, three important functions to be reckoned with when a linear structure is being analyzed - The System Function, The Characteristic System Function and the Response Function.

The repeated-load response of the three layer visco-elastic system investigated in this study was obtained

* L_2^S is an integral operator of the relaxation or creep type.

through the use of equation (61) with

$P_s(t)$ = the repeated load response

$SR(t)$ = the Response Function of the system,

and

$P(t)$ = the time-configuration of the repeated load.

To obtain the Characteristic System Function for the moving load, the same equation was utilized but this time with the following changes,

$P_s(t)$ = the Characteristic System Function,

$SR(t) = L_2^S$ = the System Function, and

$P(t)$ = time configuration of the moving load.

Application to Moving Load Problem

This section illustrates the technique of application of the principle just discussed, towards formulating the solution for the normal deflection at any point in the three-layer linear viscoelastic structure shown in Figure 11.

The analytical expression arrived at for the normal deflection at any point of the three-layer linear elastic half-space that is under a uniformly distributed stationary load is given on the next page.

$$W_e(R, Z, t) = qa \int_0^{\infty} \frac{J_1(mr)}{m} \Psi_e(t, m) dm \quad (62)$$

where $J_1(mr)$ = $J_1(ma)$ = Bessel functions

$\Psi_e(t, m)$ = material property constant of elastic response,

q = intensity of load,

a = radius of the loaded area,

m = dummy variable and,

$W_e(R, Z, t)$ = elastic normal deflection at time t ,
for a point with coordinates R, Z .

The derivation of the above equation was discussed in the earlier parts of this chapter. When the correspondence principle is applied to this elastic solution, a viscoelastic solution for the normal deflection is obtained. In this solution, the viscoelastic response is given by the viscoelastic counterpart, $\Psi_v(t, m)$, of the elastic system response, $\Psi_e(t, m)$. The viscoelastic solution may therefore be written as

$$W_v(R, Z, t) = qa \int_0^{\infty} \frac{J_1(mr)}{m} \Psi_v(t, m) dm \quad (63)$$

* The subscript 'e' and 'v' respectively refer to elastic and viscoelastic response.

where, $q, a \frac{H_1(m)}{m}$ are defined as previously and
 $W_v(R, Z, t)$ = viscoelastic normal deflection at time t , for a point with coordinates R, Z

In this formulation (equation (63)) the variable controlling the response of the system to a step load of unit magnitude is $\psi_v(t, m)$ - the System Function that producing the excitation is $H_1(m)$. The term 'qa' is merely a multiplier. $W_v(R, Z, t)$ is the Response Function of the system. The moving load solution at any point in the system can be obtained by utilizing equation (61) in which $SR(t)$ is now the System Function - $\psi_v(t, m)$.

Moving Load Solution

In equation (63), which is the stationary load solution for the vertical deflection, the step incremental load $H_1(m)$ is the product of two Bessel functions. If the stationary load were to move with a constant velocity V along a straight path on the surface (Figure 11), then the argument R in the function $J_0(mR)$ should become $R-Vt$ where R is the offset distance of the load at zero time. The incremental load exciting the system will now have the form $J_0(m\{R-Vt\}) J_1(ma)$. Since $J_1(ma)$ is a constant and does not enter the integration over the time variables, it can be dropped from the loading function. Therefore the incremental load exciting the system will hereafter be referred to as $J_0(m\{R-Vt\})$ for simplicity.

Using the concept of the response of linear systems to imposed excitations, the characteristic* system function for the moving load $\psi_{m0}(t,m)$ may be obtained from the system function $\psi_v(t,m)$ (due to the stationary load) and the excitation $J_0(m\{R-Vt\})$ as

$$\psi_{m0}(t,m) = \int_{0-}^t \frac{\partial}{\partial \tau} J_0(m\{R-V\tau\}) \psi_v(t-\tau,m) d\tau \quad (64)$$

The vertical deflection (at any point in the system) due to the moving load can then be expressed as:

$$W_M(R,Z,t) = qa \int_0^m \frac{J_1(ma)}{m} \psi_{m0}(t,m) dm \quad (65)$$

an expression which is obtained after making the appropriate substitution in equation (63). The deflection which results from loading the system in the manner described above, is caused by a superposition of effects as shown in Appendix (D). The integral on the right hand side of equation (65) can be numerically evaluated using Simpson's rule. The same approach can be utilized to obtain the other components of the stress tensor and deflection vector at any point in the system.

* Page (84)

Method of Evaluation of Moving Load Solution

There are two steps involved in this method of evaluation:

- a) the integral (64) is first evaluated and,
- b) the results obtained in (a) are later used to evaluate integral (65)

The integral (64) is evaluated using a finite difference method of integration after the system function $\psi_v(t,m)$ has been represented by a series of exponential terms. The reason for this choice of series of exponential terms is the fact that $\psi_v(t,m)$ is either a monotonically increasing or decreasing function of time -- a property also possessed by exponentials. $\psi_v(t,m)$ has this time-behavior because it is a rational function of viscoelastic functions which are themselves monotonically increasing or decreasing in time. Furthermore, an expansion of the type mentioned above has been suggested by Schapery (53) and many others to represent creep and relaxation functions which are similarly monotonically increasing or decreasing functions of time.

The numerical experiments performed in a computer (IBM 360/40) have shown very good agreement between the actual values of $\psi_v(t,m)$ and those calculated using the exponential series

$$\sum_{i=1}^n G_i^m e^{-t\delta_i}$$

representation. The coefficients G_i of this series are determined using the least squares, curve-fit method discussed in Appendix (II) of reference (71) — Tables (AII-1) and (AII-2) and Figures (AII-1) and (AII-2) of Appendix (AII), show the comparison of the results obtained.

The integral (65) is evaluated using Simpson's rule and a parabolic interpolation. The method of parabolic interpolation is described in detail in Reference (71). The $\psi_{m0}(t,m)$ terms are first evaluated for each time t_i for 13 values of m , and an interpolation is performed so as to obtain ninety-one values of the integral expression, for m varying between 0 and $9m$ (and spaced 0.1m apart)*. Each of these ninety-one values is multiplied by the corresponding Bessel term

$$\frac{J_1(ma)}{m}$$

in equation (65) and the integral is evaluated. The result so obtained is a normalized result for the deflection due to a moving load. This is achieved by using a factor H_1 , (i.e., the height of the first layer) to reduce the geometrical variables of the system to dimensionless terms, and dividing the functions $W_M(R,Z,t)$ by a factor of $qH_1D_{CRP_3}$ (in which q and H_1 are defined as previously,

* The values of $\psi_{m0}(t,m)$ from $9m \rightarrow \infty$ were not included since, when the integral expression was evaluated, this portion of integral made a negligible to $W_M(R,Z,t)$.

$D_{CRP_3}^{(\infty)}$ is the magnitude of the creep function of the third layer at infinity). The use of dimensionless parameters greatly reduces the volume of computational work, and simplifies the input to the computer program written to evaluate the integral.

The Repeated Load Solution

The vertical deflection $W_S(R, Z, t)$ obtained from the stationary load is a response function of the system. Since the system is linear, the vertical deflection due to a repeated load $Q(t)$ will be given by

$$W_R(R, Z, t) = \int_{0^-}^t \frac{\partial Q(\tau)}{\partial \tau} W_S(R, Z, t-\tau) d\tau \quad (66)$$

The time configuration used for $Q(t)$ in this study is shown in Figure (12). This usage does not place any restriction on the method, as any other time-configuration can be chosen. The half-sine wave with rest periods was selected largely because of its realistic simulation of the load application on a three-layer viscoelastic pavement structure.

The following definitions apply to Figure 12.

T = time at the beginning or at the end of the repeated load application,

$T(J) = T(J-1) + \text{duration of loading (for } J \text{ (even) i.e., } J = 2, 4, \dots)$

02

$$T(J+1) = T(J-1) + \text{period of loading (for } J \text{ (even))}$$

i.e., $J=2, 4, \dots$)

$Q(t)$ = the time configuration of the exciting force where

$$Q(t) = \begin{cases} \sin \omega t & \text{for } T(J-1) < t < T(J) \\ 0 & \text{for } T(J) < t < T(J+1) \end{cases}$$

Method of Evaluation of Repeated Load Solution

To facilitate computation non-dimensionalized terms are utilized in the computer program that was written to evaluate the integral (66). The function $W_S(R, Z, t)$ is non-dimensionalized by a factor $qH_1D_{CRP_3}(\infty)$, where q is as defined previously, H_1 is the height of the first layer, and $D_{CRP_3}(\infty)$ is the magnitude of creep function of the third layer at infinity. Equation (66) can be written as

$$\begin{aligned}
W'_R(R, Z, t) &= \int_0^t \frac{\partial}{\partial \tau} \sin \omega \tau \frac{W'_S(R, Z, t-\tau) d\tau}{qH_1 D_{CRP_3}(\infty)} \quad (67) \\
&= \int_0^t \omega \cos \omega \tau W'_S(R, Z, t-\tau) d\tau
\end{aligned}$$

where

W'_S = the dimensionless deflection factor due to the stationary load,

W'_R = the dimensionless deflection factor due to the repeated load.

If the function $W'_S(R, Z, t-\tau)$ is approximated by the Dirichet series

$$\sum_{i=1}^n G_i e^{-(t-\tau)\delta_i}$$

using a least squares curve method (71), the G_i 's are the coefficients determined from the set of simultaneous equations which result when the δ_i 's are chosen in a particular way (53). Equation (67) then becomes

$$\begin{aligned}
W'_R(R, Z, t) &= \int_0^t \omega \cos \omega \tau \sum_{i=1}^n G_i e^{-(t-\tau)\delta_i} d\tau \\
&= \sum_{i=1}^n G_i e^{-t\delta_i} \omega \int_0^t \cos \omega \tau e^{\tau\delta_i} d\tau \quad (68)
\end{aligned}$$

The integral $\int_0^t \cos \omega \tau e^{-\tau \delta_i} d\tau$ can be expressed as a sum of integrals. When this is done, equation (68) becomes

$$W'_R(R,Z,t) = \sum_{i=1}^n G_i e^{-t \delta_i} \omega \sum_{j=2}^L \int_{t_{j-1}}^{t_j} \cos \omega \tau e^{-\tau \delta_i} d\tau \quad (69)$$

for j even.

This expression can be evaluated after L repetitions of load at any specified frequency. The same technique is utilized to obtain the solutions of the other stress and displacement variables of the system.

The next chapter discusses the development of the cumulative damage model.

V. THE GENERAL CUMULATIVE DAMAGE THEORY

A cumulative damage theory is developed to account for the progressive deterioration of a pavement system in different failure modes. This theory utilizes the basic concepts presented by Dong (35) in his theory of cumulative damage.

It is assumed that a fixed distribution of weak regions exist within the structure and that damage in the form of cracks, and/or 'plastic' zone formations progresses from each region in the same manner. The theory is therefore deterministic in its approach and if the statistical method is to be used the necessary modifications must be made. The basic assumptions and the mathematical formulation of the general theory are:

1. The materials in the structure and the structure itself are subjected to an arbitrary load history in the form of a stress tensor, a strain tensor, or their derivatives.

In the most general case, all these tensors can be independent functions in the functional responsible for causing damage in the structure. For our discussion, only a simple case is considered, i.e., the functional causing damage is a function of the history of the tensor $(H)_{ij}$ - which can be of the stress or strain type.

2. The materials in the structure are non-aging, and temperature conditions are isothermal.

3. The accumulation of damage and its recovery can be accounted for.

4. The life remaining in the structure has full value at zero history of loading, and no value at failure.

When these assumptions are made, the damage functional may be written in the following form:

$$A_{ij}(S) = F \left[\frac{d}{ds} \textcircled{H}_{ij}(s) \right]_{s=-\infty}^{s=S} \quad (70)$$

where $A_{ij}(S)$ is the concentration or intensity of damage in a given volume, at any 'S',

F is a functional of damage in the form of the derivative of $\textcircled{H}_{ij}(s)$ with respect to 's',

s is the generic value of 'S', and

S is the value of a parameter which represents the unit in which damage is accumulated. (e.g., number of load repetitions, time, etc.). S is non-decreasing with time.

The expression (70) indicates that at any instant 'S', the degree of damage accumulated in the material depends on the rate of change of $\textcircled{H}_{ij}(s)$ with respect to 's' in the interval $-\infty < s < S$.

The functional, F, can be expanded into an infinite series of hereditary integrals as follows:

$$A_{ij}(S) = \int_{-\infty}^S \beta_{ij}(S-s_1) \frac{\partial}{\partial s_1} \mathbb{H}_{ij}(s_1) ds_1 + \int_{-\infty}^S \int_{-\infty}^S \beta_{ijKl}(S-s_1, S-s_2) \frac{\partial}{\partial s_1} \mathbb{H}_{ij}(s_1) \frac{\partial}{\partial s_2} \mathbb{H}_{Kl}(s_2) ds_1 ds_2 + \dots + \dots \quad (71)$$

where β_{ij} and β_{ijKl} are damage kernels.

$\mathbb{H}_{ij}(s_1)$, $\mathbb{H}_{Kl}(s_2)$ are arbitrary histories of the damage tensors.

The above expression can be written in one-dimensional form, for ease of discussion and use, with no loss of generality:

$$A(S) = \int_{-\infty}^S \beta_1(S-s_1) \frac{\partial}{\partial s_1} \mathbb{H}(s_1) ds_1 + \int_{-\infty}^S \int_{-\infty}^S \beta_2(S-s_1, S-s_2) \frac{\partial}{\partial s_1} \mathbb{H}(s_1) \frac{\partial}{\partial s_2} \mathbb{H}(s_2) ds_1 ds_2 + \dots + \dots + \int_{-\infty}^S \dots \int_{-\infty}^S \beta_N(S-s_1, \dots, S-s_N) \frac{\partial}{\partial s_1} \mathbb{H}(s_1), \dots, \frac{\partial}{\partial s_N} \mathbb{H}(s_N) ds_1 \dots ds_N \quad (72)$$

The set of integrals illustrates that a cause C_n applied at any instant S_n modifies the effect produced by a cause C_k applied at an instant S_k , providing $n \leq k$. The contribution of the increment $\partial \mathbb{H}(s_1)$ to the damage - accumulation is given by the damage kernel $\beta_1(S-s_1)$,

that for a combination $\partial \textcircled{H}(s_1) \partial \textcircled{H}(s_2)$ is given by $\beta_2(S-s_2, S-s_2)$ and so on.

$\beta_1 ()$ is a linear damage kernel and is thus independent of the magnitude of $\partial \textcircled{H}(s_1)$, and the manner in which it is applied. When convolved with $\partial \textcircled{H}(s_1)$, however, history-effects are present in the results obtained. The kernel therefore represents physical linearity.

The kernels $\beta_2() \dots \beta_N ()$, are non-linear kernels. They depend on the history of the application of the quantity $\partial \textcircled{H}(s_1) \dots \partial \textcircled{H}(s_n)$. As a result of this, these kernels account for any physical nonlinearity that a material might display under an arbitrary loading history.

The arguments $(S-s_1, S-s_2 \dots S-s_n)$ in the β_i functions, for $i > 1$, are symmetrical with respect to each other; this insures that the equations will be form-invariant with respect to s , and consequently guarantees material symmetry.

Using the damage functional as defined above, the life remaining in a given region of the material or structure at any time for which the independent variable causing the damage has a value $\textcircled{H}(S)$ is given by

$$l_R(S) = L + A(S) \tag{73}$$

where $l_R(S)$ = value of life in a given region of the material at any 'S'.

L = value of life in a given region of the material or structure at zero history of loading.

$A(S)$ = the concentration of damage in a given region at any 'S'

In normalized form we will have

$$l(S) = \frac{L}{L} + \frac{A(S)}{A_f} = 1.0 + \frac{A(S)}{A_f} \quad (74)$$

$l(S)$ = value of life at any S in percent of total life of the structure or material

A_f = maximum concentration of damage in a given volume of the material or structure

Equation (74) indicates that at zero history of loading, the life remaining is one-hundred percent of its full value. At failure, it is zero percent and at any other time between zero history of loading and time of failure life is at some percentage between zero and hundred.

i.e., $l(0) = 1.0$ for $S = 0$, no loading

$l(S_f) = 0.0$ for $S = S_f$, failure

$0.0 < l(S) < 1.0$ for $0 < S < S_f$

Implicit in the use of the damage functional is the fact that a damage curve, a failure curve, a damage surface or a failure surface, each depending on the choice of \mathbb{H} (one-dimensional, two-dimensional, or three-dimensional respectively), is not necessarily unique. Various histories may yield different failure curves or surfaces. Linear and non-linear damage

behavior can be handled. Finally, and most importantly, for a given damage surface or curve, the effect of the sequence of events and prior history can be accounted for. (See equation 80).

The discussion above gives very generally the framework within which the cumulative damage theory has been developed. The manner in which it may be utilized to analyze the failure of pavement systems (as a result of crack formations by repeated loading) is described below.

Determination of H

In Chapter III, pavement systems were broadly classified according to their manner of resisting structural impairment in a given traffic and climatic environment. This approach helped to identify the pertinent stress or strain quantities which can be monitored so as to predict damage progression in each classification.

In a frictional-type pavement, the damage parameter H is associated with shear stresses and shear strains, since cumulative shearing action is responsible for the type of damage that occurs. The magnitude of H at any time is commensurate with a certain percentage of damage concentration in a given volume. Information on this magnitude therefore yields information on the progression of damage.

In a flexural-type pavement, the materials in the layers respond to load application by flexing. Their

performance is therefore dependent on their capability of resisting tensile stresses by flexure. Damage in such pavements propagates in the fatigue-loading mode and (H) is associated with tensile stresses and strains. Here again, the magnitude of the developed stresses and strains is equivalent to a particular concentration of damage. Therefore by monitoring the developed stresses and strains the progression of damage can be predicted.

The third type of pavement is impaired by the destructive cumulative tensile and shear action that is manifested within the layer components. The damage parameter (H) is therefore associated with both tensile and shear actions. In the literature survey of the 'fatigue-behavior' of frictional-flexural pavement, however (H) was shown to be associated only with the tensile strain at the bottom of the surface layer.

In order to develop a damage progression model for different pavement structures, the primary model (discussed in chapter IV), may be utilized to determine the accumulation of the critical stresses and strains which develop within such a facility under a given repeated load application. The damage model can then be used to predict the number of the load repetitions to failure after the appropriate kernel functions (β_i 's) have been determined (see next section for determination of kernels). If the damage accumulation is attributed to the development of shear strains within the structure, then the damage concentration factor

$\left(\frac{A(S)}{A_f}\right)$ yields the size of the 'plastic' - zone within the structure at any instant. If the damage progresses under the action of tensile stresses and strains the damage concentration factor $\left(\frac{A(S)}{A_f}\right)$ is then, equivalent to the crack distribution at any instant.

One important fact to realize here is the flexibility of the damage model as presented. The model can be used to determine the progression of damage within the whole structure if the kernel functions are representative of the damage behavior of the whole pavement structure (i.e., the damage behavior of the individual layers, interact to produce unique β_i -functions which are combinations of the damage kernels for each layer). The same model may also be used to investigate the damage that takes place in each layer, if the appropriate (β_i 's) are used. This capability is an added advantage in that if the surface layer for example is known to exhibit fatigue under loading, the β -functions for fatigue can be determined and the service life on the structure in this mode of response can be predicted. The kernel functions therefore change depending on the mode of failure being investigated, and on the mechanical properties of the materials in the structure.

The Determination of β_i 's

The linear kernel function $\beta_1(s)$ is a curve. The other functions $\beta_1(s_1, s_2 \dots s_i)$ $i > 1$ are surfaces. For example $\beta_2(s_1, s_2)$ is a three-dimensional surface;

$\beta_3(s_1, s_2, s_3)$ is a four-dimensional surface and so on.

The functions $\beta_1, \beta_2, \beta_3$ can be determined by setting up careful experimental loading programs for a pavement structure.

Let us consider for this discussion a frictional-flexural pavement system. This structure may be assumed to have adequate shear support so that the predominating factor of damage propagation is tensile action. In other words, cracks form early within the flexural surface material and propagate to failure in fatigue.

The fatigue properties of the material in the surface must be determined. As discussed in Chapter III, if this material is asphaltic concrete, it can be assumed that the tensile strain at the bottom of the surface layer is the damage determinant and β_1 can be determined as follows: (35)

For the linear portions of the damage theory, the life remaining in the material can be represented as,

$$l(N) = 1 + \int_{-\infty}^N \beta_1(N-\eta) \frac{\partial E_T(\eta)}{\partial \eta} d\eta \quad (75)$$

where $E_T(\eta)$ is the tensile strain as a function of the number of repetitions η or N .

Several loading programs of the constant repeated load type can be conducted on the surface of a pavement structure, using plate loading tests, and the tensile strain developed at the bottom of the surface layer can be measured.

With failure in fatigue defined as the number of repetitions at which the surface deflection exceeds a particular value or as when tension cracks appear on the surface, a curve of E_T vs. N can then be plotted. In other words a fatigue failure curve as shown schematically in Figure 13, can be obtained.

Assuming that this curve is unique for other loading programs, the β_1 - function can be determined for loading programs which are arranged to produce a constant level of sinusoidal strain at the bottom of the structure.

At failure, therefore, for all such loading programs,

$$1(N_f) = 1 + \int_0^{N_f^*} \beta_1 (N_f - \eta) \frac{\partial E_T(\eta)}{\partial \eta} d\eta \quad (76)$$

where N_f is the number of repetitions to failure.

$E_T(\eta) = E_f H(\eta)$, where E_f is the failure strain

and $H(\eta) = 0$ for $\eta < 0$.

1 for $\eta > 0$.

Equation (76) therefore yields at failure,

$$0 = 1 + \beta_1 (N_f) E_f \quad (77)$$

$$\therefore \beta_1(N_f) = - \frac{1}{E_f} \rightarrow \text{Figure 14} \quad (78)$$

*The portion of the integral from $-\infty$ to 0 is assumed to be zero since the structure is undisturbed in this time period.

12

For different values of E_f and N_f a curve of $\beta_1(N)$ can be traced. The kernel function is therefore the negative inverse of the failure curve. The sequence of events can be handled for all other types of strain which develop at the bottom of the structure. Figure 15 contains some hypothetical strain history programs.

For program 1,

$$E_T(N) = E_1 H(N) + E_2 \left[H(N-N_1) - H(N-N_2) \right] \quad (79)$$

and the life remaining in the structure at any number of load repetitions, N , is given by

$$l(N) = \beta_1(N)E_1 + E_2 \left[\beta_1(N-N_1) - \beta_2(N-N_2) \right] \quad (80)$$

and for program 2,

$$E_T(N) = (E_1 + E_2)H(N) - E_2 H(N-N_1) \quad (81)$$

and,

$$l(N) = \beta_1(N)(E_1 + E_2) - \beta_1(N-N_1)E_2 \quad (82)$$

The two results are obviously not the same at any N indicating the importance of the order of the application of the load.

The Determination of β_2

It was mentioned before that the kernel functions β_i () for $i > 1$ are symmetrical with respect to their

arguments; with this provision, the surface β_2 in Figure 16, is symmetrical about a vertical plane bisecting the positive s_1 and s_2 axes. In order to determine the shape of the surface for any material or structure, only that portion which is on one side of the vertical bisecting plane is needed. An experiment should therefore be devised to create loading paths 1 and 2 as shown in figure Path 1 will yield the curve $\beta_2(s_1, s_2)$ for any arbitrary but equal values of s_1 and s_2 , and path 2 will yield the curve $\beta_2(s_1 - s'_1, s_2)$ for any value of s_2 and arbitrarily fixed values of s'_1 . The whole surface can therefore be evaluated for arbitrary values of s'_1 , in the function $\beta_2(s_1 - s'_1, s_2)$. The four dimensional hypersurface β_3 can be evaluated using the same technique if $\beta_3(s_1 - s'_1, s'_2, s_3)$ is evaluated for arbitrary values of s'_1 and s'_2 (35).

If the fatigue damage behavior can be described by the expression given below,

$$\frac{A(N)}{A_f} = \int_0^N \beta_1(N - N_1) \frac{\partial}{\partial N_1} \textcircled{H} (N_1) dN_1 + \int_0^N \int_0^N \beta_2(N - N_1, N - N_2) \frac{\partial}{\partial N_1} \textcircled{H} (N_1) \frac{\partial}{\partial N_2} \textcircled{H} (N_2) dN_1 dN_2 \quad (83)$$

where $\frac{A(N)}{A_f}$ = the damage concentration factor
 N = the number of load repetitions

then the curve β_1 and the surface β_2 can be determined by using the damage determinant \textcircled{H} in the following manner:

If the following histories of the \textcircled{H} are considered,

$$\textcircled{H}_1(N) = K_1 H(N) \quad (84)$$

$$\textcircled{H}_2(N) = K_2 H(N) \quad (85)$$

at failure, when they are individually substituted into equation (83), they give:

$$1.0 = K_1 \beta_1(N_{f_1}) + K_1^2 \beta_2(N_{f_1}, N_{f_1}) \text{ for equation (84) - (86)}$$

and

$$1.0 = K_2 \beta_1(N_{f_2}) + K_2^2 \beta_2(N_{f_2}, N_{f_2}) \text{ for equation (85) - (87)}$$

with N_{f_1} or 2 = number of repetitions at failure.

By performing such experiments for different values of K_1 and K_2 and knowing β_1 () from the previous section, the curve $\beta_2(N, N)$ can be determined for any N . If in figure 16 we replace s_1 and s_2 by N_1 and N_2 then $\beta_2(N_1, N_2)$ is the curve traced on the surface by the vertical bisecting plane of the positive N_1 and N_2 axes.

To determine the rest of the surface $\beta_2(N_2, N_1 - N_1')$, another experiment has to be performed with the following

\textcircled{H} history.

$$\textcircled{H}(N) = K_3 H(N) + K_4 H(N - N_1) \quad (88)$$

* $H(N)$ = Heaviside step function, K_1 and K_2 are constants.

** K_3, K_4 are constants.

when this history is substituted into equation (83) the following expression is obtained at failure.

$$\begin{aligned}
1.0 = & K_3\beta_1(N_f) + K_4\beta_1(N_f-N_1) + K_3^2\beta_2(N_f,N_f) \\
& + 2K_3K_4\beta_2(N_f,N_f-N_1) + K_4^2\beta_2(N_f-N_1,N_f-N_1) \quad (89)
\end{aligned}$$

In the above equation every β -value, except $\beta_2(N_f,N_f-N_1)$ is known. Therefore, the performance of several experiments with \textcircled{H} - histories like that in equation (88) should yield the curves $\beta_2(N, N-N_1)$ for any arbitrary N_1 .

The above process is tedious and becomes cumbersome as the 'i' in $\beta_i()$ increases. To use the non-linear theory with many terms, therefore, becomes very difficult. However, approximations can be made to reduce the number of terms in order to make possible the conduction of a reasonable number of experiments depending on the domain of interest and the range of load magnitudes applied on the material or structure.

Comments on the Determination of β_1 and β_2 .

In the above two sections, only failure conditions have been utilized to determine the kernel functions β_1 and β_2 . However, a more logical procedure would be one in which the damage behavior of the material or structure in question can be identified from its conception to its final destructive stage, so that β_1 and β_2 may be

determined more directly. In this manner, the parameter responsible for damage is closely monitored with the number of load repetitions in a specially prepared specimen until failure occurs. During the conduction of the experiment, the compliance of the specimen can be related to the crack length at each number of load repetition. This may be done for several loading rates and the compliance versus crack length curve plotted. From this latter curve the crack length at any instant for any of several loading programs can be predicted by measuring the compliance of the specimen at each load repetition.

Such a technique can be utilized to measure the fatigue properties of the material in the surface layer of the pavement, by utilizing a specially prepared beam specimen. A plot of the ratio of the crack length $C(N)$ at any instant to the final, crack length $C_f - \left[\frac{C(N)}{C_f} \right] -$ versus the number of load repetitions N - will then represent the damage curve $\frac{A(N)}{A_f}$, for each loading program.

Using the equations (86) to (89) with $\frac{A(N)}{A_f}$ inserted for the value of unity on the left hand side of the equations, and N for N_f on the right hand side, β_2 can be calculated easily.

The experimental information necessary for the calculation of the non-linear damage Kernel β_2 using any of the suggested approaches is not available at the present time (1969). To obtain such information it is necessary to conduct a very large number of experiments as indicated above

100

with carefully selected loading programs. In the absence of such information use is made of what is now available to obtain the linear damage kernel β_1 for a pavement structure. The damage behavior is predicted as a first approximation using the failure curve in the manner previously discussed. An example of the use of such an approach is presented in the next chapter.

VI - APPLICATIONS OF DEVELOPED MODELS

Introduction

In the previous sections, two models were developed to account for the primary and ultimate response behaviors of pavement structures. The primary response model describes the behavior of the physical system when it is subjected to load inputs under isothermal conditions. The system responses or output functions obtained from the primary model are measurable quantities such as the developed deformations and stresses. When these primary responses attain a limiting value, distress in the form of rupture, disintegration or distortion occurs. The system performance can therefore be estimated by monitoring (over time) the values of the output functions in terms of the number of load applications.

The second model which has been called the cumulative damage model establishes the link between the primary and ultimate responses of the pavement structure. This model relates the level of the developed deformations and stresses to the internal damage concentration in a given volume. By identifying or monitoring the manner in which the internal damage develops, the amount of life remaining in the structure after a given number of load repetitions can be predicted. The damage model therefore not only describes the performance of the structure under load, but also

yields information about the limiting value of a critical output function or functions causing the type of distress investigated.

In order to be representative of a pavement structure, the primary model must be able to account for the observed pavement performance in terms of significant pavement parameters. These parameters may be grouped under three separate headings: a) the mechanical properties of the materials in the layers b) the loading characteristics and c) the geometric parameters.

Within such a framework, under heading a) the quality of each layer and that of the combination of layers are important. Equally important, are the trade-offs between the quality and the thickness of the layers.

Under heading (b), the pertinent parameters are the magnitude of the load, its duration, (static, repeated or moving), and the frequency of the repetition.

Under heading c), the thickness of each layer, the offset distance of the load, the location of the point of interest, and relation between the thickness of the layers, are all known to be significant in determining the system response.

The following presentation is therefore divided into three broad sections. A discussion is first presented on the dimensionless system parameters, which describe the pavement system. Then the capabilities of the primary model are discussed with the aid of several pavement structures.

Finally, an illustration of the use of the cumulative damage model to predict the fatigue-failure of a flexural-frictional pavement system is presented.

1. Dimensionless System Parameters:

A dimensionless system is defined as a three layer pavement structure with a given set of material properties in each layer (Figure 17). For the examples presented each layer is assumed to be incompressible -- i.e., Poisson's ratio = 0.5. The material in each layer is represented by a dimensionless creep function of the types shown in Figures 17 through 21. As shown in these figures, when a layer is elastic, its creep function does not vary with time.

For ease of computation and use, the normalising factor for the creep function of all the systems is the value of the creep function for the third layer at infinite time. This means that if the third layer is elastic, its dimensionless creep function has a value equal to unity. If it is viscoelastic, its asymptotic value is unity. Each of these functions has been approximated by a Dirichlet

series
$$\sum_{i=1}^n A_i e^{-t\alpha_i}$$
 where the α_i 's are fixed and

A_i 's are determined using a least squares curvefit method described in (71). This type of representation has been chosen because most of the available published data on the properties of the paving materials are presented in and are easily convertible to the creep form.

All the components of the stress tensor at any point in the three-layer pavement system are expressed in terms

105

of the intensity of the load. For the components of the displacement vector, the normalising factor is the product of the intensity of the load q , the creep function of the third layer at infinity $D_3(\infty)$, and the height of the first layer H_1 .

The geometric variables considered are: the offset distance of the load R , the height of the first and second layers, H_1 , and H_2 respectively, the depth of interest Z , and the radius of the loaded area A -- all of which are represented in dimensionless forms in terms of the height of the first layer H_1 -- See Figure 17.

In addition all times are dimensionless and are expressed in terms of an arbitrary time factor. The variables representing the period and the duration of the loading are also dimensionless. In all the examples presented the arbitrary time factor is equal to ten.

The use of dimensionless terms is desirable because it greatly facilitates the computation and execution time of the computer programs written to determine the developed stresses and displacements.

2. The Primary Response Model

The response of the primary model is discussed in two sections: First, the influence of the mechanical properties of the layers on the system response of various pavement systems is discussed. Second, the influence of the loading and geometric variables on the response of two pavement systems are considered.

The Mechanical Properties of the Layer-Materials

In this section five different systems were selected to investigate the effect of the mechanical properties of the materials used in each layer on the response of the pavement. The material in each layer is assumed to be linear, homogeneous and isotropic.

System No. 1 is composed of completely elastic materials (Figure 18). System No. 2 is completely viscoelastic (Figure 17). Layer one in System No. 3 is assumed to be viscoelastic and the second and third layers are considered elastic (Figure 19). System No. 4 is assumed to be partially viscoelastic by considering that only the third layer is viscoelastic (Figure 20). Finally, System No. 5 is assumed to be similar to System No. 3 but with the spectrum of the creep function of the first layer shifted to the left in one case and to the right in the other (Figure 21), to permit the determination of the influence of viscoelastic properties on the pavement response.

System No. 2 (Figure 17) is used as the basis for comparison. In this system each layer is viscoelastic and the creep compliance function of each layer has the same value at infinite time. This provision serves as a check on the results of the static loading condition. At very large times, the creep functions of the three layers have the same value; the system acts as a homogeneous elastic half-space and Boussinesq's elastic solution should thus be obtained.

The creep functions in each layer of System No. 1 correspond to the values of the creep functions in the corresponding layers of System No. 2 at zero time in non-dimensionalized form. However, when they are translated into dimensionless creep functions, the initial values for System No. 1 no longer coincide with those for System No. 2. The creep functions for dimensionless System No. 3 are obtained by using the same technique, but this time the first layer of System No. 2 is kept viscoelastic. System No. 4 is obtained from System No. 3 by performing shifts in the spectrum of the creep function as was previously mentioned.

In dimensionless form, therefore, Systems 2 and 4 have the same initial values for the creep functions of the materials in their layers. Systems 1, 3 and 5 also have the same initial values for the creep functions of the materials in their layers.

Before presenting the results in detail the effect of the time-temperature superposition is briefly discussed. This principle states that short time effects obtainable at high temperatures are convertible by superposition on the time scale to long time effects at a fixed lower temperature (79). This implies that though the creep functions for the viscoelastic layers in the systems considered in this study are presented for a fixed temperature over a broad range of time, the spectrum of temperatures encountered in the field are, however, represented. Therefore results obtained at a

108
given time and a fixed temperature can be transferred through the use of a shift factor, to results at other temperatures (79). The analysis therefore considers temperature effects implicitly.

The output functions or system responses utilised to investigate the influence of the mechanical properties of the layer materials are the vertical deflection, the vertical stress and the shear stress developed at the first interface -- that between layer 1 and layer 2 -- for System Nos. 1, 2, 3, 4 and 5 under the application of a stationary load.

The results of the stationary load are used for most of the discussion because the repeated and moving load solutions are obtainable from the stationary load response by the superposition principle. Consequently, any effect observed for the stationary load as far as the material variables are concerned must also be observed in a general form for the repeated and moving loads.

Since conditions on the axis of the load are usually the most severe the offset distance factor for the vertical stress and vertical deflection are set equal to zero and that for the shear stress is set equal to one because the shear stress on the axis of the load is zero. Conditions on the first interface are used for discussion because at the surface the shear stress factor is zero and the vertical stress factor is unity under the load and zero elsewhere.

Vertical Deflection:

Figure 22 presents the vertical deflection under the center of the loaded area on the first interface for Systems 1 through 4. It can be noted from this figure that when the system is elastic, the response -- vertical deflection -- does not vary with time. It was mentioned before that the zero time value of the creep functions for System 1 and 3 are the same; therefore at zero time (not shown because of the logarithm scale) the two systems undergo the same magnitude of deflection. However, as the load is maintained, System 3 continues to deflect due to the viscoelastic characteristics of its top layer. This indicates that the stiffer the surface material, the lesser would be the deflections of the pavement.

Systems 2 and 4 have the same initial values of deflection. System 2, however, accumulates more deflection than System 4. The reason for this is that the upper two layers of System 4 are considerably stiffer than those of System 2. Since the third layers of both systems possess the same mechanical properties, the discrepancy in results must be due to the uppermost layers, which supports Burmister's conclusion that when better quality materials are used in the base and surface course of the pavement, the pavement provides a blanket effect around the subgrade.

All the systems shown in Figure 22 are elastic at long times with System 4 displaying the least deflection and System 2 the greatest. In terms of stiffness, at long

times, System 2 is the weakest of all the systems and, therefore, deflects the most. Since Systems 2 and 3 are later used to investigate the influence of the loading conditions and geometric variables on the mechanical response, it will be worthwhile to examine them more closely at the present time.

For very small values of time, System 2 is stiffer than System 3. Therefore, at short loading times the deflection for System 2 is less than that for System 3 when loads of the same magnitude are used. With the passage of time, however, System 2 becomes less stiff when compared to System 3. From the shape of the deflection curves, this occurs at dimensionless time of approximately one. When this event occurs, the deflection on the first interface of System 2 exceeds that of System 3 and continues to do so until it reaches a plateau.

For the stress (Figure 26), however, System 3 consistently displays higher values of developed stresses than System 2 except at very short times where the stresses of System 2 are greater than those for System 3 (not shown in figure). The reason for this behavior is that the two lower layers of System 3 are elastic and have stiffness values which do not change with time. The stresses developed on the first interface of System 3 increase considerably with time because of the rigidity of the bottom two layers. The lower layers of System 2 offer no such resistance; therefore, the stresses developed are not as

great as those for System 3.

Figure 23 illustrates that the spectrum of the creep function has a significant influence on the system response. The curves presented are for the vertical deflection factor of Systems 3 and 5 on the first interface, and under the center of the loaded area.

The creep functions of the two different first layers assumed for the System 5 have the same initial and final values as the creep function of the first layer of System 3 (Figures 19 and 21), but their time dependent behavior is not the same. Curve A of System 5 is obtained by shifting the creep function of the first layer of System 3 to the left, while Curve B is obtained by shifting the creep function in layer 3 to the right. The vertical deflection factors obtained for these curves also have followed similar shiftings as shown in Figure 23. This indicates that by adjusting the mechanical properties of the materials in the first layer, keeping those in the lower layers fixed, the system response can be controlled. This demonstrates that in the selection of asphaltic mixtures for the surface course of a pavement one should be concerned with the form of the creep function over large time intervals rather than relying upon the initial or an arbitrarily selected time value of the creep function. If for instance minimal deflections are desirable during the transient response period, the vertical deflection curve for System 5 - curve B would seem appropriate and the paving material should be

designed in such a manner that a rather flat spectrum of retardation time functions would result.

Vertical Stress:

Figure 26, shows the curves obtained for the vertical stress factor on the first interface for Systems 1, 2, 3 and 4 (Figures 17 through 20). The stresses similar to vertical deflection start with the same initial values for Systems 2 and 4, and for Systems 1 and 3.

However, while the stress on the first interface of System 2 (Figure 19) increases with time that on the System 4 (Figure 20) decreases. This may be due to the fact that the stiffness of the upper two layers of System 4, remain fixed while that of the lower layer decreases with time. The overall effect is to cause a decrease in the stresses on the first interface. For elastic System 1, the stresses remain constant with time as expected.

In Figure 26, the stresses developed on the first interface of System 3 exceed those of System 2. This is not surprising, for reasons depending on the differences of the mechanical properties in the layers of both systems. These reasons have been previously discussed. The influence of the spectrum of the creep function on the vertical stresses developed in the first interface are shown in Figure 27 for System 5. As is noted in this figure, the pattern is similar to that of variations of deflection with the creep spectrum.

Shear Stress:

Figure 28 shows the effect of the mechanical properties of the layer-materials on the shear stress developed on the first interface directly under the edge of the loaded area. The effect is almost similar to that for vertical stress except for System 4, for which the shear stress slightly increases with time while the normal stress showed a slight decrease. The reason for this may be due to the fact that the deflection on the interface under the axis of the load is increasing, causing an increase in the curvature of the interface. This would definitely cause an increase in the shear stress because such stresses, as Burmister shows, are deflection dependent (80). Figure 29 shows the shear stress developed at the interface for the two creep functions assumed for System 5. As can be seen, the spectrum of the creep function has the same effect on shear stress as it did on the vertical stress.

In order to demonstrate the capability of the primary response model in determining the radial stress and radial deflection, typical curves for these components are presented in Figure 24 and 25 for the first interface of System 2.

The results obtained thus far indicate that the nature of the system response depends upon the mechanical characteristics of the materials in the layers. The interaction between the material properties of each layer pro-

duces what may be called a system function which is not only a function of the location of the point of interest, but of the kind of the response function being investigated (i.e. a stress or a deformation output.)

Loading Conditions:

Only three system responses -- the vertical stress, the vertical deflection and occasionally the shear stress -- will be used to investigate the effect of the loading conditions and geometric variables. The results for other components of stress and displacement are not presented in order to avoid the lack of clarity associated with the handling of numerous variables. What is presented is a clear illustration of what the model is capable of doing using the components of stress and displacements that are frequently discussed in the pavement literature.

The stationary loading condition: For the stationary loading condition, the magnitudes of the components of the stress and displacement factors generally increase with the increase in dimensionless time for all systems, as shown in Figures 22, 26 and 28 for vertical deflection, vertical stress, and shear stress respectively.

It is interesting to note that for both Systems 2 and 3, the magnitude of all the three responses tend towards an asymptotic value at a value of dimensionless time corresponding to that when the dimensionless creep compliance functions become asymptotic. The system response therefore depends on the response characteristics of the layer materials. The extensive variation in stress and deformation with time under the constant load for both systems, is

a marked contrast to the constant distribution (of these quantities) exhibited by a structure with elastic properties. This phenomenon may have an important influence in the design of such structures. The rational design of the structural components (especially those exhibiting viscoelastic response) should, therefore, utilize the complete history of the stress and displacement distribution, rather than a single value of these components.

At values of dimensionless time greater than one thousand, the magnitudes of the stress and displacements components are equal to those obtained when the system behavior is elastic i.e., the mechanical properties of the materials in the layers are equivalent to those of the given creep functions at infinity.

This capability serves as a check on the validity of the viscoelastic representations, since the results thus obtained are comparable to those acquired by other authors for elastic systems having the appropriate properties. The model can therefore account for the manner of variation of all the pertinent stress and deflection factors at any point in three-layer pavement structure for this boundary condition.

The repeated loading condition: For this loading condition, the influence of the duration and period of the loading on the response of Systems 2 and 3 was investigated using the vertical deflection on the surface directly under the center of the loaded area, the vertical stress on the first inter-

face but with offset distance factor equal to one.

The stress on the first interface was selected because on the surface the value is unity and repeated applications of the load do not cause accumulations. At the first interface, however, the stress develops with time, as already observed, under a constant load condition.

The shear stress on the first interface at the offset distance factor of unity was chosen because the magnitude of shear stress under the load is zero.

A load repetition is considered to be completed at the end of the period of the loading (see Figure 12) and the magnitude of the stress or deflection factor is measured at this time. The results which are presented for a dimensionless period of 0.05 and durations of the loading equal to .005, .01 and .02 can be noted in Figures 30 through 32; the stress and deflection factors of the systems increase with increasing number of load repetitions.

Figure 30 shows the results obtained for the vertical deflection on the surface. The magnitudes of the deflection factor for System 3 are consistently lower than those for System 2. This indicates that System 2 behaves more viscously; a result which is evident from the dimensionless creep compliance functions for this system (Figure 17). The reason for this difference was discussed in the section on the influence of the mechanical properties of the layer materials on the response of the system.

Figures 31 and 32 show the curves obtained for the

vertical stress and shear stress factors on the first interface. The stresses developed in System 3 are consistently higher than for System 2. This is because of the fact that for the same load the system that is more stiff will develop the greater stresses for the same value of deflection. An examination of the creep functions for System 2 and 3 in Figures 17 and 19 respectively shows System 3 to be more stiff.

For each system, the greater the duration of the loading the greater is the developed stress or deflection factor. This indicates that the severity of the structural response is directly related to the duration of the loading. The longer the load remains on the system, the greater is the damaging effect.

The moving-load boundary condition: Figures 33 through 36 illustrate the manner in which the Systems 2 and 3 respond to the application of a moving load travelling with a constant velocity along a straight line on the surface (See Figure 11). The curves in Figures 33, 34, 35 are for the vertical deflection on the surface. The vertical stress and the shear stress on the first interface are shown in Figures 36 and 37 respectively.

The curves indicate that the system response in terms of stress and deflection factors is not symmetrical with respect to time. The viscoelastic behavior of the systems is

such that there is a time-lag between the observance of a response and the time of application of the agent causing it. Therefore, at the time when the load is directly over the point of interest, the magnitudes of the response in terms of stress and deflection factors are not at the maximum. In addition, it must be noted that the maximum value of either a stress or deflection factor is obtained not before but after the load has passed over the point. However, when all the layers in the system are elastic, no such lag effects are observed, as shown in Figure 34. This figure presents the results obtained for dimensionless System 2 which is converted into a homogeneous elastic system with the creep properties of all the layers being equal to that of the viscoelastic system at infinity.

This technique in fact serves as a check on the moving load analysis, because its elastic solutions should match those obtained from the stationary load-analysis at the pertinent offset distances. The degree of agreement between the solutions obtained through both methods of analysis is seen to be satisfactory. In order to ensure the accuracy of these solutions, they were rechecked using the homogeneous half space solutions of Alvin and Ulery (46). The results compared well with the tabulated values. The observed time-lag in the viscoelastic responses is also velocity dependent. The greater the velocity of the moving load, the smaller the time lag. This

velocity dependence is discussed using the solutions obtained for the vertical deflection of Systems 2 and 3. Figure 33 shows the curves so obtained for the vertical deflection of System 2. It is seen that the peak deflection of the system increases with decreasing velocity factors, indicating that the longer the load remains within the region of influence the greater is the damaging effect that it has on a point of interest within the structure. It is also interesting to note that the lag in response time increases with decreasing velocity factors for the same reasons as above.

The same behavior is displayed by System 3. Figure 35 is presented to show the difference between the magnitudes of the response for both systems. As observed before, the deflection for System 3 attains a maximum value lower than those for System 2. This is so because System 3 is stiffer than System 2.

The results obtained for the vertical stress and shear stress factors on the first interface of System 2 and 3 also show a consistent behavior as indicated in Figures 36 and 37 respectively. In the case of the shear stress factor, however, there are two peaks in the curve. This indicates that as the load approaches the point the shear stress builds up to some limiting value and starts to decrease. At the time when the load is directly over the point, the shear stress is zero. However, the superposition of effects from previous loads actually prevent the total

shear stress from going to zero. The effect of the decrease is to cause a marked reduction in the shear stress. As this load moves away from the point, the shear stress builds up again to a maximum peak and decreases.

The Geometric Variables

The Height Factor of the Second Layer: The influence of this variable on the system response is investigated using the vertical deflection factor on the surface of Systems 2 and 3 when they are subjected to repeated loading. The surface vertical deflection factor is selected over the deflection or stress in any other location so as to obtain a better indication of the influence of this variable on the response of the system.

Figure 38 illustrates that for both systems the deflection increases with the number of repetitions for a fixed value of the height factor. The deflection factors for a given number of repetitions, however, decrease with increasing H_2/H_1 indicating that the thicker the system, the lower are the deflections. An alternative method of lowering surface deflection as has been discussed already is to have stiffer materials in the layers.

The dependence of the surface vertical deflection factor on the height factor of the second layer is more marked for System 3 than for System 2. For System 3, this marked dependence is displayed at every load repeti-

tion. At lower numbers of load repetition, the dependence is pronounced. At higher levels, it is absent. This is not surprising when the mechanical properties of System 2 are taken into account (Figure 17). Since all the creep functions tend toward the same value at long times, one would expect the system to become homogeneous eventually. When this occurs, the deflection at the surface is independent of H_2/H_1 because the system is a semi-infinite homogeneous mass.

The Depth Factor: The influence of this factor is investigated using the vertical deflection and vertical stress factors under the center of the loaded area. The shear stress factor is investigated at the first interface but at an offset distance factor equal to one. The curves so obtained for both Systems 2 and 3 are shown in Figures 39 through 41.

There is a marked reduction in vertical deflection through the layers as shown in Figure 39. The reduction is greater as the number of load repetitions increase. For points within the third layer, an increase in the number of repetitions does not cause significant increase in the deflection. However, this effect is more severe for points that are nearer to the point of load application. Figures 40 and 41 show that a similar effect is displayed in the case of the vertical and shear stress factors.

In Figure 41, for the shear stress factor, it is shown that the first interface of both systems undergo a more severe damaging effect than the second interface.

The radius factor: The effect of this variable was investigated using the vertical deflection factor on the first

interface directly underneath the load. The curves generally indicate that as the radius of the loaded area is increased, the deflection is accordingly increased. Again System 2 deflects more than System 3 for reasons previously discussed.

The damaging effect on the first interface increases considerably with the increase in the size of the loaded area confirming the rather obvious result that for a given period and duration of loading heavier loads do more damage than lighter ones.

The offset distance factor: Figure 43 indicates that the surface deflection factor decreases with increasing offset distance for both Systems 2 and 3. This result is what is expected because the effect of the applied load is more severe near the point of interest. Figure 44 illustrates that the vertical stress factor on the first interface displays a similar behavior.

Permanent deformation: The preceding discussion has served to emphasize the fact that the physical characteristics of the pavement system include among other things geometric measurements such as thickness, arrangement of the component layers and the basic properties which characterize material behavior. The system response consequently involves the behavior of the physical structure when it is subjected to load and climatic inputs. When these act on the system a condition which describes the mechanical state results. Measurable quantities such

as the deformation and stress are then acquired. These quantities have been used in this dissertation to represent the primary responses of the system as described by the Hudson et al chart (Figure 1.0). When they attain a limiting value, distress in the form of rupture, distortion, or disintegration occurs in the ultimate response mode.

One such form of distress is the permanent deformation which results from the shear displacements of a roadway structure. This deformation can be estimated using curves like those presented in Figure 43. Using this procedure, the potential for rutting type distress can be investigated for different systems under different loading conditions.

3. The Damage Model

The limiting response of a pavement structure has been described conceptually as a function of the degree of cracking, distortion and disintegration (Chapter I). Through the use of a mechanistic model such as the primary response model, the distress function can be expressed as continuously increasing with time until a limiting performance criterion is attained. When this level is reached then the failure of the roadway structure will be said to have occurred. For this study, distress in the form of fatigue is investigated.

In order to use the damage theory, the following steps are taken.

1. The temporal variation of the tensile strain on the underside of the surface layer of the selected three-layer pavement structure is determined by utilising the mechanistic model discussed in the previous section.
2. The tensile strain function $E_T(N)$ so obtained from the above step, is inserted into the damage equation:

$$\frac{A(N)}{A_f} = \int_0^N \beta_1(N-\eta) \frac{\partial E_T}{\partial \eta}(\eta) d\eta$$

3. The above integral is evaluated for any N , and the life used or remaining in the structure is predicted using equation (75). When $l(N) = 0$, the surface of the facility will have a given distribution of cracks, and failure in fatigue will have resulted.

Performance criterion: The performance criterion utilised in this case is a phenomenological factor which describes how well the pavement is accomplishing its objective of resisting the impairment that results from fatigue action. The study makes use of a damage concentration factor, $A(N)/A_f$, (e.g., distribution of cracks in a given volume) and a life factor $l(N)$, all of which are related to the level of tensile strain at a critical point of the structure. The distress function $A(N)/A_f$ yields at any instant

of time the degree of damage that has been caused by the formation of fatigue cracks due to a particular number of load repetitions. From this information, one can predict how well the structure is performing by estimating the remaining life, using the equation given below

$$l(N) = 1 + A(N)/A_f$$

Failure Criterion: The failure criterion of the structure may be designated as a point on the distress curve.

When the distress function exceeds a set value defined by this point, failure is said to have occurred. As far as the damage theory is concerned, limiting distress has occurred when $l(N) = 0.0$ or $A(N)/A_f = -1.0$ in equation 91.

The fatigue curve of the surface layer is assumed to be that utilised by Monismith et al (68) for MORRO Bay pavement. The failure curve in fatigue is given by the expression

$$N_f = 8.78 \times 10^{-11} \left(\frac{1}{E_T} \right)^{4.46} \quad (92)$$

where N_f = number of repetitions at failure E_T = tensile strain at failure. From the previous discussion on the determination of the linear damage kernel β_1 , the following expression is obtained for β_1 :

$$\beta_1(N) = - \left(\frac{10^{11}}{8.78} \right)^{1/4.46} (N)^{1/4.46} \quad (93)$$

The plotted curve is shown in Figure 46..

127

The foregoing techniques were utilised in the dimensionless System 6 (Figure 45) (whose creep functions are obtained from AASHO road test results (81)) to predict the occurrence of distress in the surface layer when the structure is subjected to repeated loading of the type shown in Figure 12. The surface layer is composed of asphaltic concrete, the second layer has gravel, the third layer clay.

The tensile strain obtained when this is done is shown in Figure 47. The function was calculated using the following formula:

$$E_T = \frac{\partial U_R}{\partial R} \quad \text{where}$$

E_T = tensile strain

U_R = radial deflection

R = cylindrical coordinate

Several plots of radial deflection factor versus the number of load repetitions were obtained for points within the vicinity of the point of interest. For this example, four points were chosen at $R/H_2 = 0.05, 0.10, 0.15, 0.20$. A curve is drawn for radial deflection factor versus offset distance factor for each load repetition. The shapes of these curves at $R = 0.1$ yield a curve for the tensile strain as a function of the number of load repetitions.

Figure 48 illustrates the manner in which damage progresses when the duration of the applied load is one-tenth of the period. Failure does not occur until 10^{15} repetitions of the load. This value is extrapolated with the assumption that the rate of damage growth is constant after 10^7 repetitions because of the space and time limitations on the computer. Failure will occur sooner if the assumption is unwarranted.

To find out what will happen if large strains were to develop, a tensile strain function with strain magnitudes of the order of one to six percent was assumed (Figure 49). For such a development of strains, failure occurs at approximately ten thousand repetitions of the load (Figure 50), indicating that the level of strain determines the number of load repetitions that the structure can withstand.

This example though simple serves to illustrate the basic ideas of the cumulative damage model. The analysis can be done for complicated load applications by using the principles of the response of linear systems to imposed excitations. It is conceivable that packaged computer programs for different configurations of load applications can be written and the response of the system to such loads evaluated. The main aim here, however, is to show how the linear damage model may be utilised. As

129

has been illustrated, this method of approach yields not only the number of repetitions to failure but the manner in which that number is attained. The results indicate that the degree of internal damage and rate of growth at any instant depend on the characteristics of the applied load for given material properties. If the layer materials should change, different results will be obtained. As is indicated in the section on the primary model, a stiffer material will produce lesser deflections and strains. In addition, the height of the layers could be increased to produce the same effect. Therefore, the optimum combination which may be utilised to sustain the imposed loads may be obtained by a trial and error method of approach.

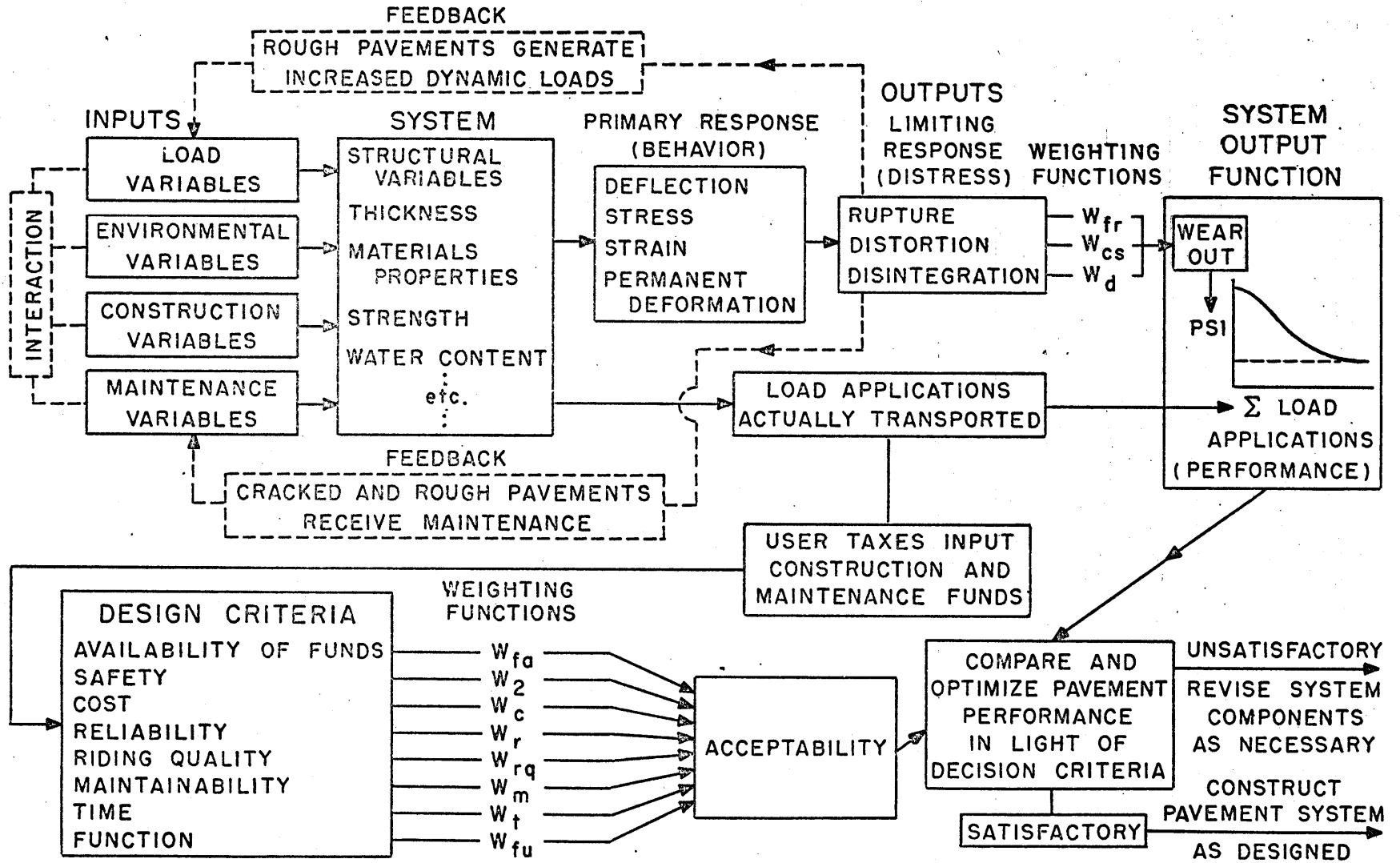


FIGURE I. BLOCK DIAGRAM OF THE PAVEMENT SYSTEM (AFTER HUDSON, ET AL).

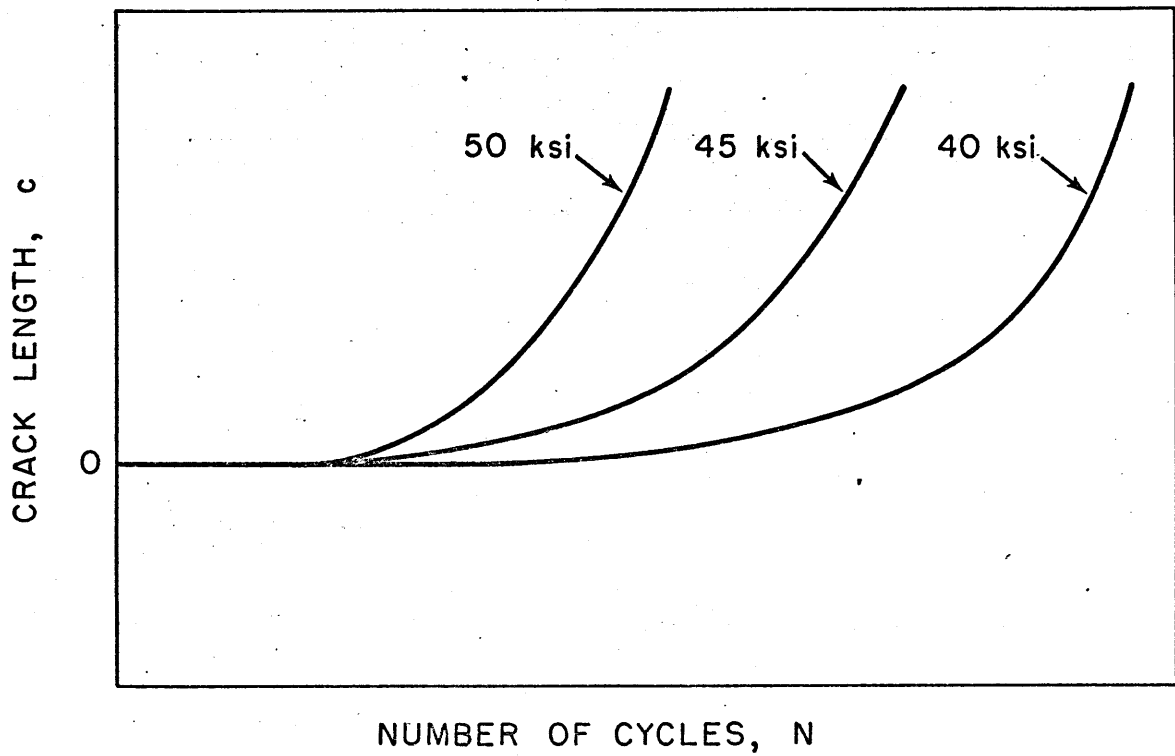


FIGURE 2. CRACK LENGTH vs. NUMBER OF CYCLES OF LOAD, AFTER DEFOREST ON SAE 1020 STEEL SPECIMENS.

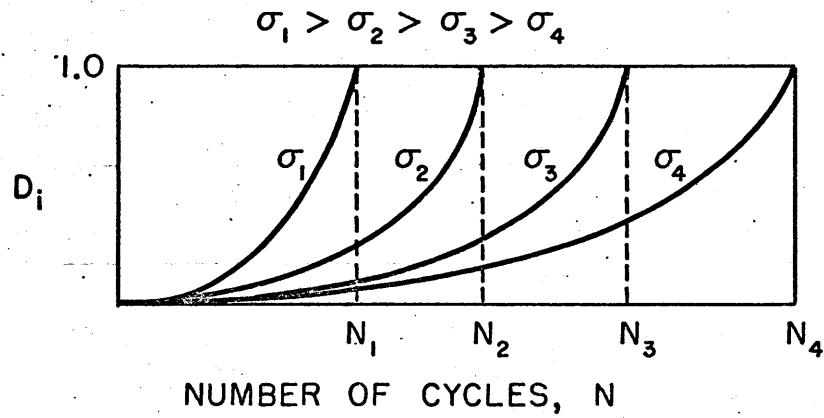


FIGURE 3. DAMAGE vs. NUMBER OF LOAD CYCLES FOR DIFFERENT CONSTANT STRESS LEVELS.

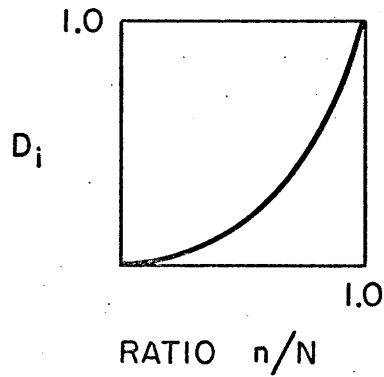


FIGURE 4. INTERACTION FREE DAMAGE LAW.

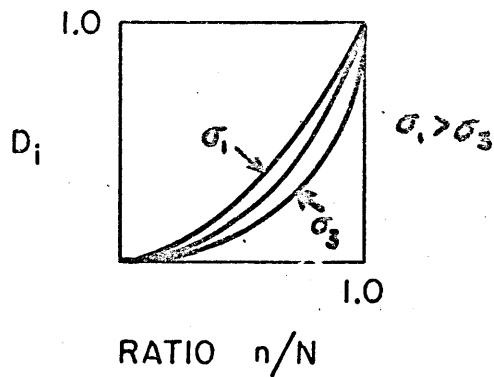


FIGURE 5. NON-INTERACTION FREE DAMAGE LAW.

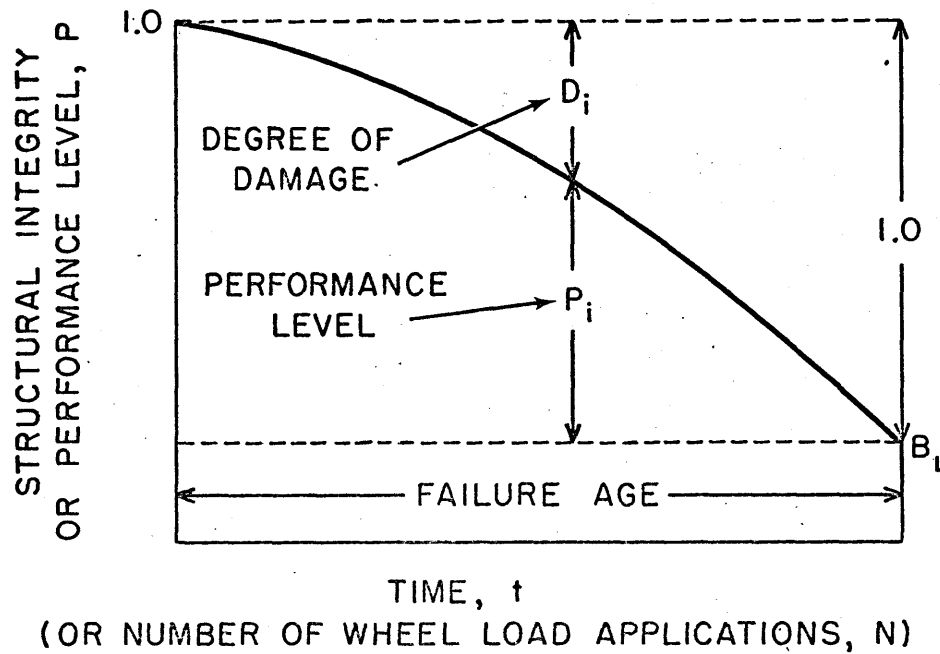


FIGURE 6. TWO-DIMENSIONAL SIMULATION OF THE PERFORMANCE OF A PAVEMENT STRUCTURE.

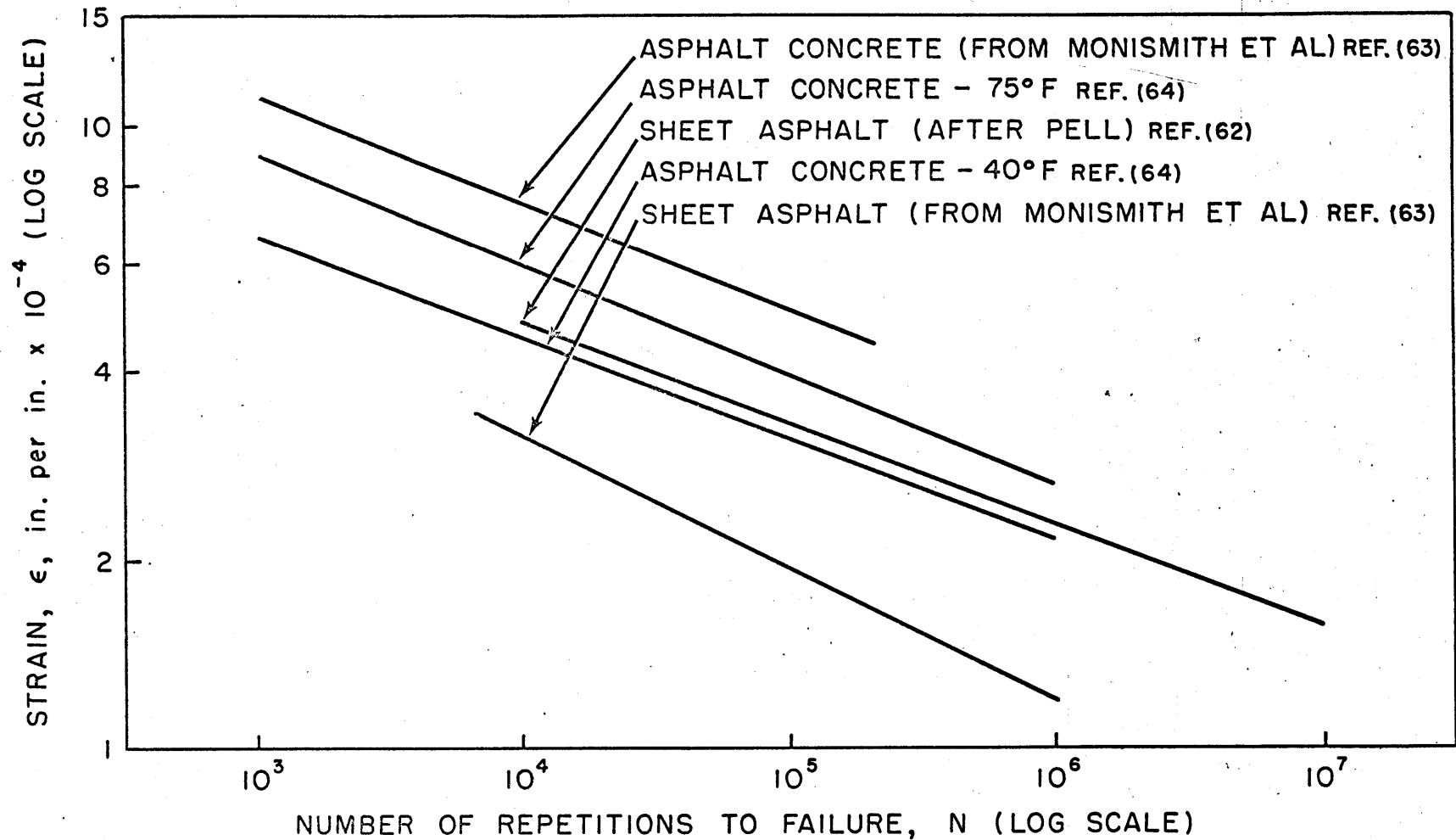


FIGURE 7. TYPICAL FATIGUE TEST RESULTS ILLUSTRATING STRAIN FAILURE CRITERIA - ASPHALT MIXTURES.

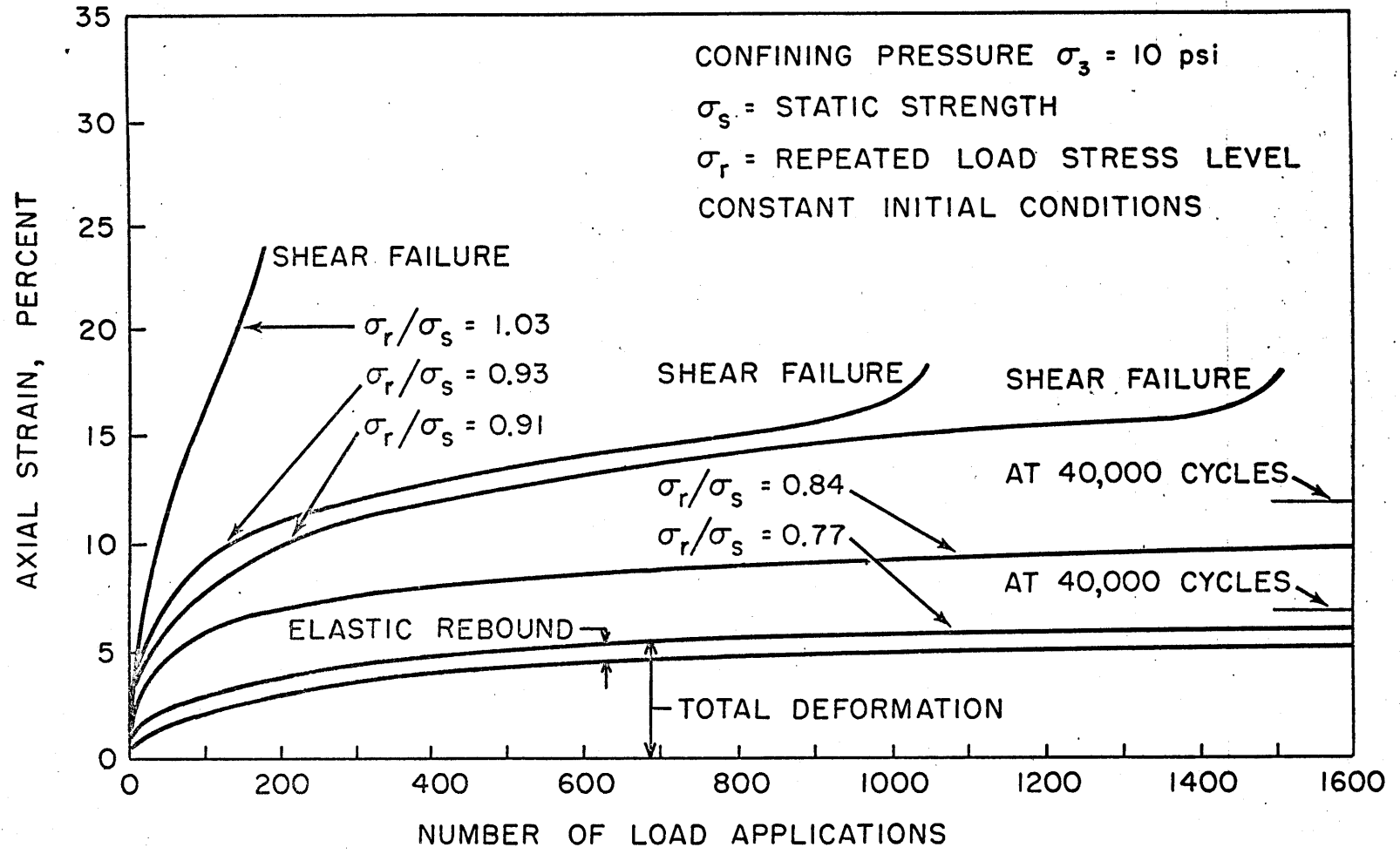
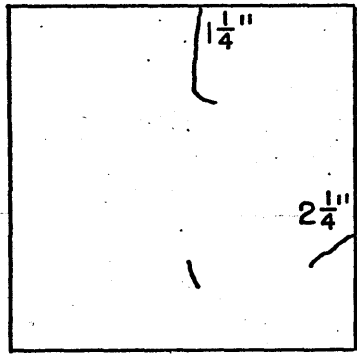
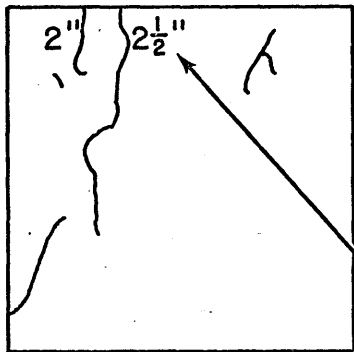


FIGURE 8. TYPICAL REPEATED LOAD TEST RESULTS ILLUSTRATING CRITICAL STRESS FAILURE CRITERIA - RESIDUAL CLAY. REF. (66)

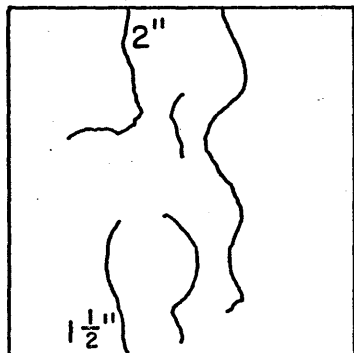


TEST HOLE No. 1
 STATION 624 + 81
 NBTL RWT
 →
 DIRECTION OF TRAVEL

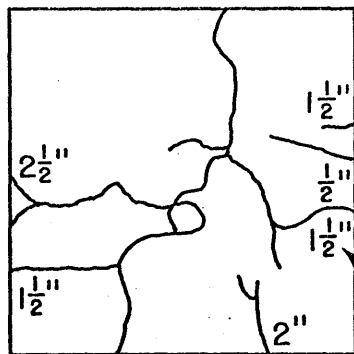


TEST HOLE No. 2
 STATION 624 + 83
 NBTL RWT
 →
 DIRECTION OF TRAVEL

(CRACK DEPTH MEASURED FROM BOTTOM)



TEST HOLE No. 3
 STATION 625 + 12
 NBTL RWT
 →
 DIRECTION OF TRAVEL



TEST HOLE No. 4
 STATION 625 + 14
 NBTL RWT
 →
 DIRECTION OF TRAVEL

(CRACK DEPTH MEASURED FROM BOTTOM)

FIGURE 9. CRACK PATTERNS ON BOTTOM OF SLABS OBTAINED IN VICINITY OF STA. 625 + 00.

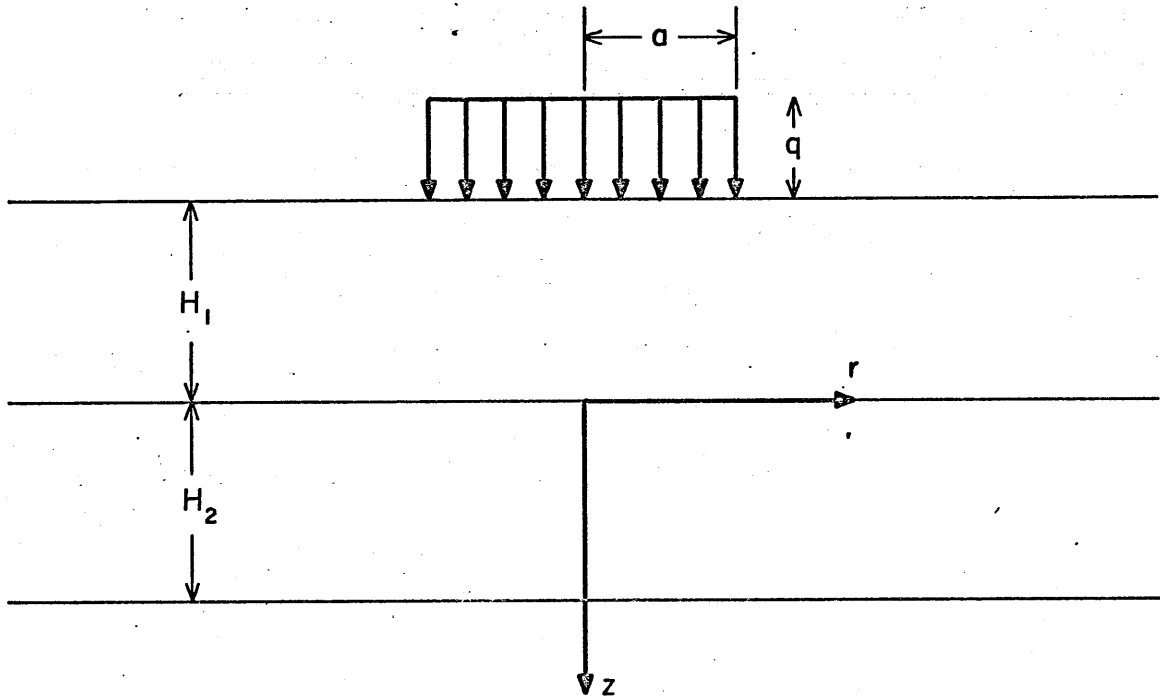
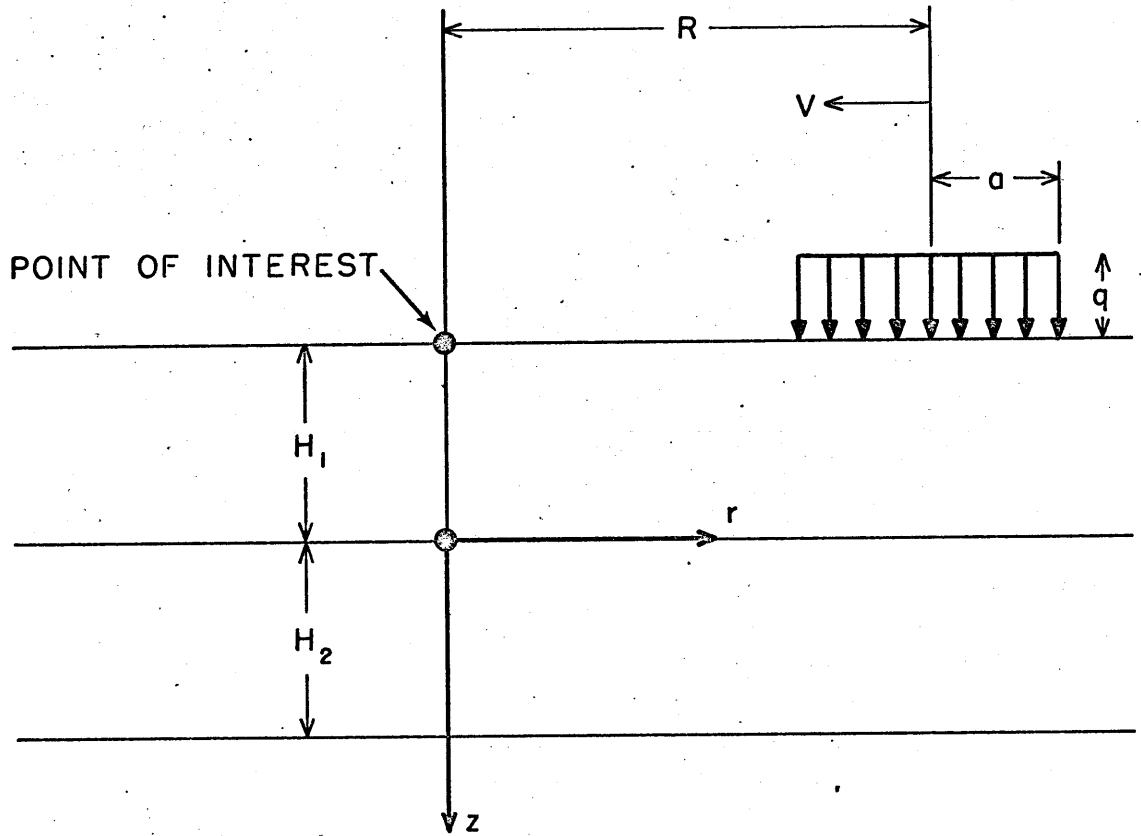
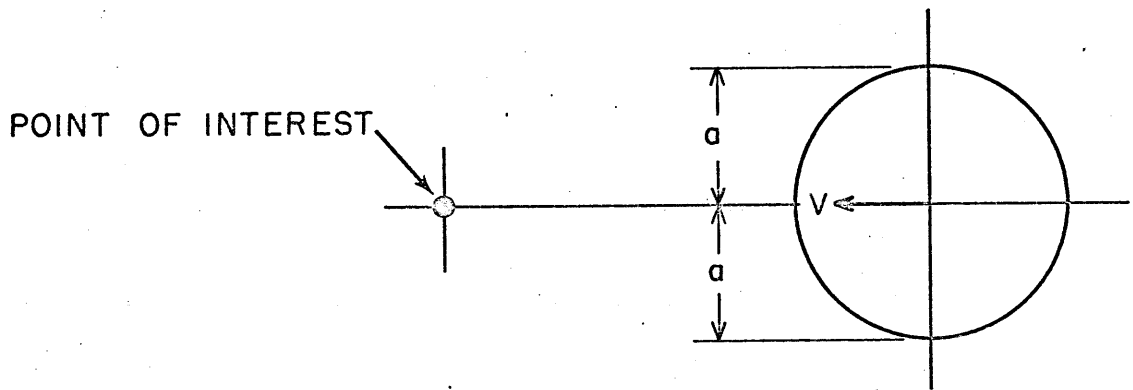


FIGURE 10. CROSS-SECTION OF THREE-LAYER SYSTEM.

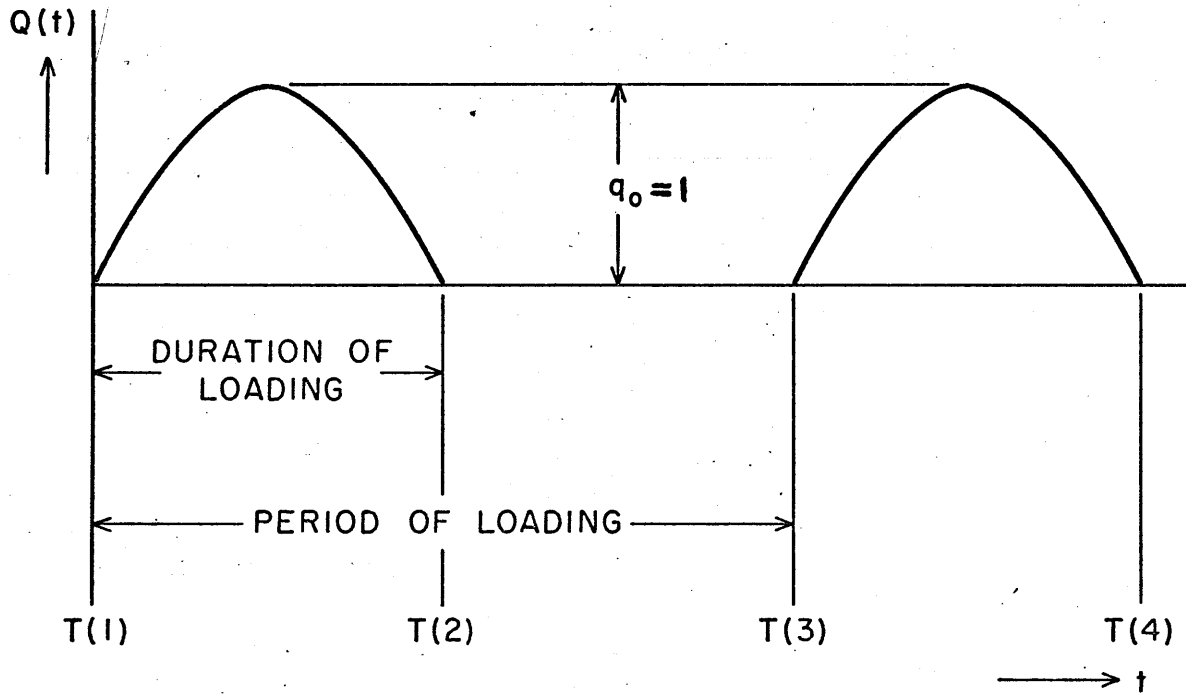


ELEVATION VIEW



PLAN VIEW

FIGURE II. MOVING LOAD ON VISCOELASTIC HALF SPACE.



WHERE $Q(t) = \begin{cases} q_0 \sin \omega t, & 0 < t < \frac{1}{2} \text{ (PERIOD OF SINE WAVE).} \\ 0, & \frac{1}{2} \text{ (PERIOD OF SINE WAVE)} < t < \text{(PERIOD OF EXCITING FORCE).} \end{cases}$

FIGURE 12. TIME-VARYING REPEATED LOAD CONFIGURATION.

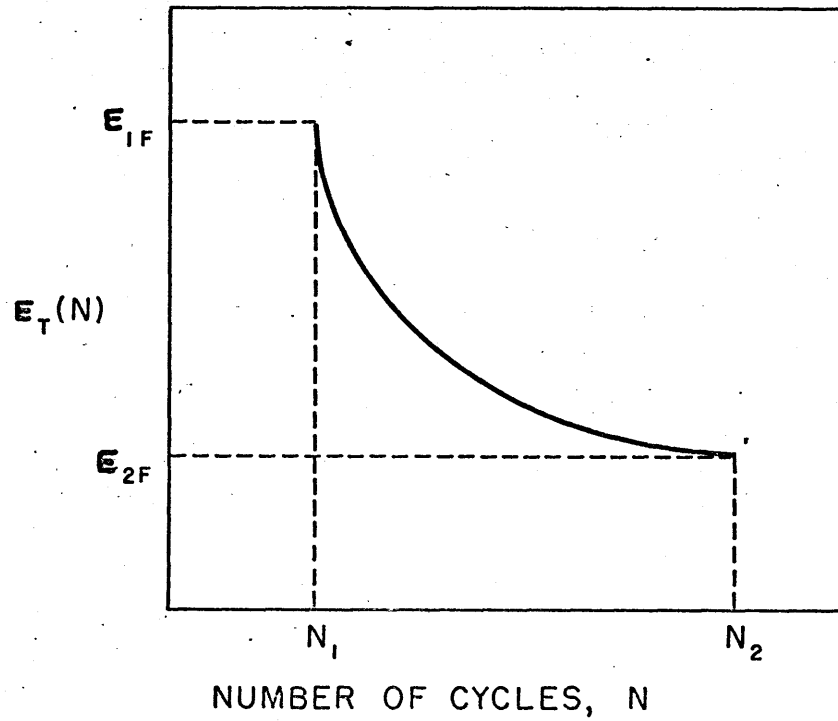


FIGURE 13. ASSUMED FATIGUE CURVE FOR THE DETERMINATION OF β_1 .

THE LINEAR KERNEL FUNCTION, β_1

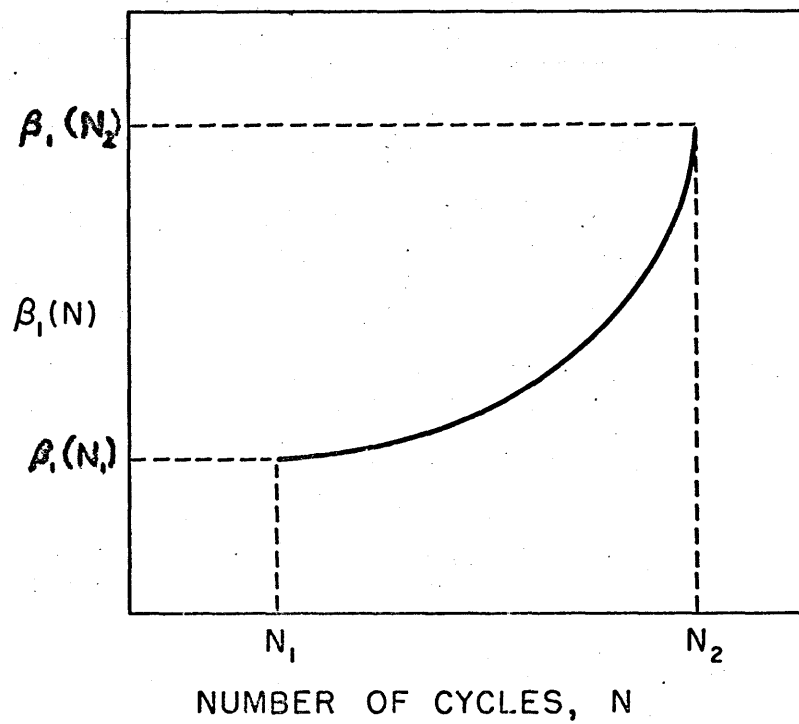


FIGURE 14. β_1 CURVE OBTAINED FROM ASSUMED FATIGUE CURVE.

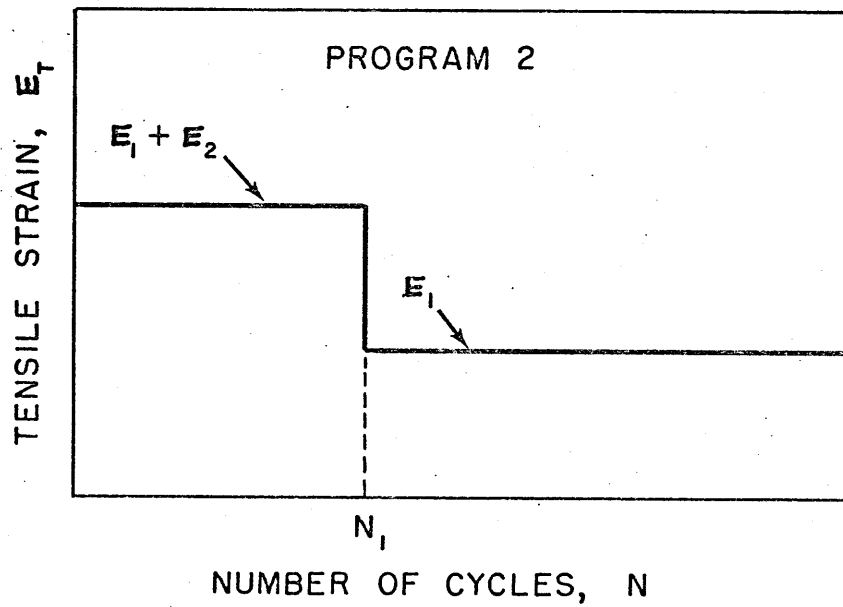
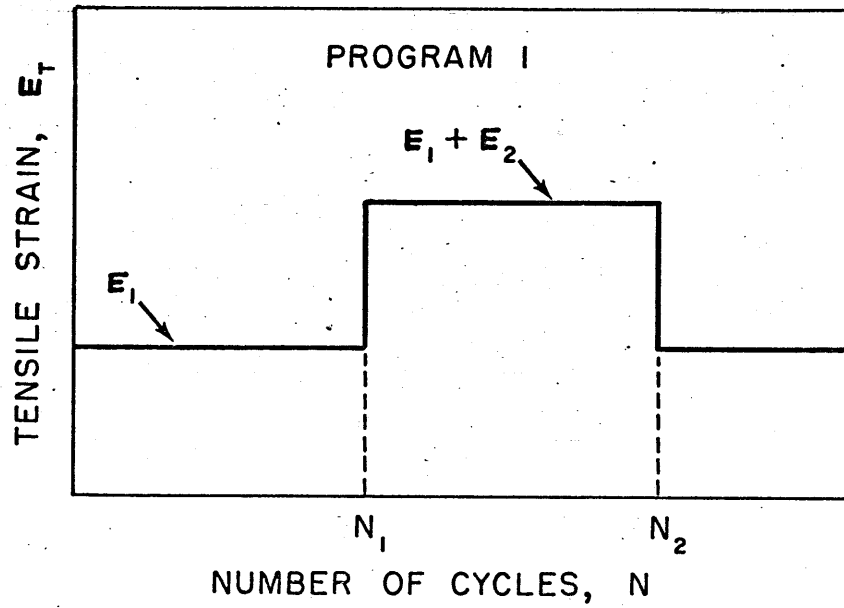


FIGURE 15. LOADING PROGRAMS.

THE NON-LINEAR KERNEL, β_2

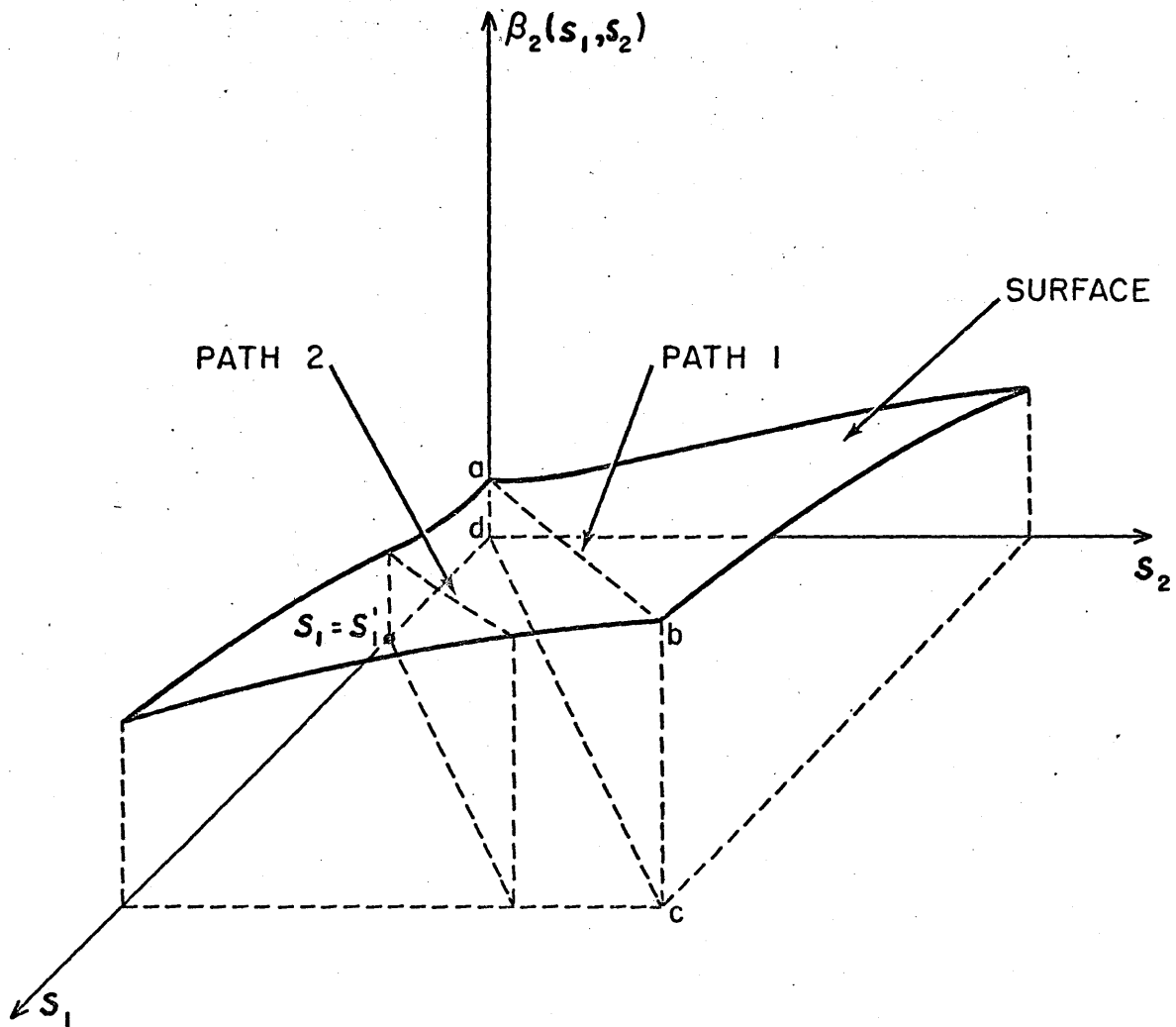


FIGURE 16. HYPOTHETICAL $\beta(s_1, s_2)$ SURFACE.

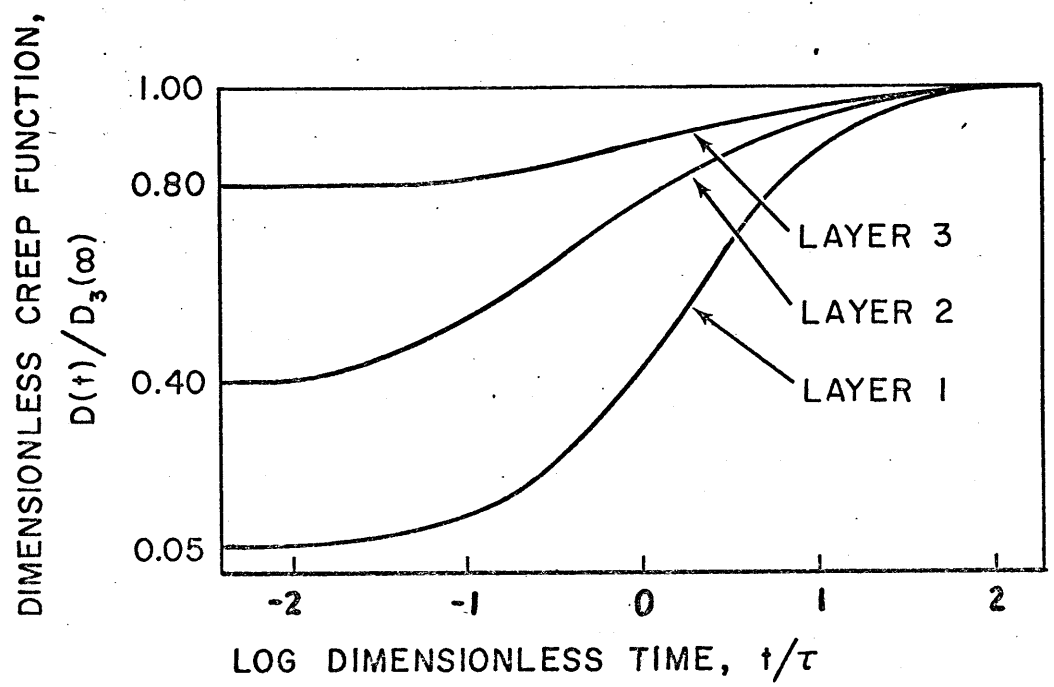
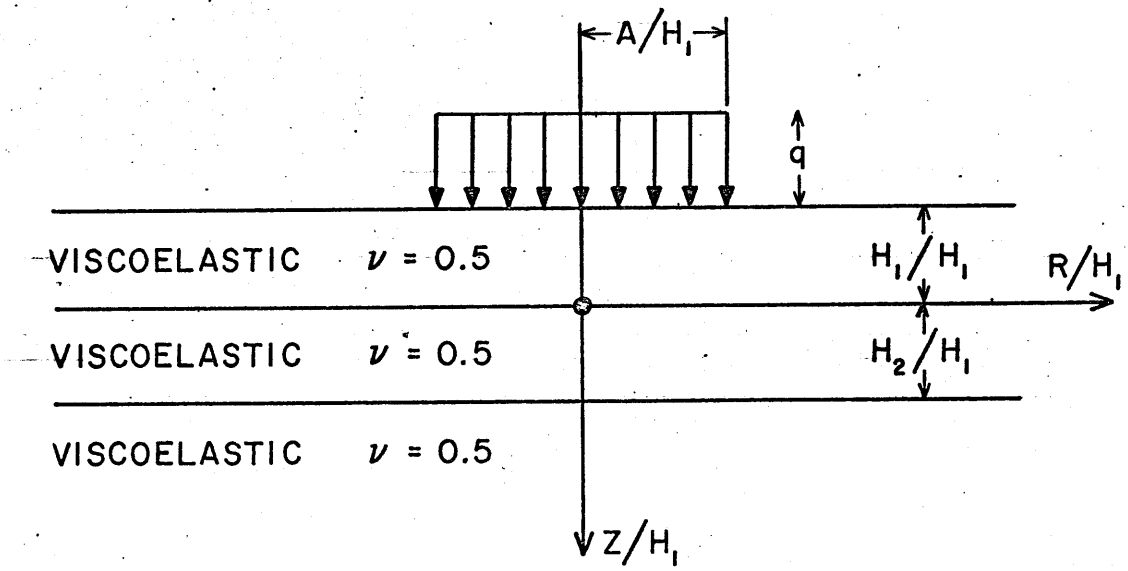


FIGURE 17. DIMENSIONLESS PAVEMENT SYSTEM NO. 2

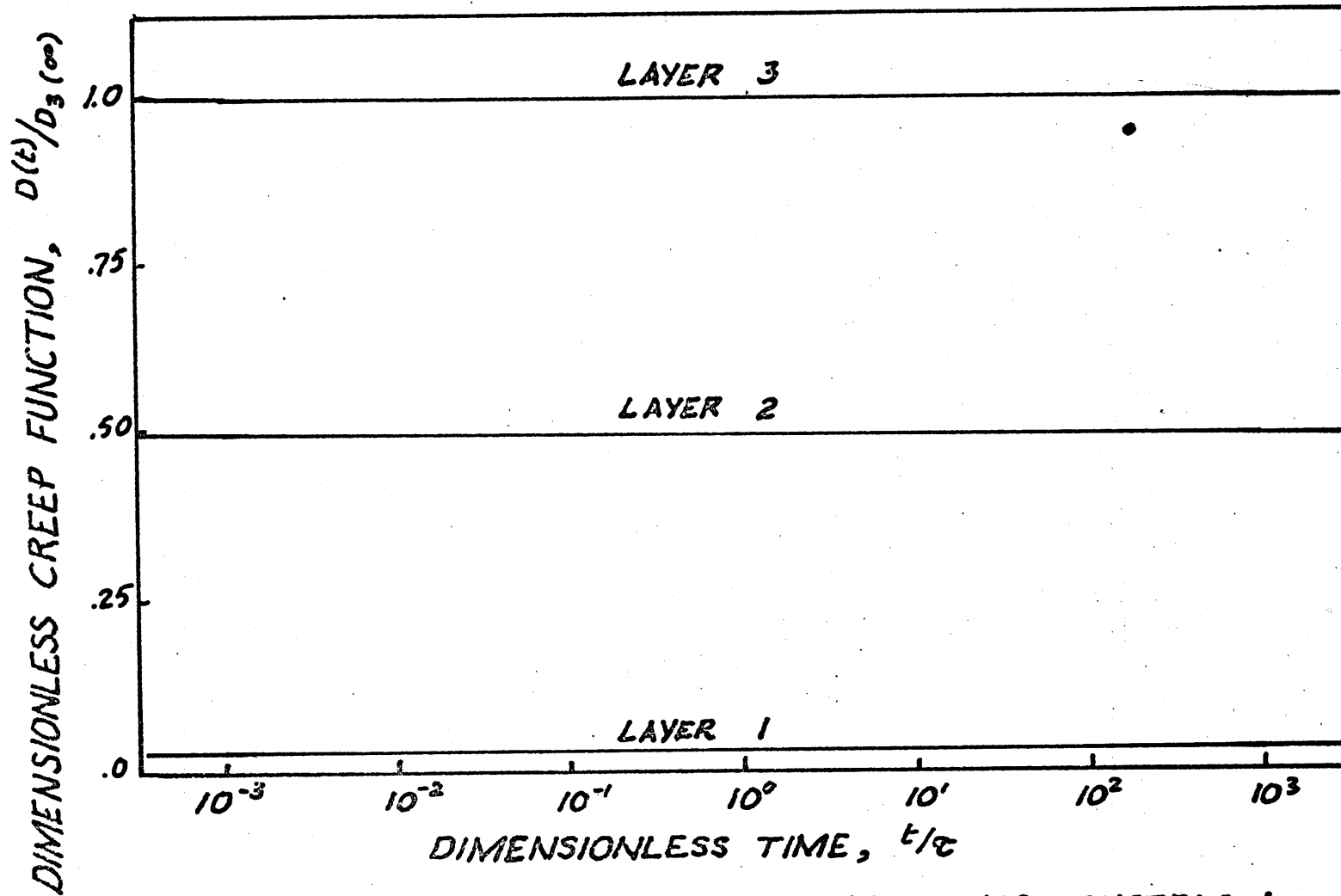


FIGURE 18.- DIMENSIONLESS CREEP FUNCTIONS - SYSTEM 1.

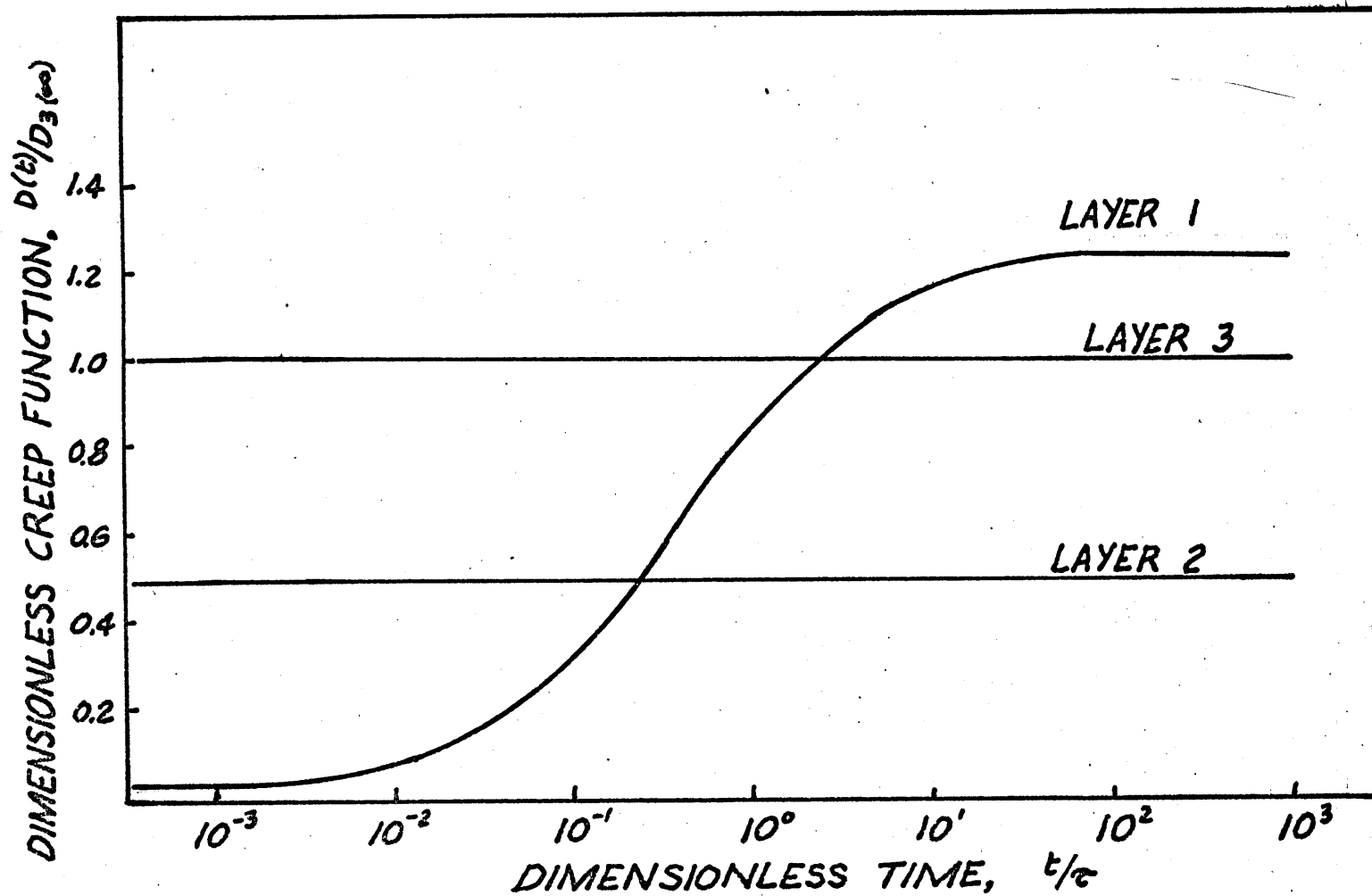


FIGURE 19. - DIMENSIONLESS CREEP FUNCTIONS - SYSTEM 3

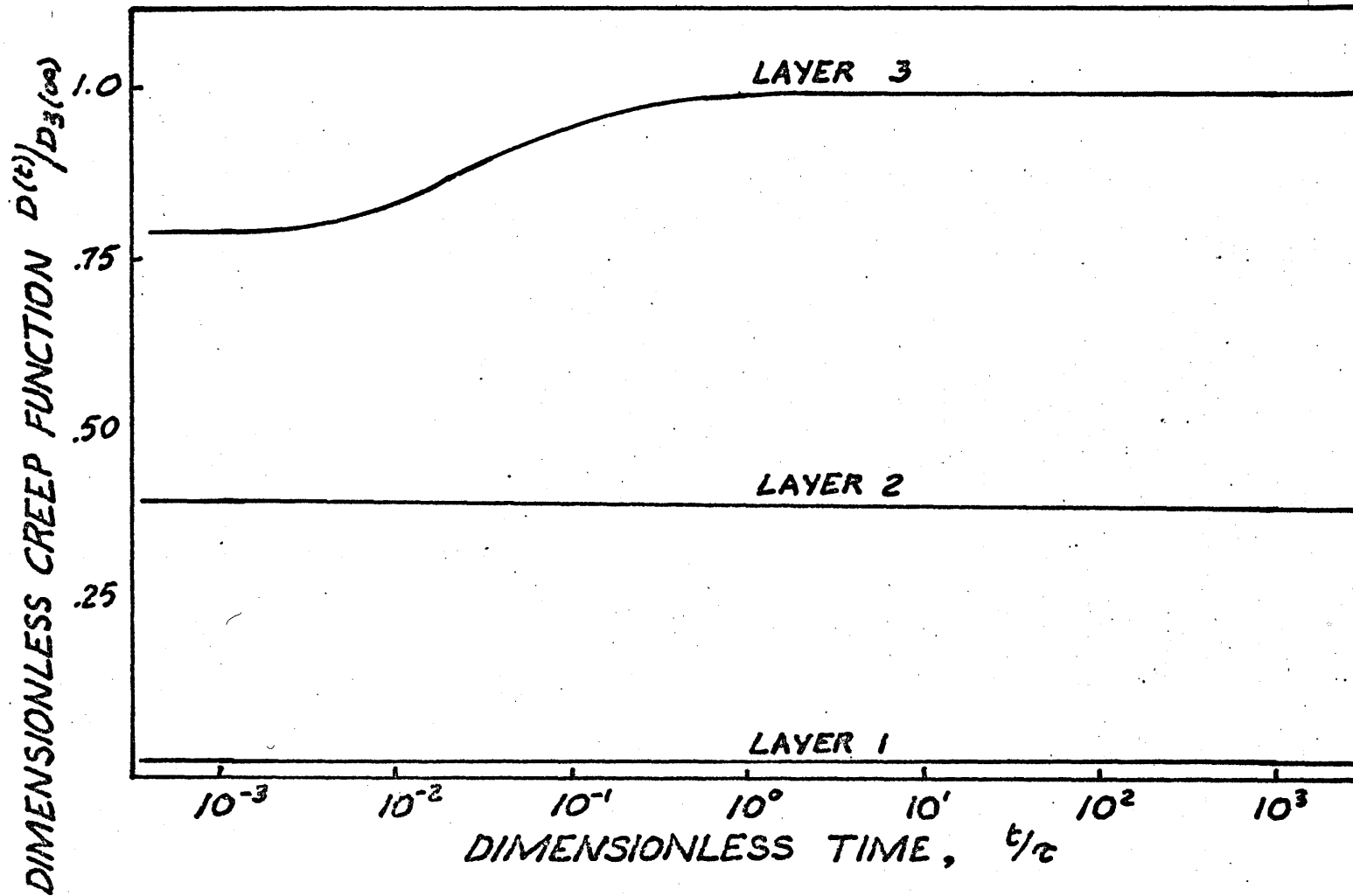


FIGURE 20.-DIMENSIONLESS CREEP FUNCTIONS-SYSTEM 4

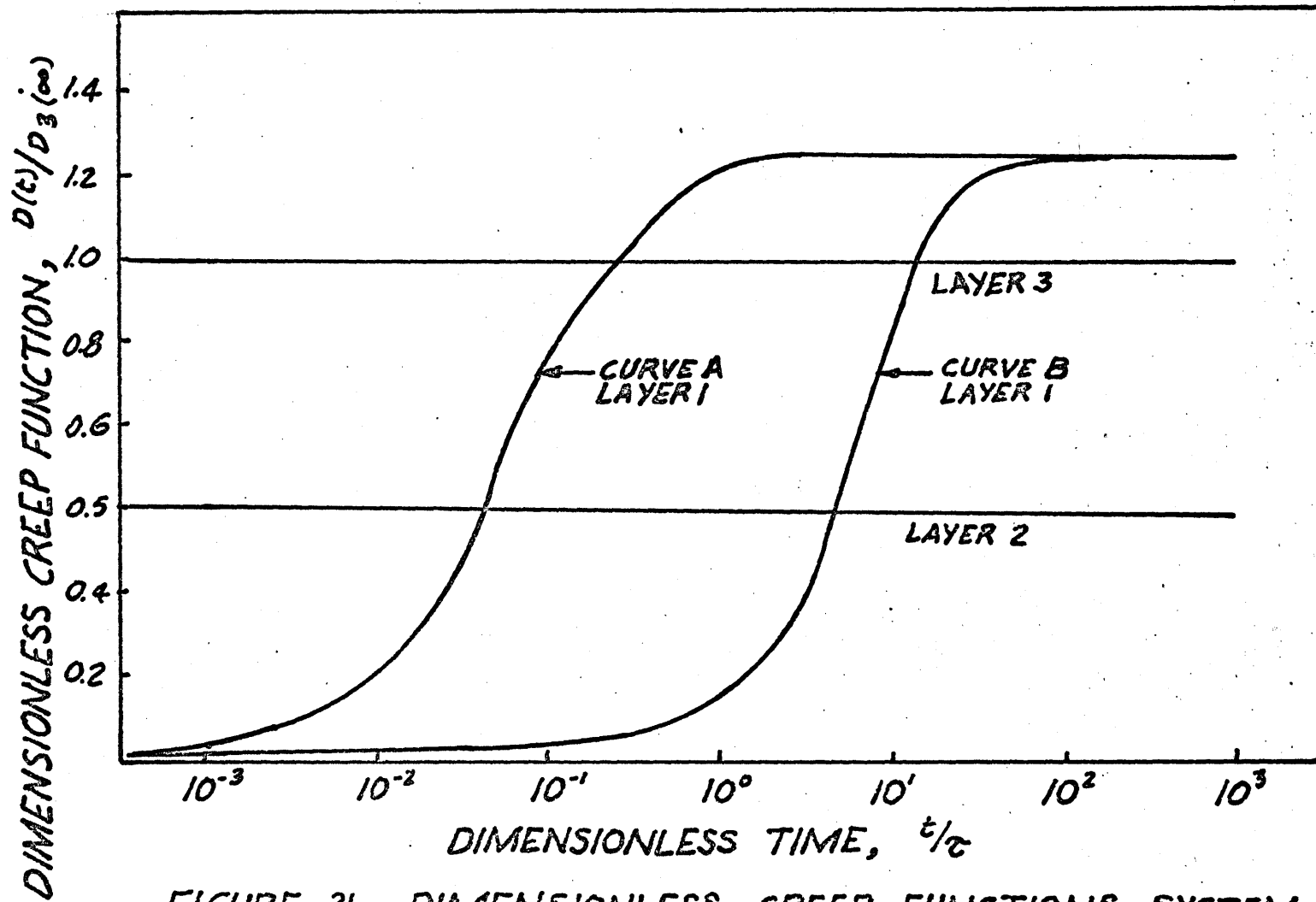


FIGURE 21. - DIMENSIONLESS CREEP FUNCTIONS - SYSTEM 5

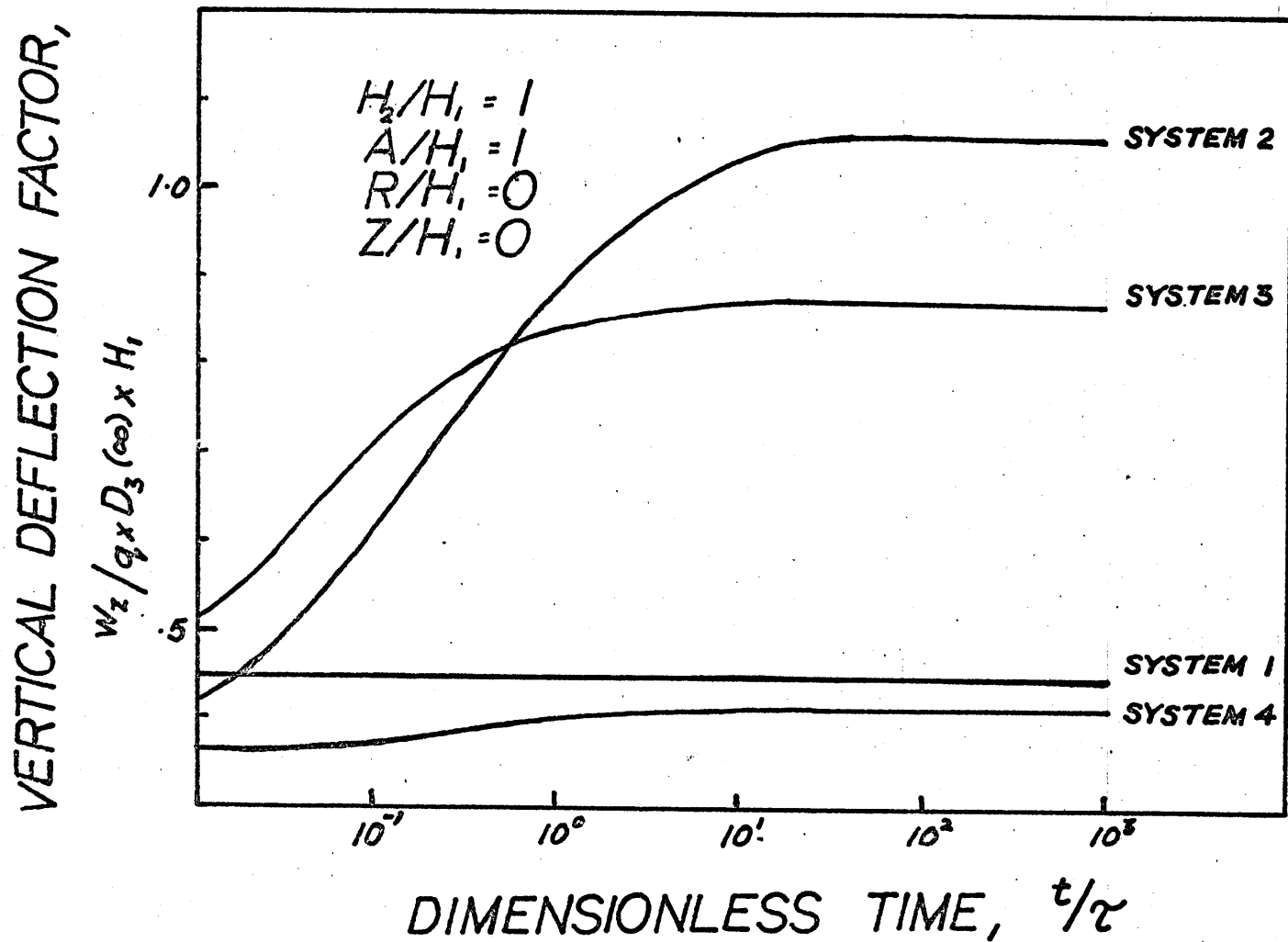


FIGURE 22. INFLUENCE OF MATERIAL VARIABLES ON VERTICAL DEFLECTION FACTOR - 4 SYSTEMS.

VERTICAL DEFLECTION FACTOR,

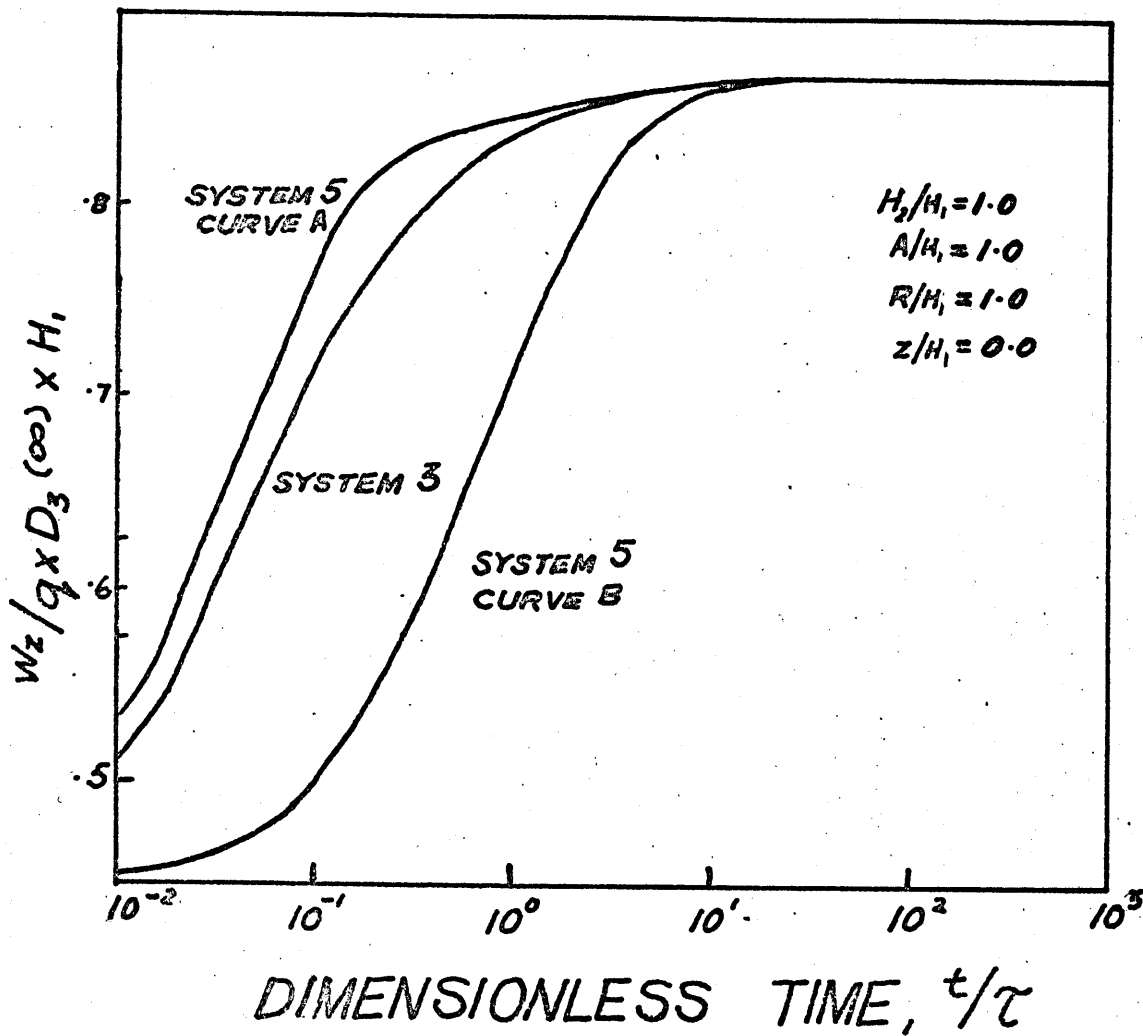


FIGURE 23. INFLUENCE OF MATERIAL VARIABLES ON VERTICAL DEFLECTION FACTOR - SYSTEM 5.

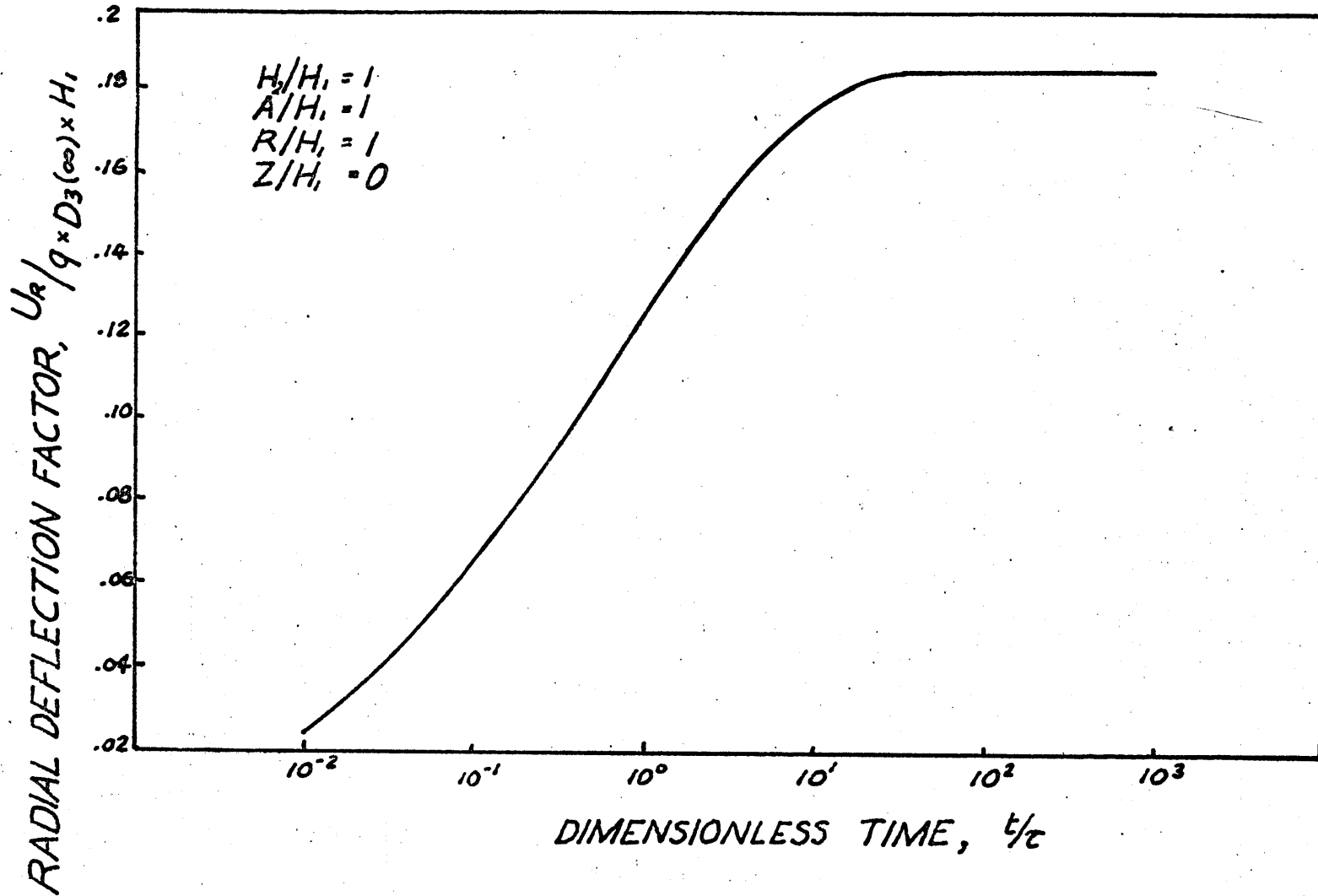


FIGURE 24. RADIAL DEFLECTION FACTOR FOR SYSTEM 2

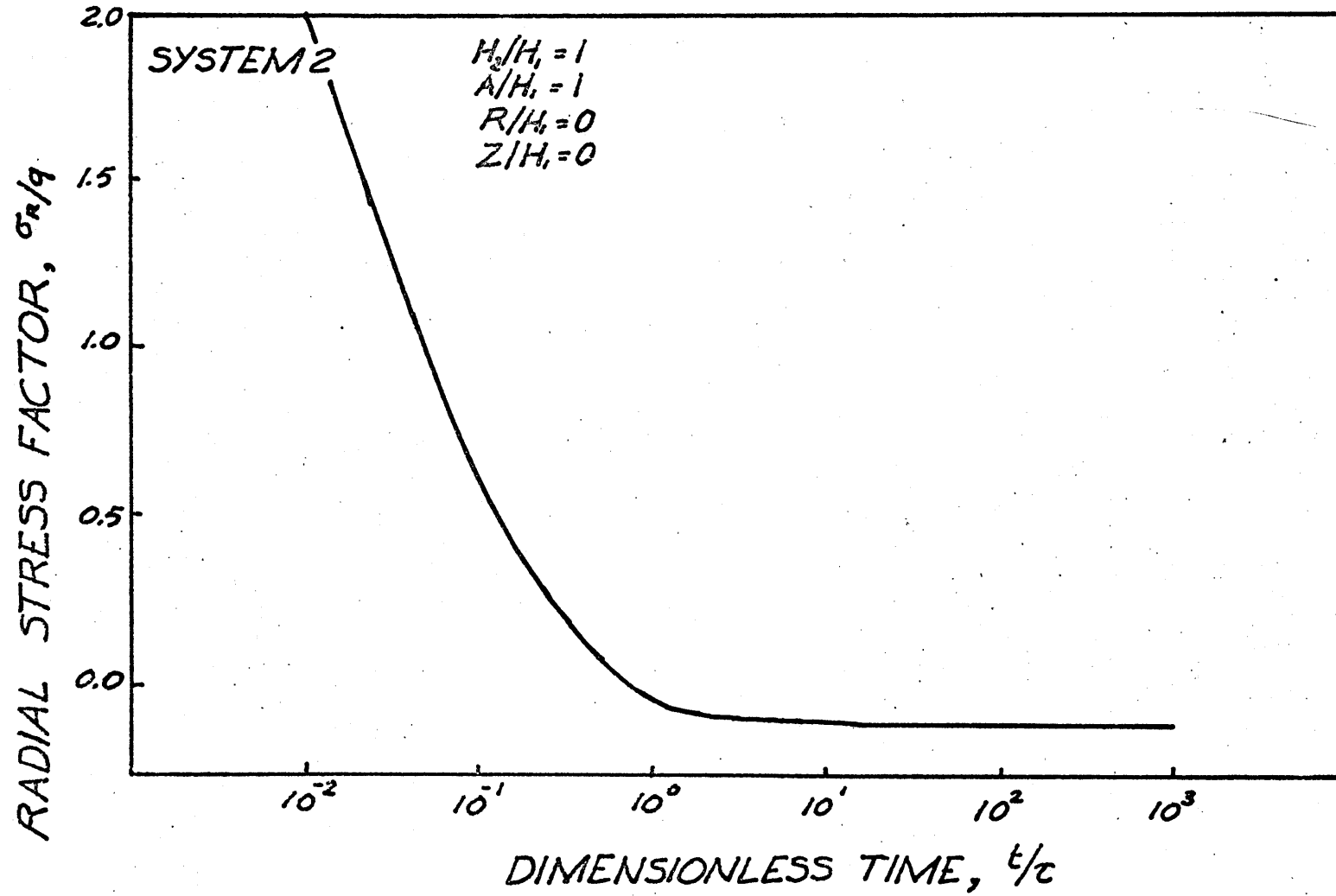


FIGURE 25. RADIAL STRESS FACTOR FOR SYSTEM 2

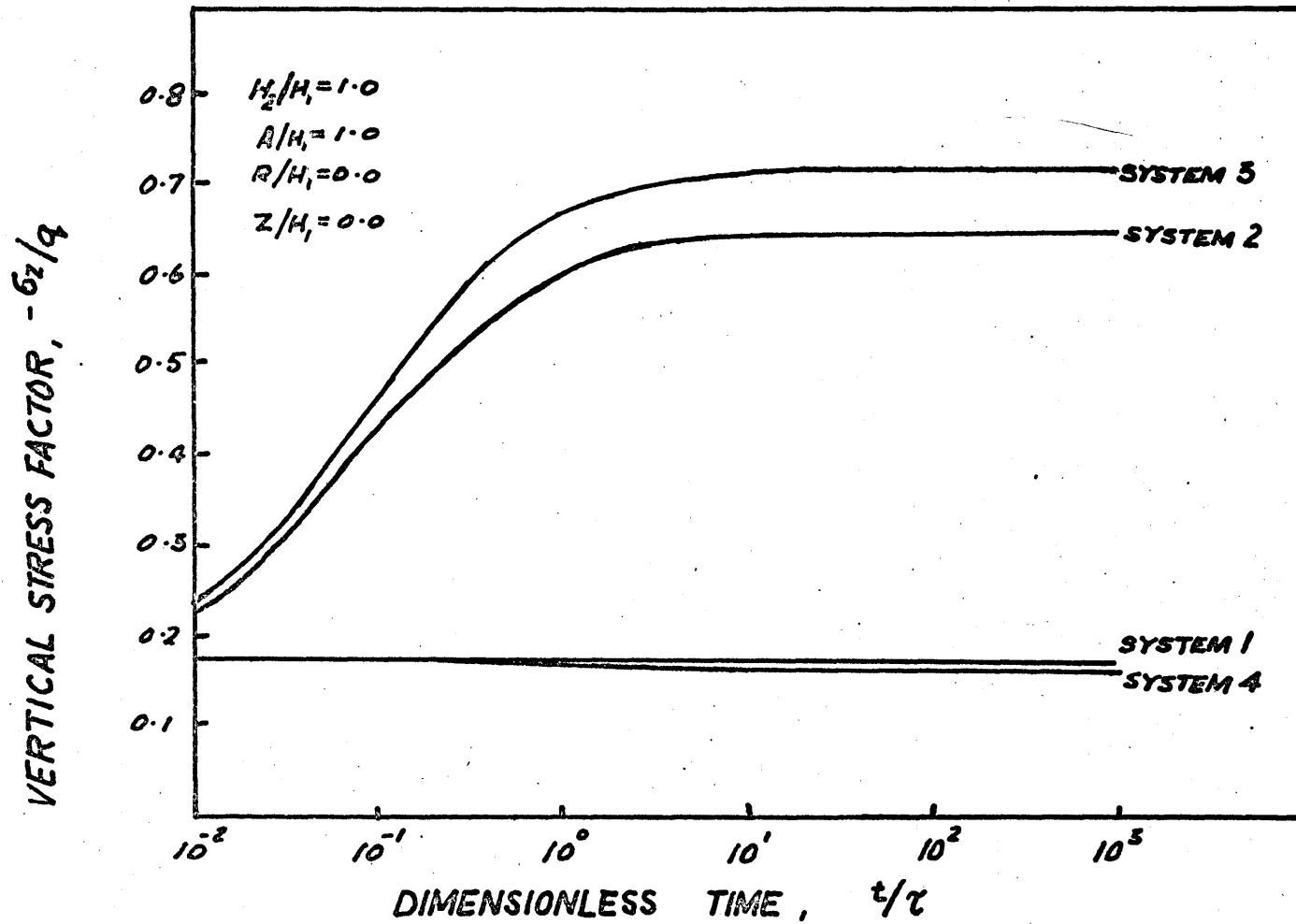


FIGURE 26. INFLUENCE OF MATERIAL VARIABLES ON VERTICAL STRESS FACTOR. - 4 SYSTEMS

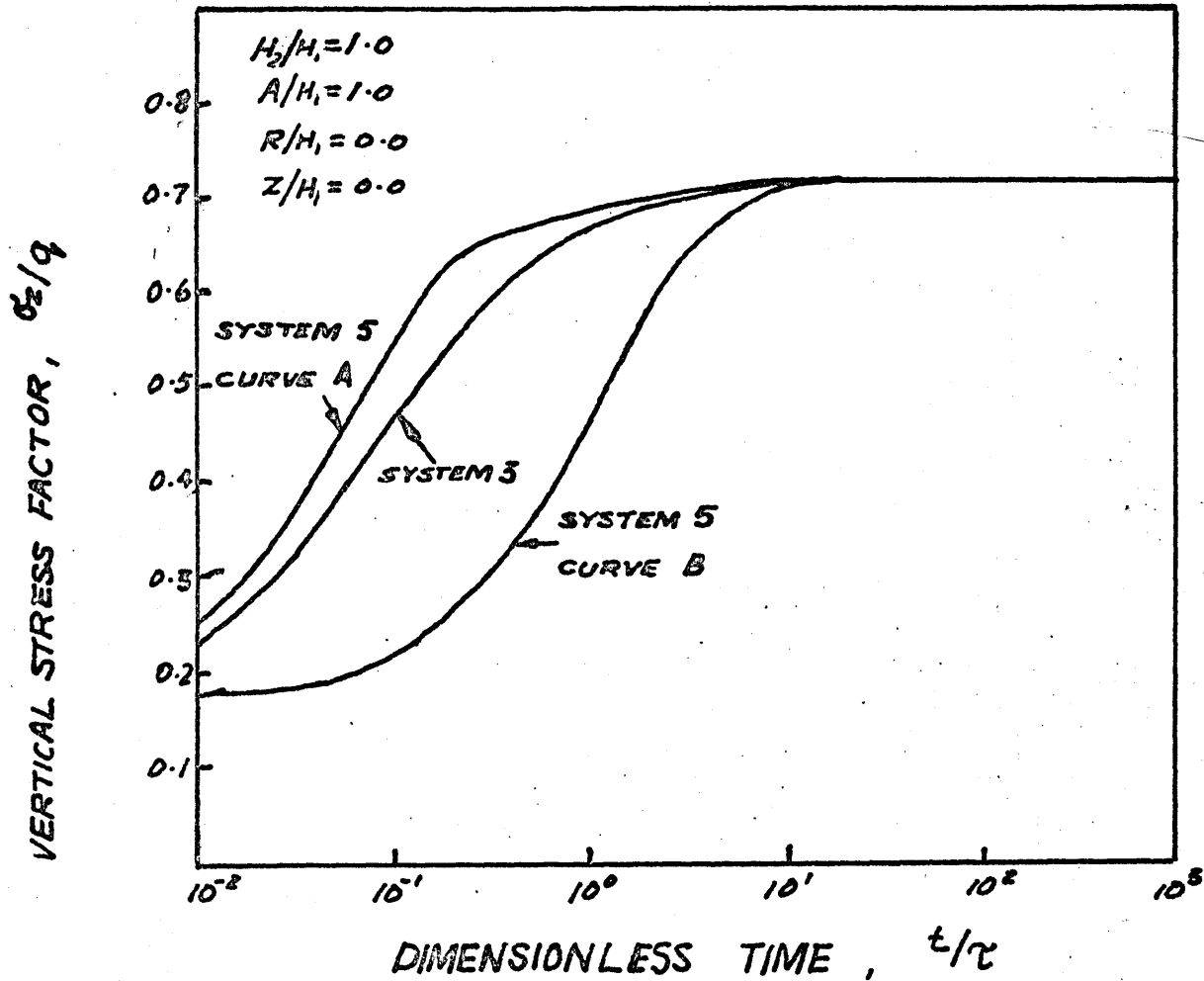


FIGURE 27. INFLUENCE OF MATERIAL VARIABLES ON VERTICAL STRESS FACTOR.- SYSTEM 5

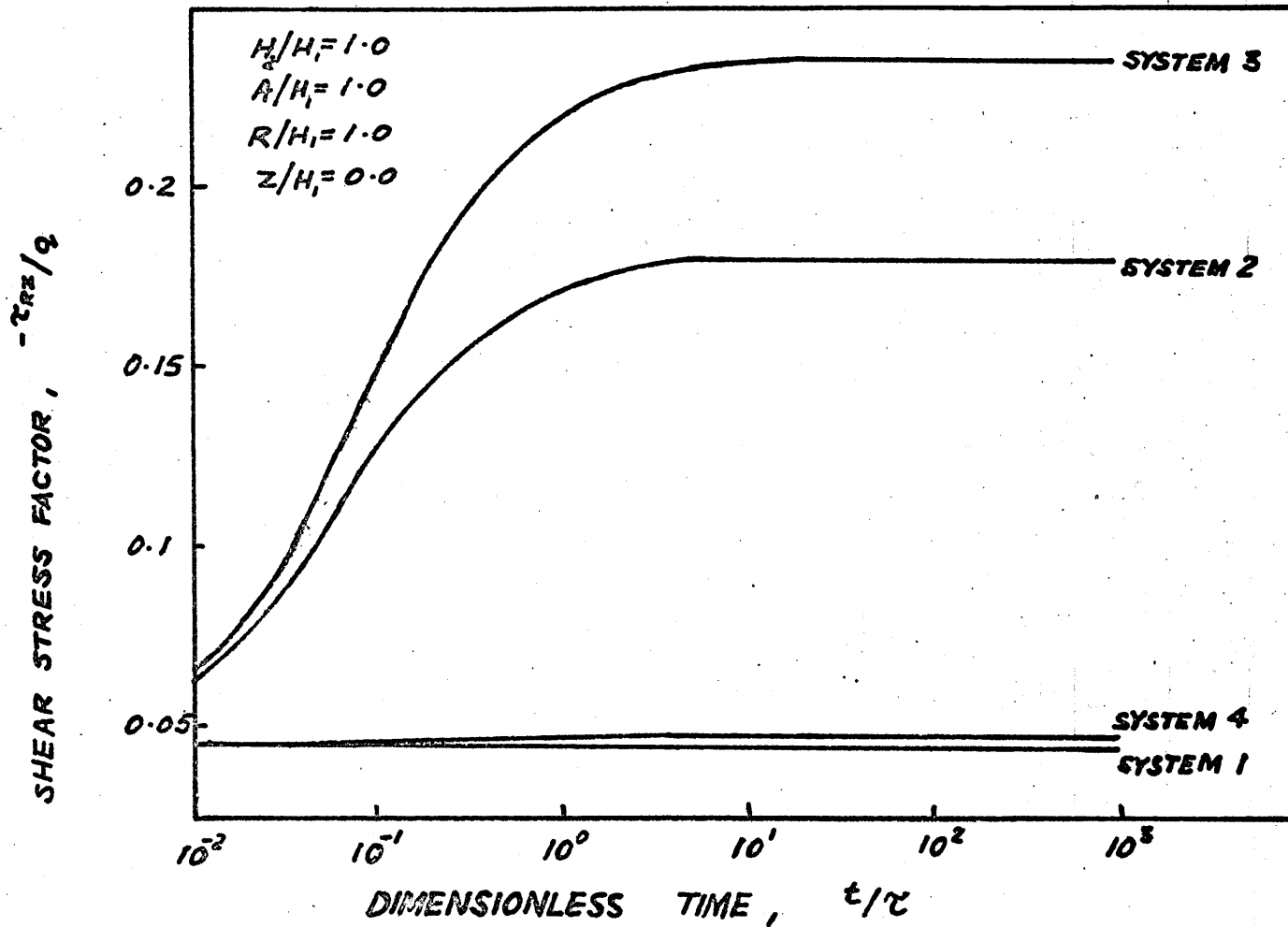


FIGURE 20. INFLUENCE OF MATERIAL VARIABLES ON SHEAR STRESS FACTOR. - 4 SYSTEMS

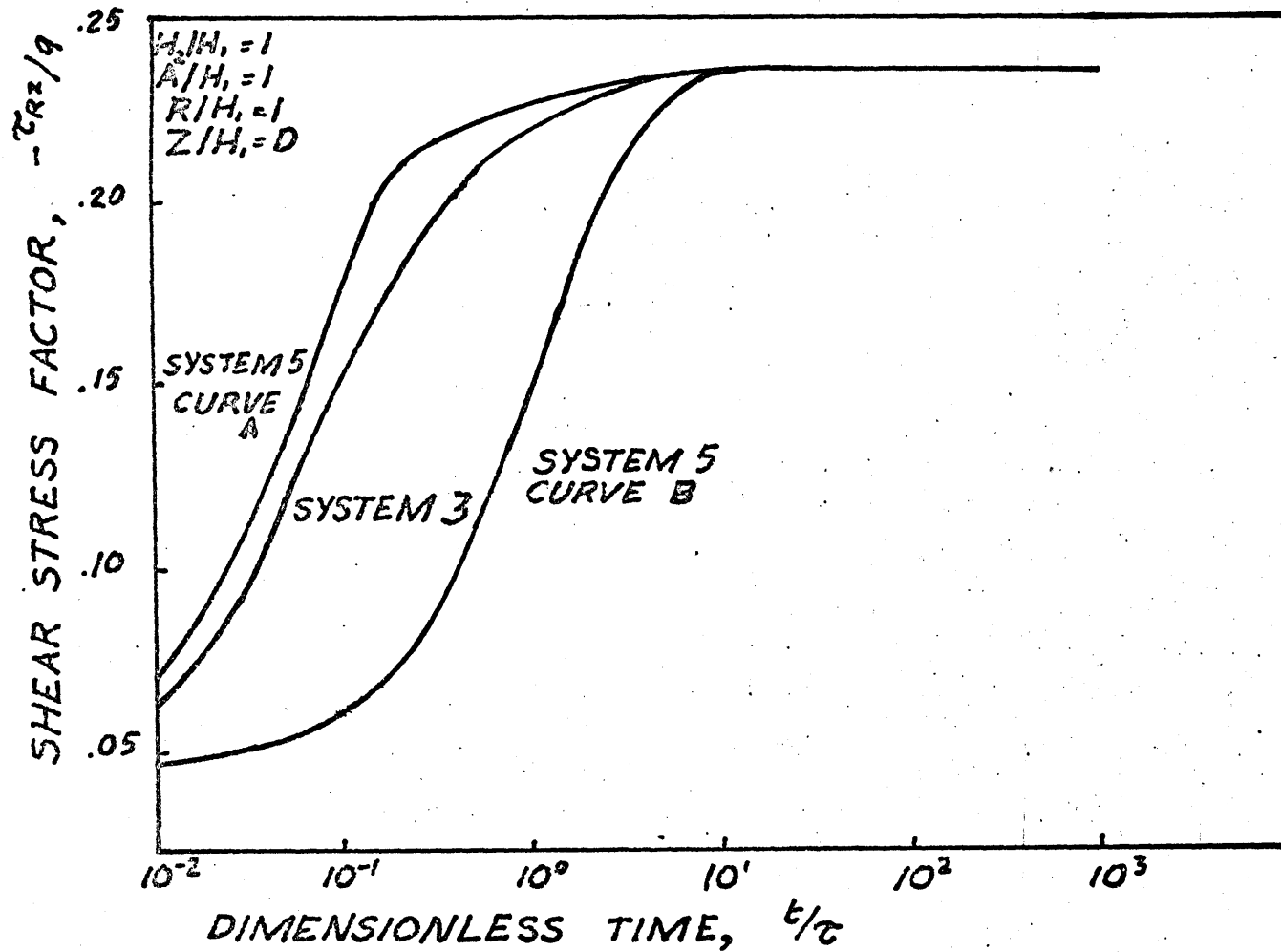


FIGURE 29. - INFLUENCE OF MATERIAL VARIABLES ON SHEAR STRESS FACTOR. - SYSTEM 5

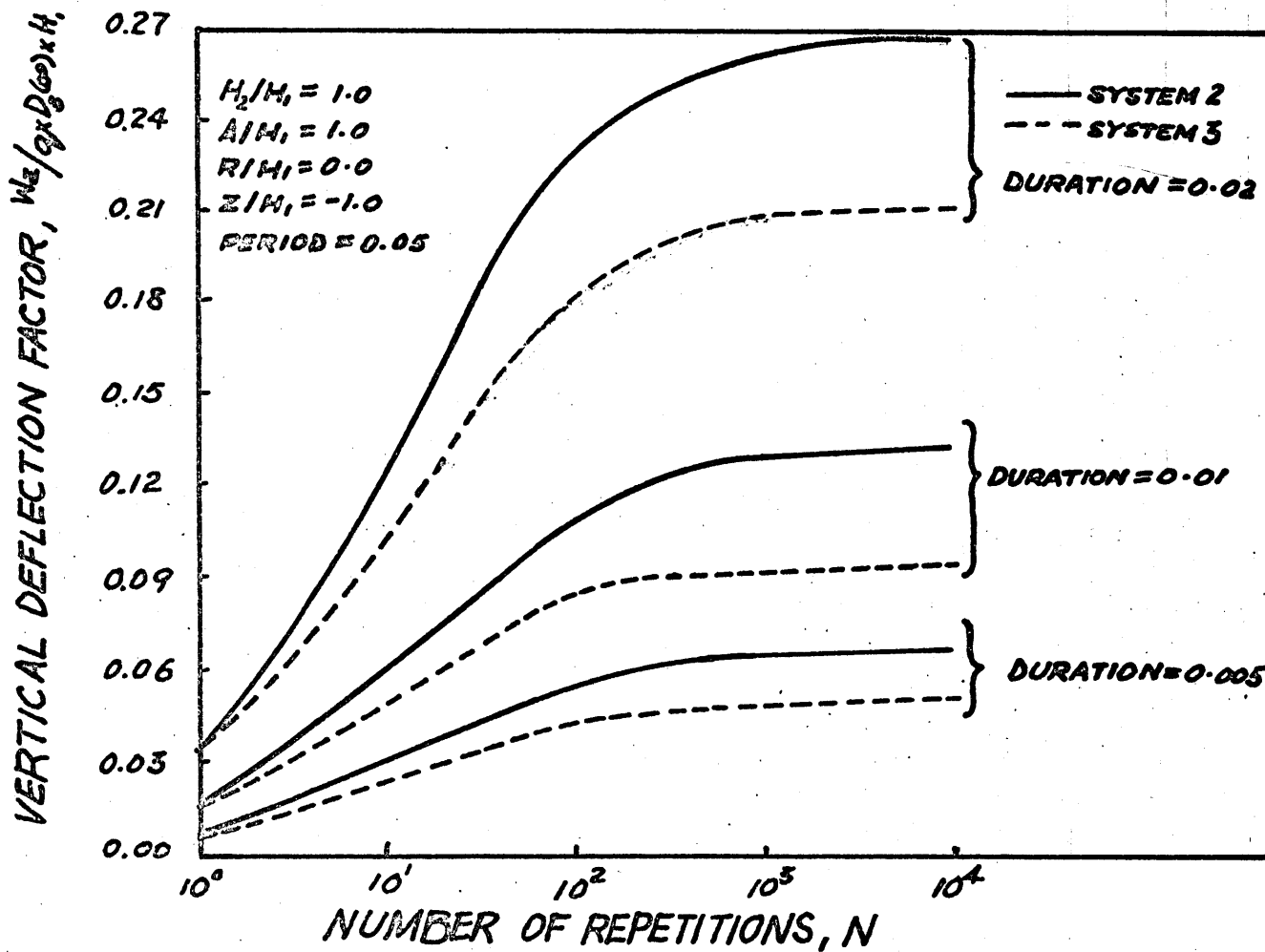


FIGURE 30. INFLUENCE OF DURATION ON VERTICAL DEFLECTION FACTOR

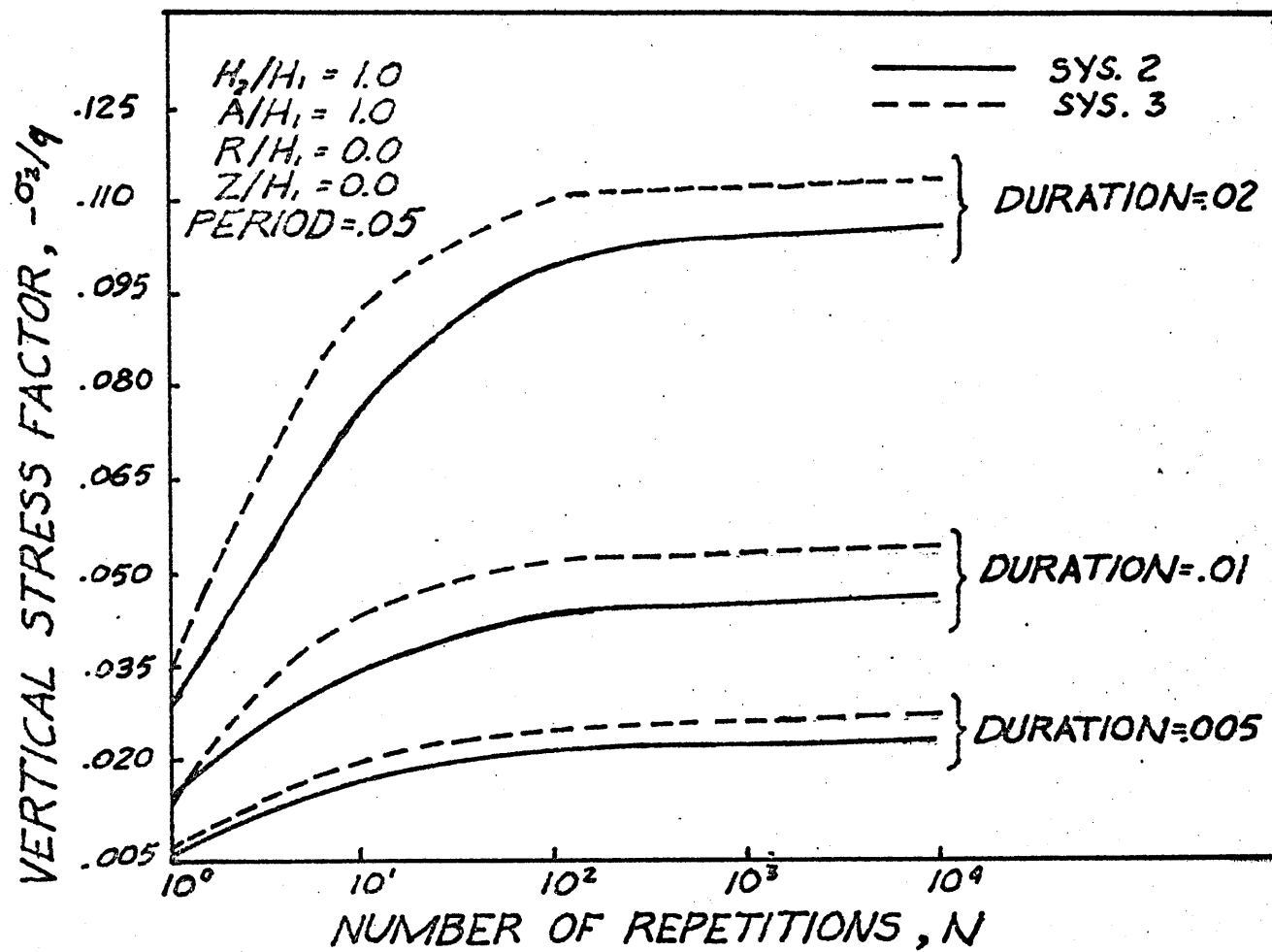


FIGURE 31. INFLUENCE OF DURATION ON VERTICAL STRESS FACTOR

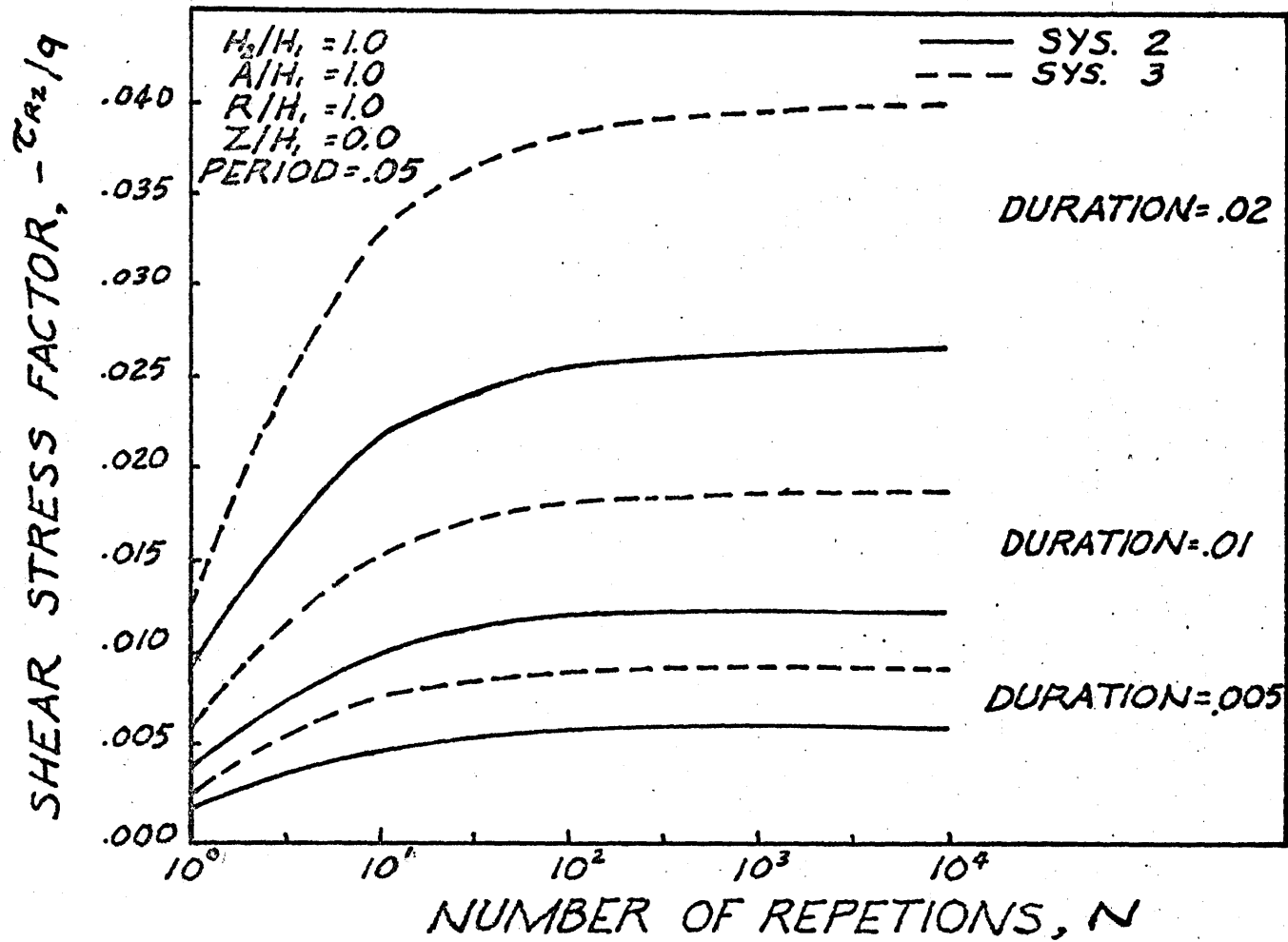


FIGURE 32. INFLUENCE OF DURATION ON SHEAR STRESS FACTOR

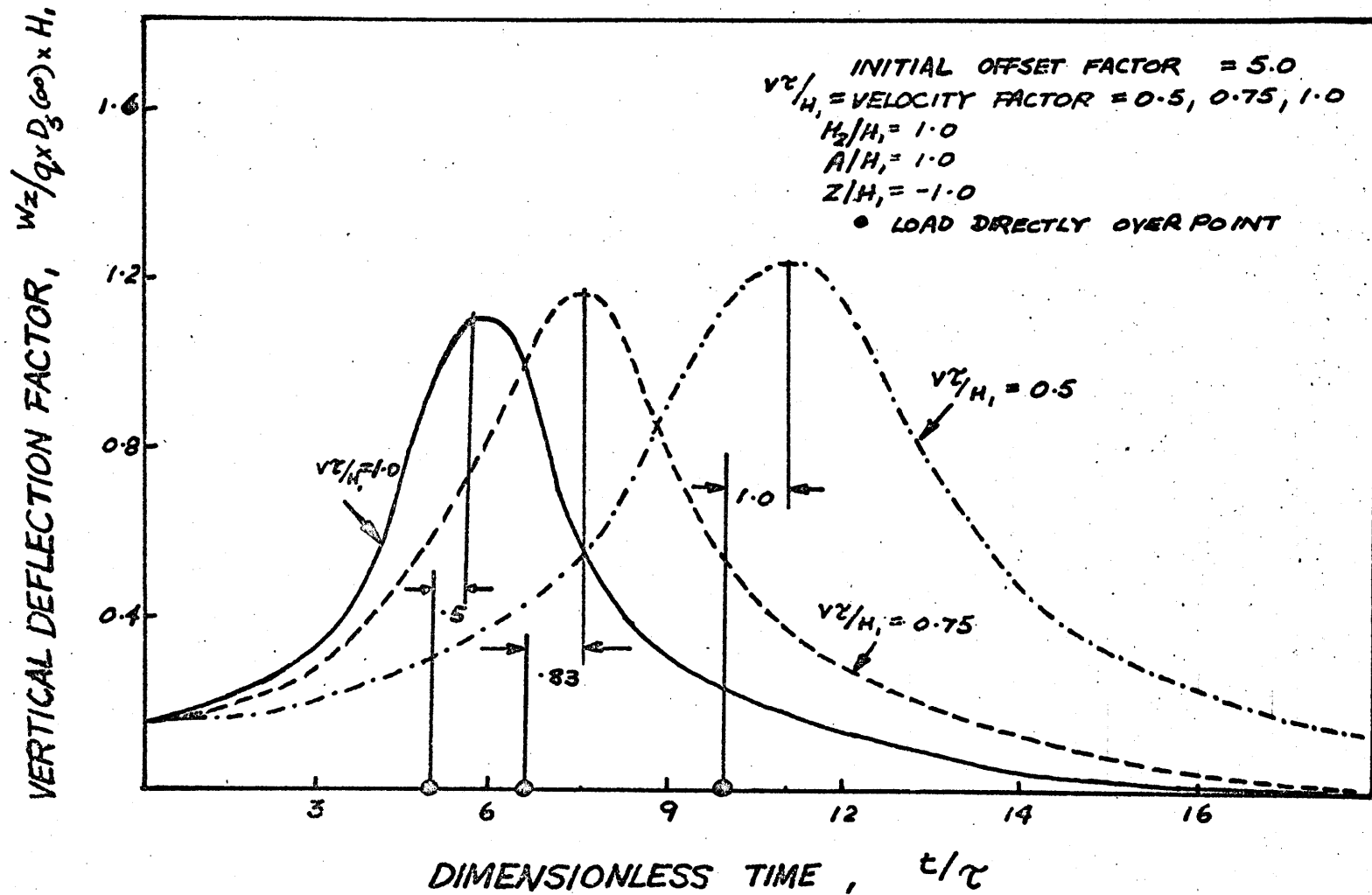


FIGURE 33. MOVING LOAD - VERTICAL DEFLECTION FACTOR
SYSTEM 2

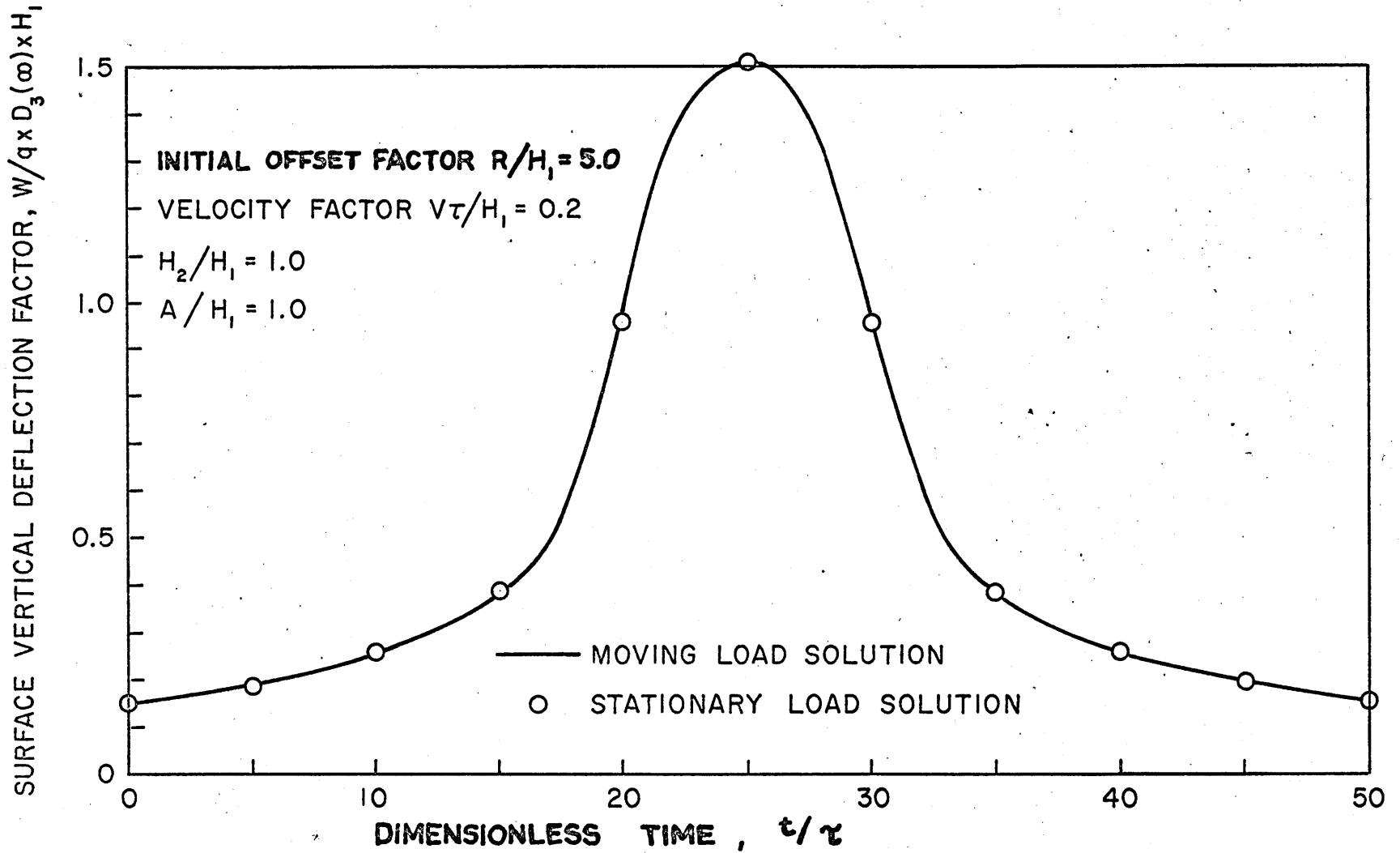


FIGURE 34. MOVING LOAD - VERTICAL DEFLECTION FACTOR ELASTIC SYSTEM.

VERTICAL DEFLECTION FACTOR, $w_z/q \times D_5(\infty), H_1$

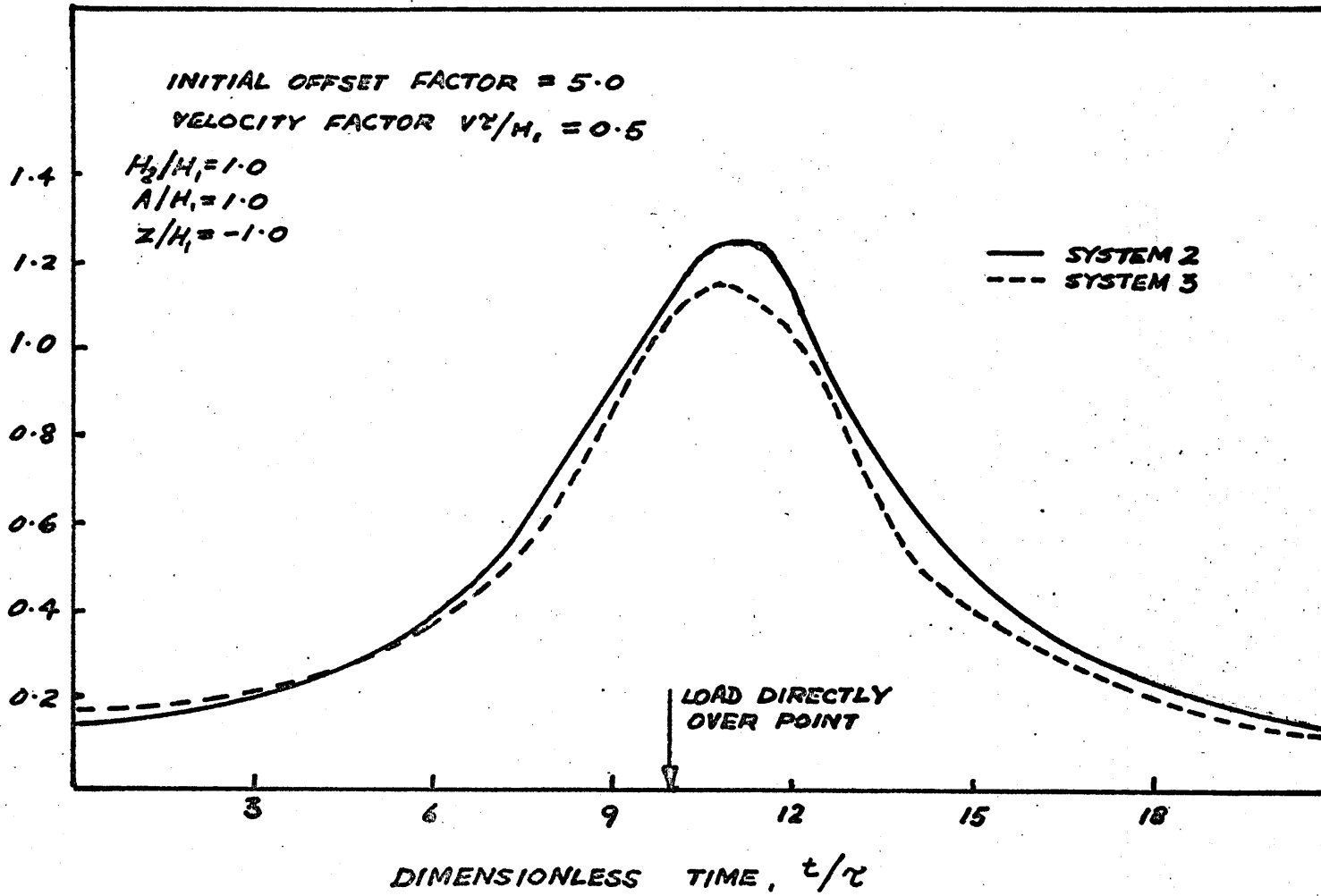


FIGURE 35. MOVING LOAD COMPARISON - VERTICAL DEFLECTION FACTOR

VERTICAL STRESS FACTOR, $-\sigma_z/q$

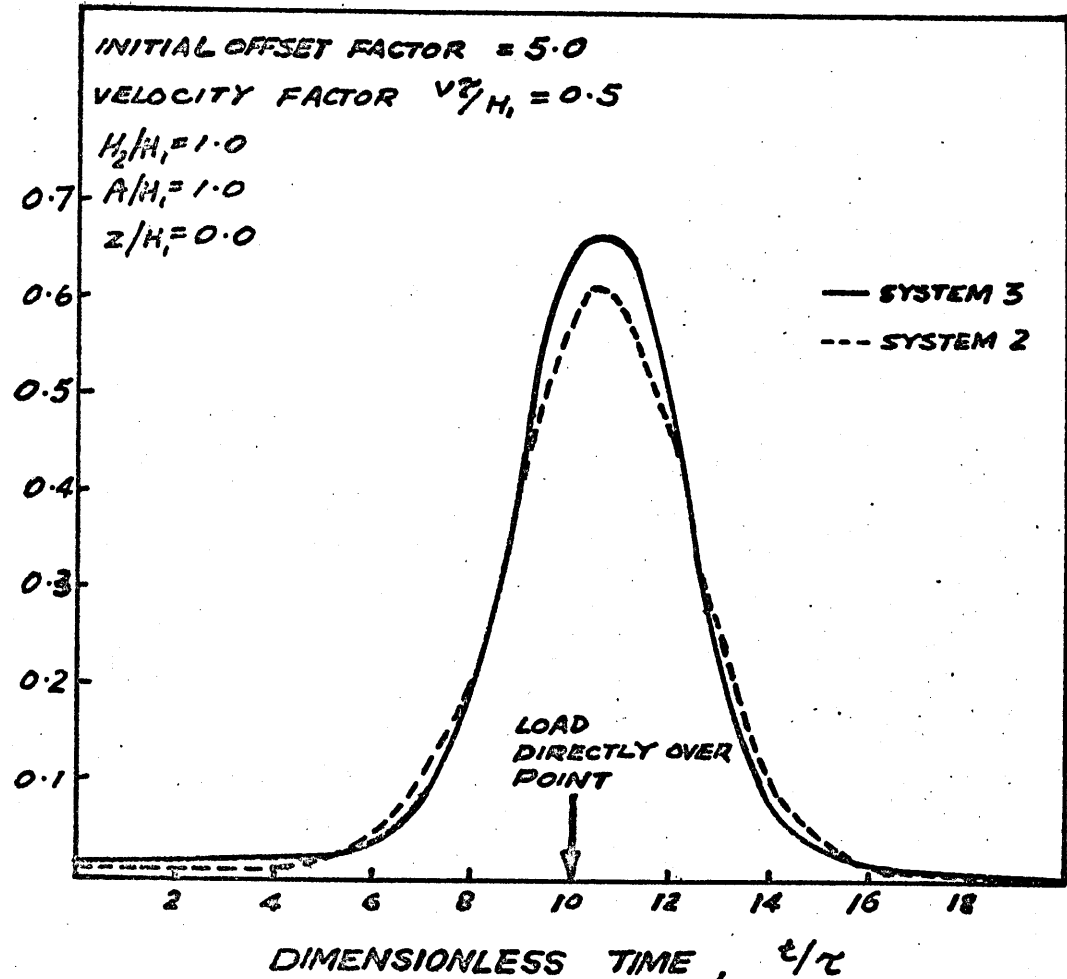


FIGURE 36. MOVING LOAD COMPARISON - VERTICAL STRESS FACTOR

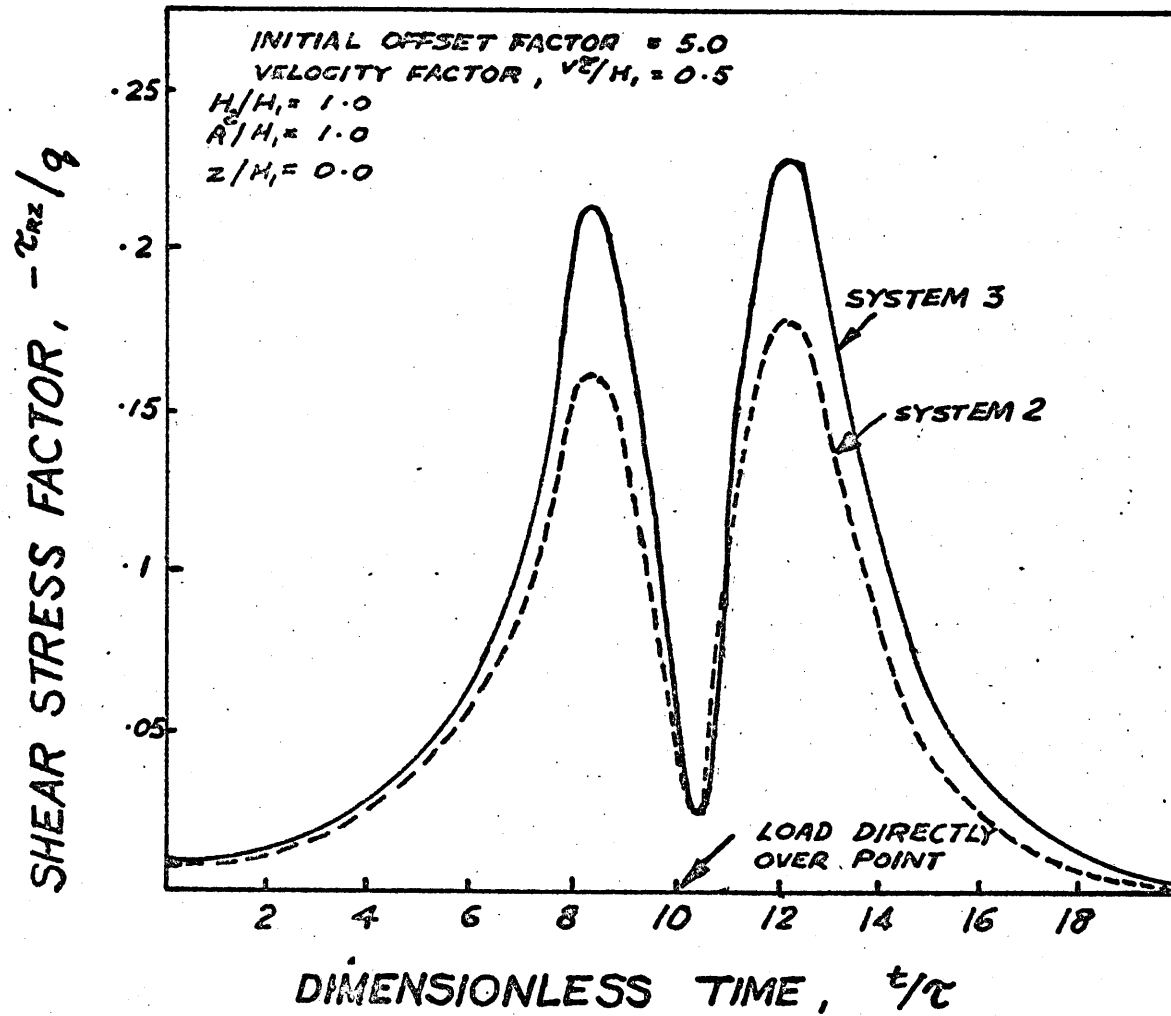


FIGURE 37. MOVING LOAD COMPARISON -
SHEAR STRESS FACTOR
SYSTEMS 2 AND 3

VERTICAL DEFLECTION FACTOR,

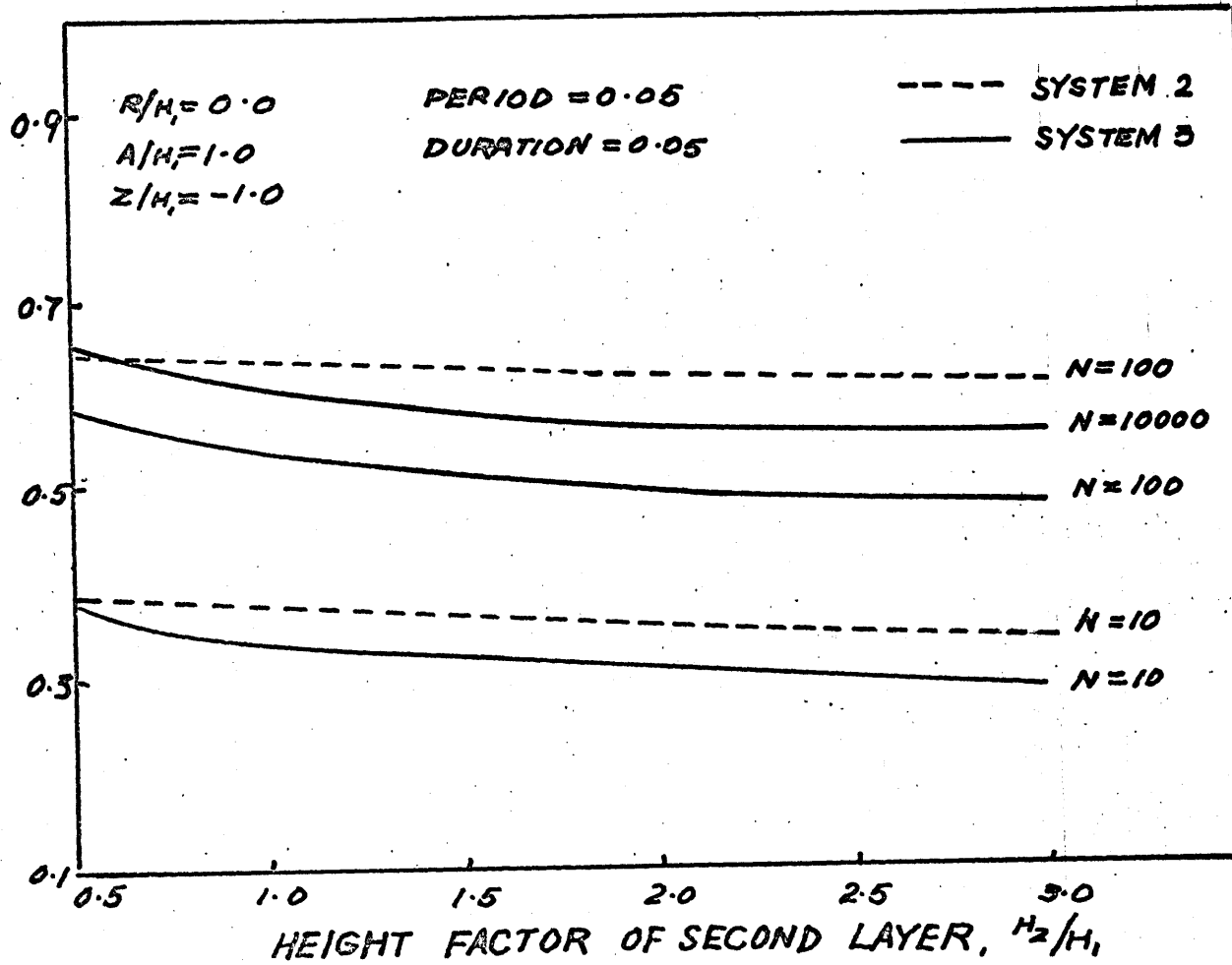
 $w_z / q \times D_3 (\infty) \times H_1$ 

FIGURE 38. INFLUENCE OF HEIGHT FACTOR ON VERTICAL DEFLECTION FACTOR

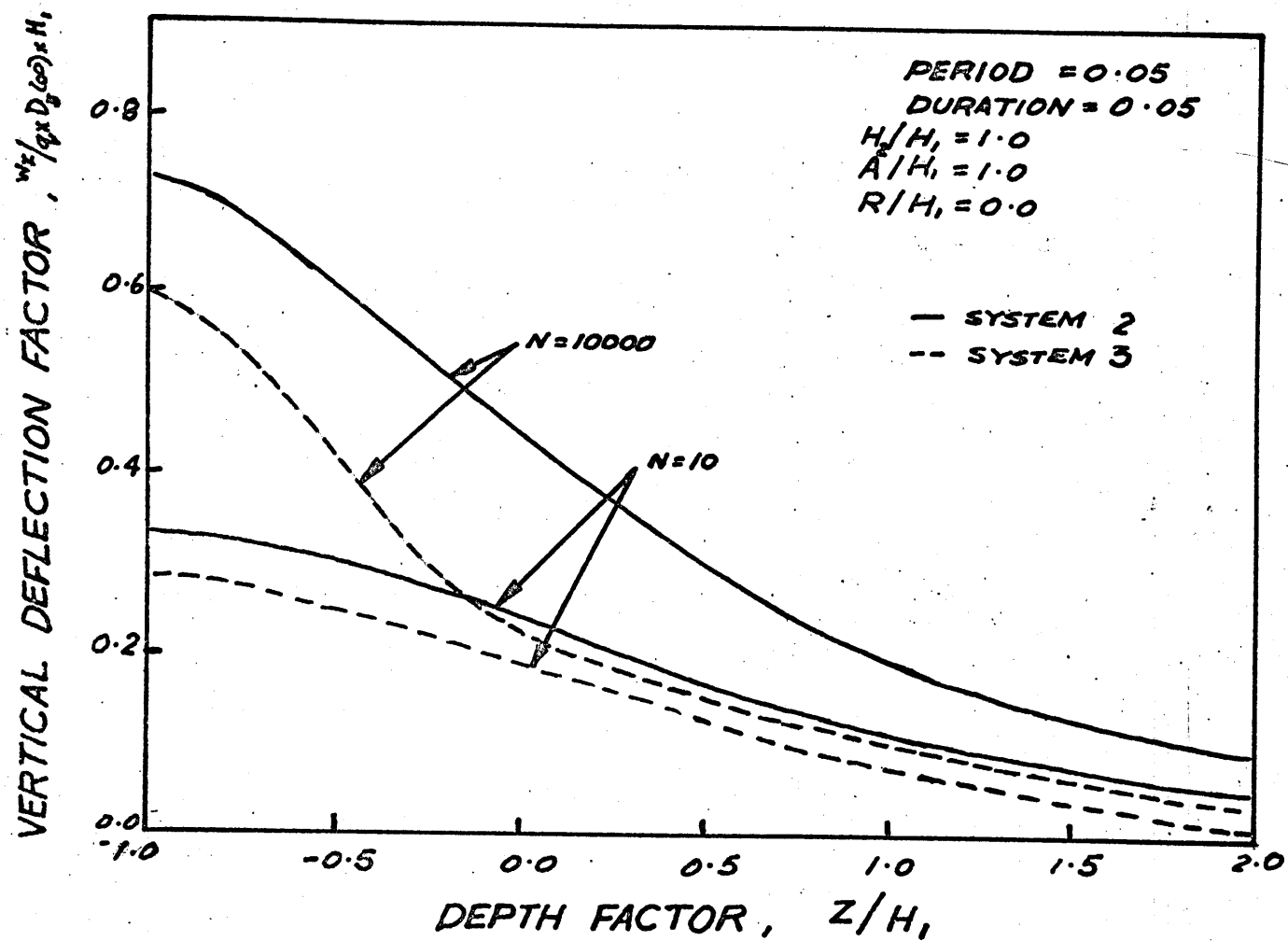


FIGURE 39. INFLUENCE OF DEPTH FACTOR ON VERTICAL DEFLECTION FACTOR.

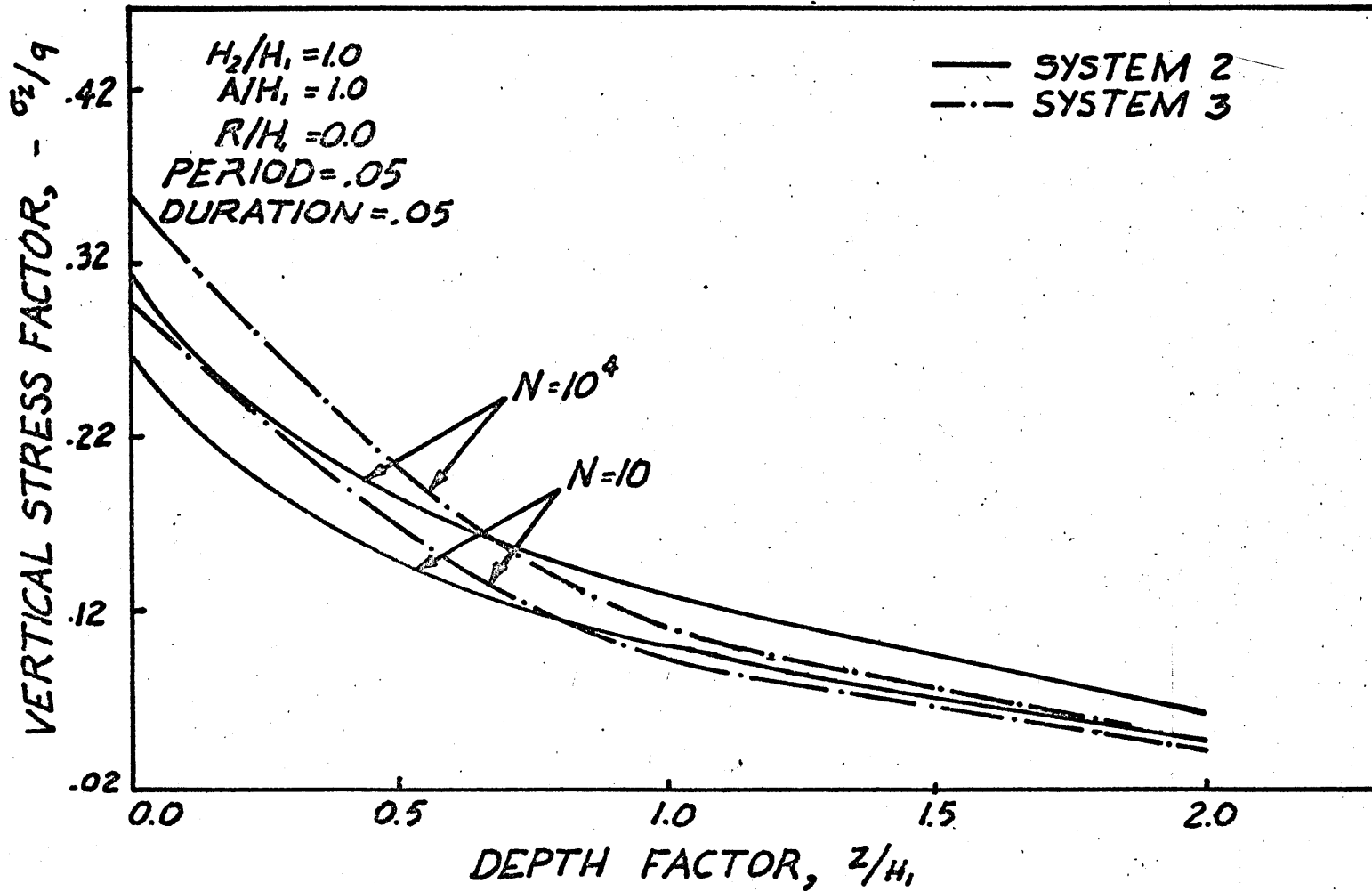


FIGURE 40.-INFLUENCE OF DEPTH FACTOR ON VERTICAL STRESS FACTOR.

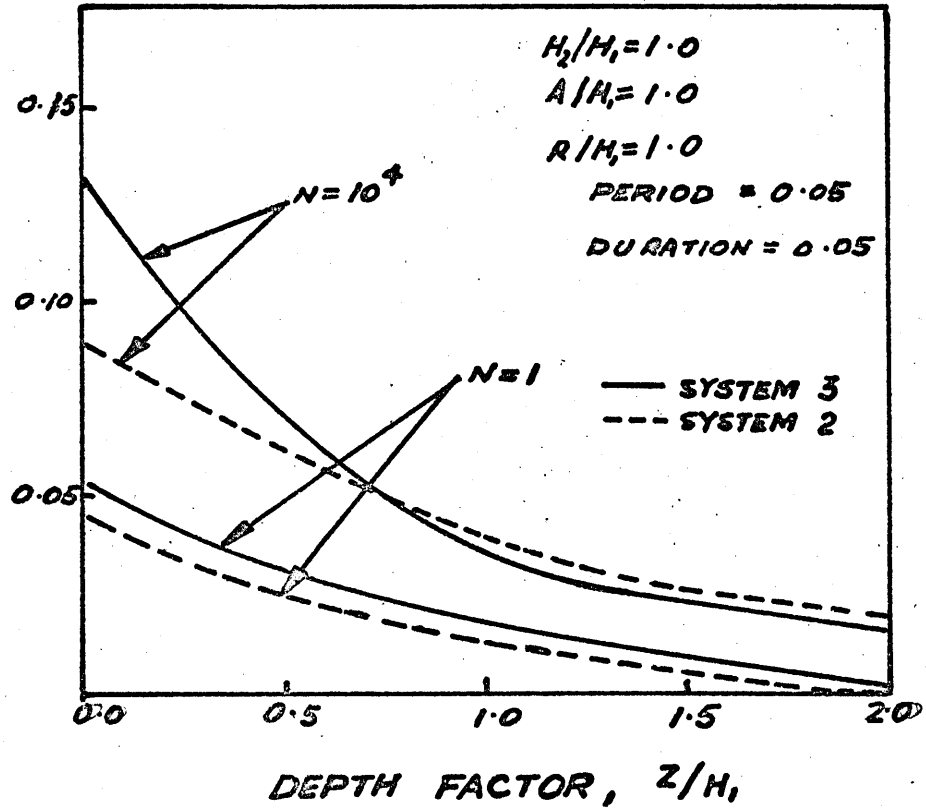
SHEAR STRESS FACTOR, $-\tau_{rz}/q$ 

FIGURE 41. INFLUENCE OF DEPTH FACTOR ON SHEAR STRESS FACTOR

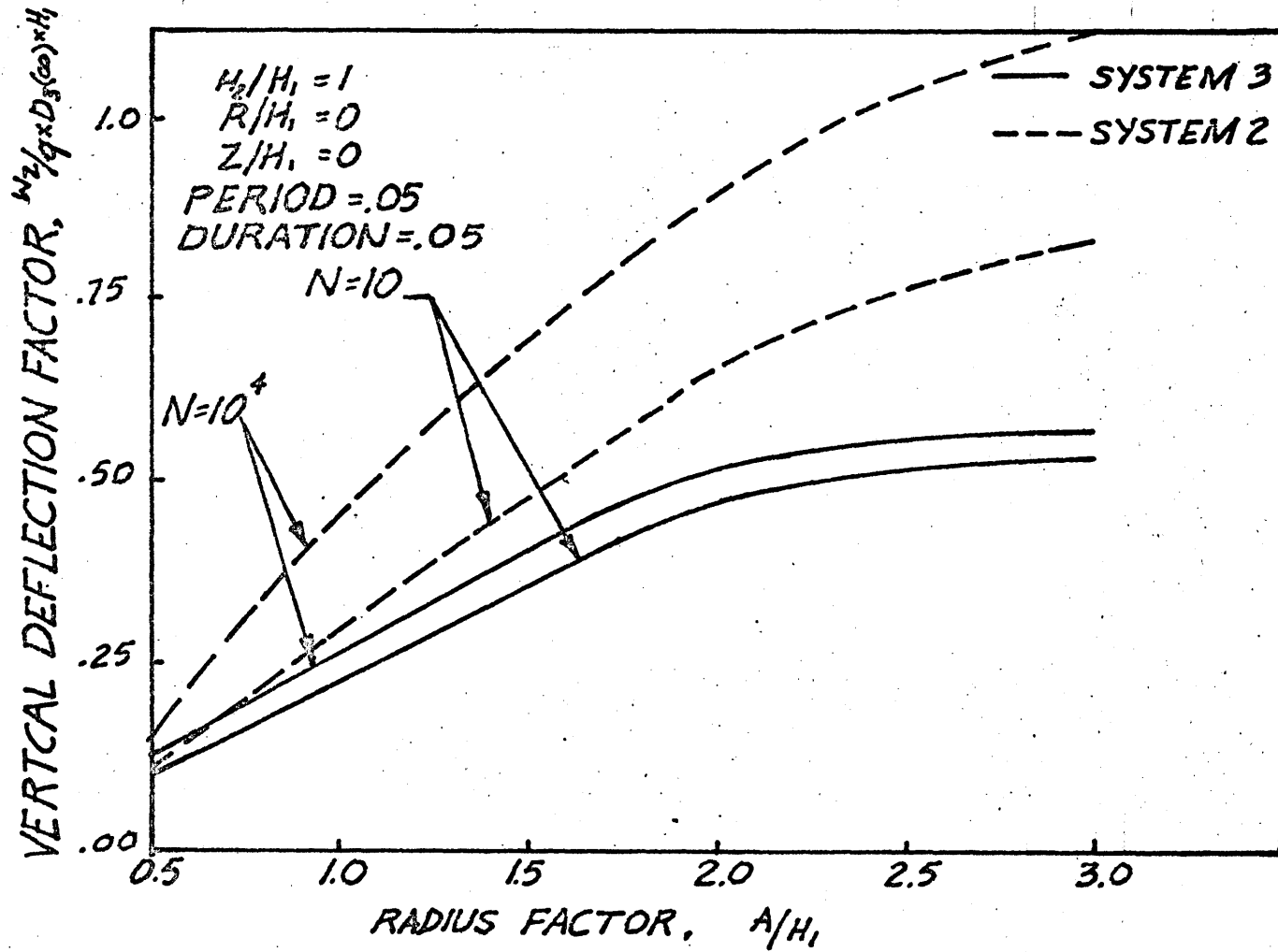


FIGURE 42.-INFLUENCE OF RADIUS FACTOR ON VERTICAL DEFLECTION FACTOR

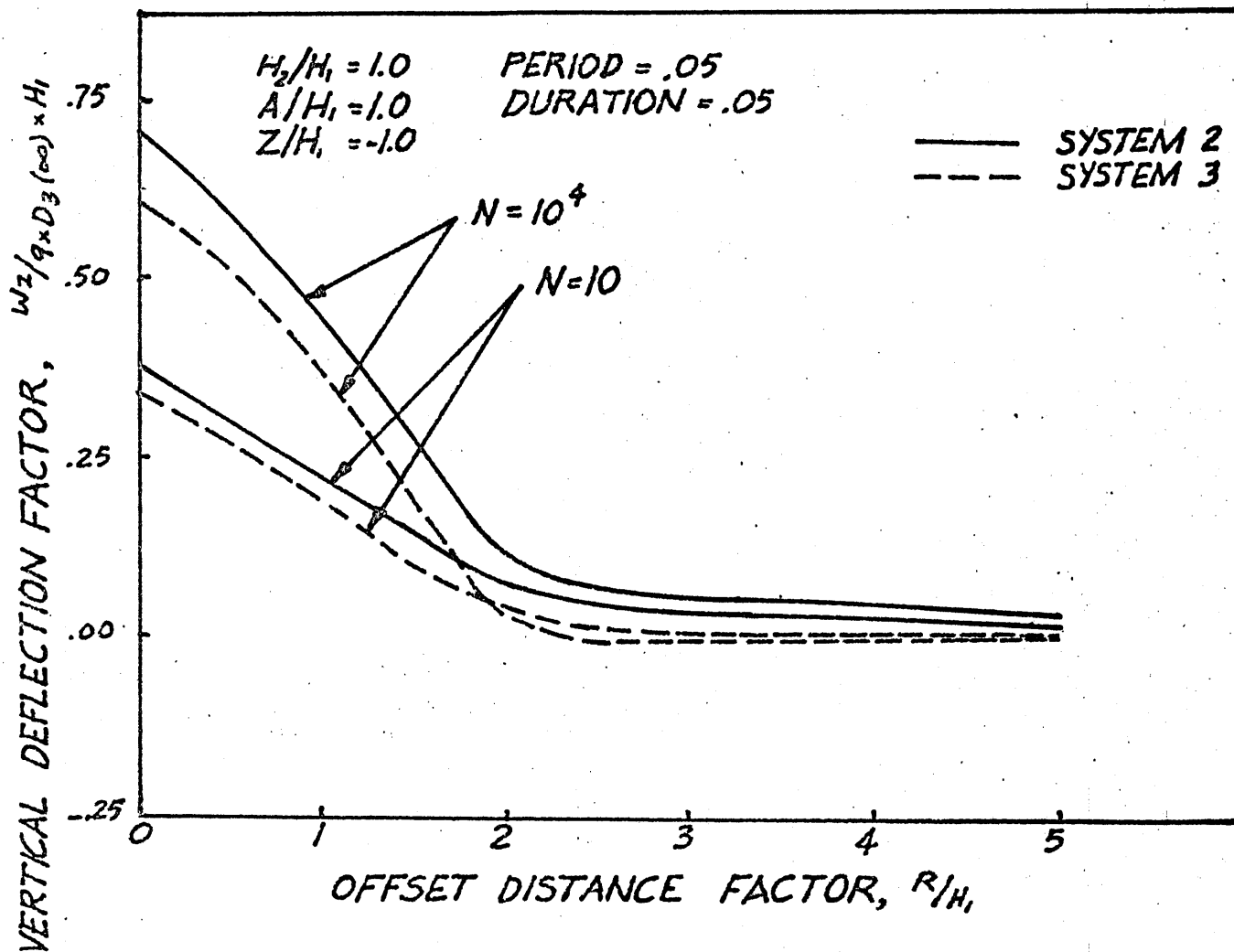


FIGURE 43.—INFLUENCE OF OFFSET DISTANCE FACTOR ON VERTICAL DEFLECTION FACTOR.

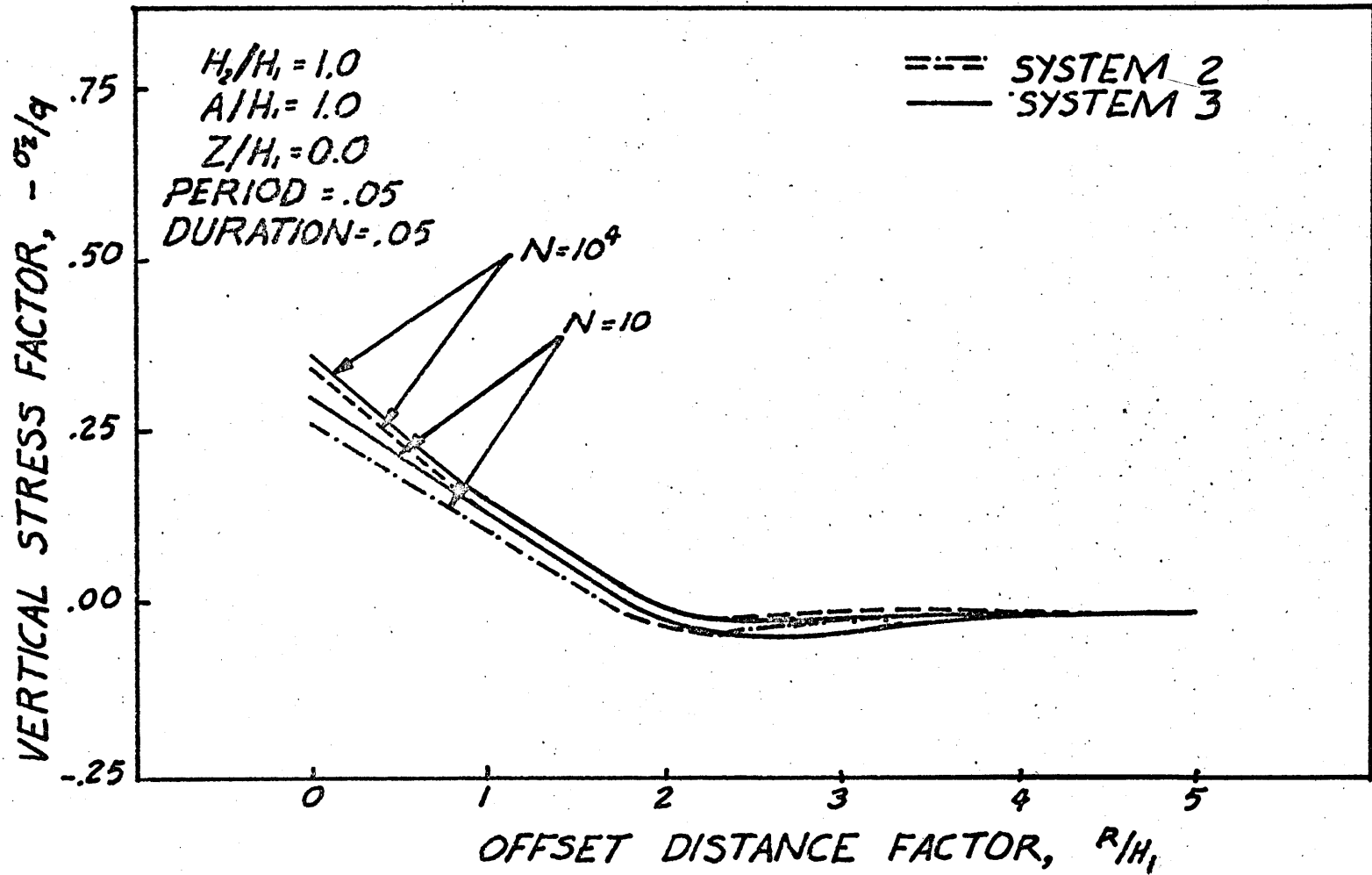


FIGURE 44. -INFLUENCE OF OFFSET DISTANCE FACTOR ON VERTICAL STRESS FACTOR.

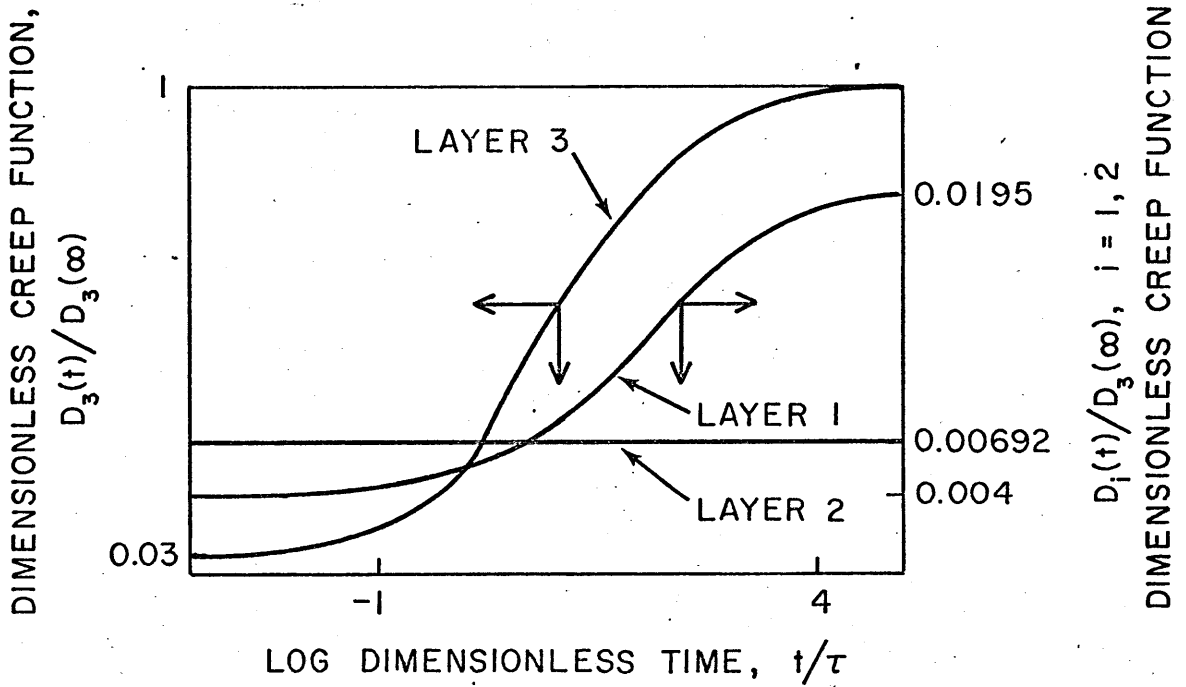
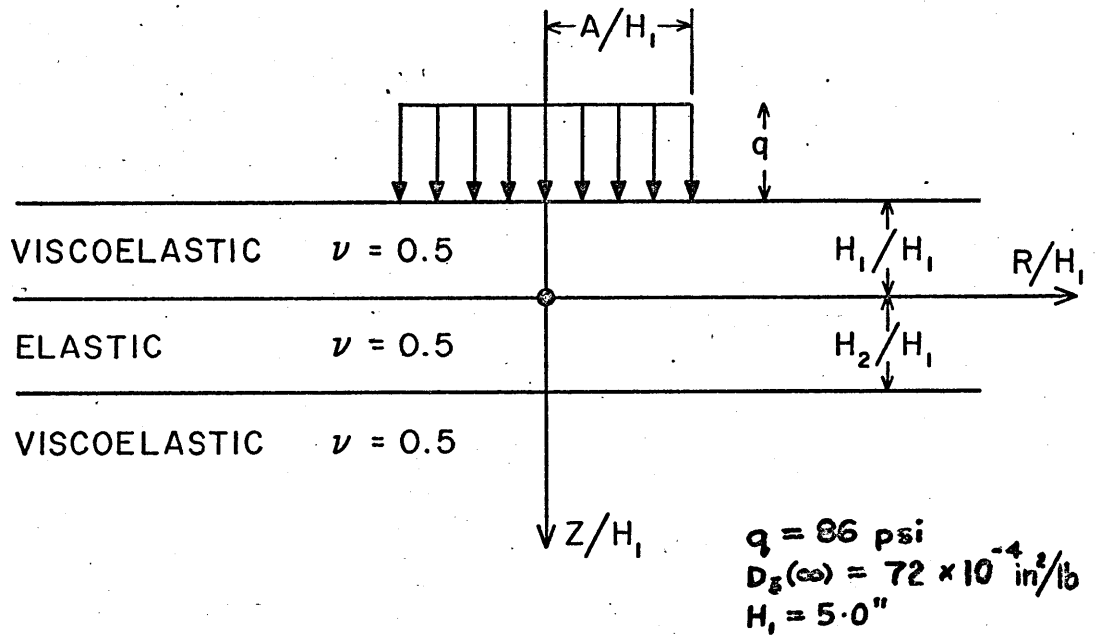


FIGURE 45. DIMENSIONLESS PAVEMENT SYSTEM NO. 6.

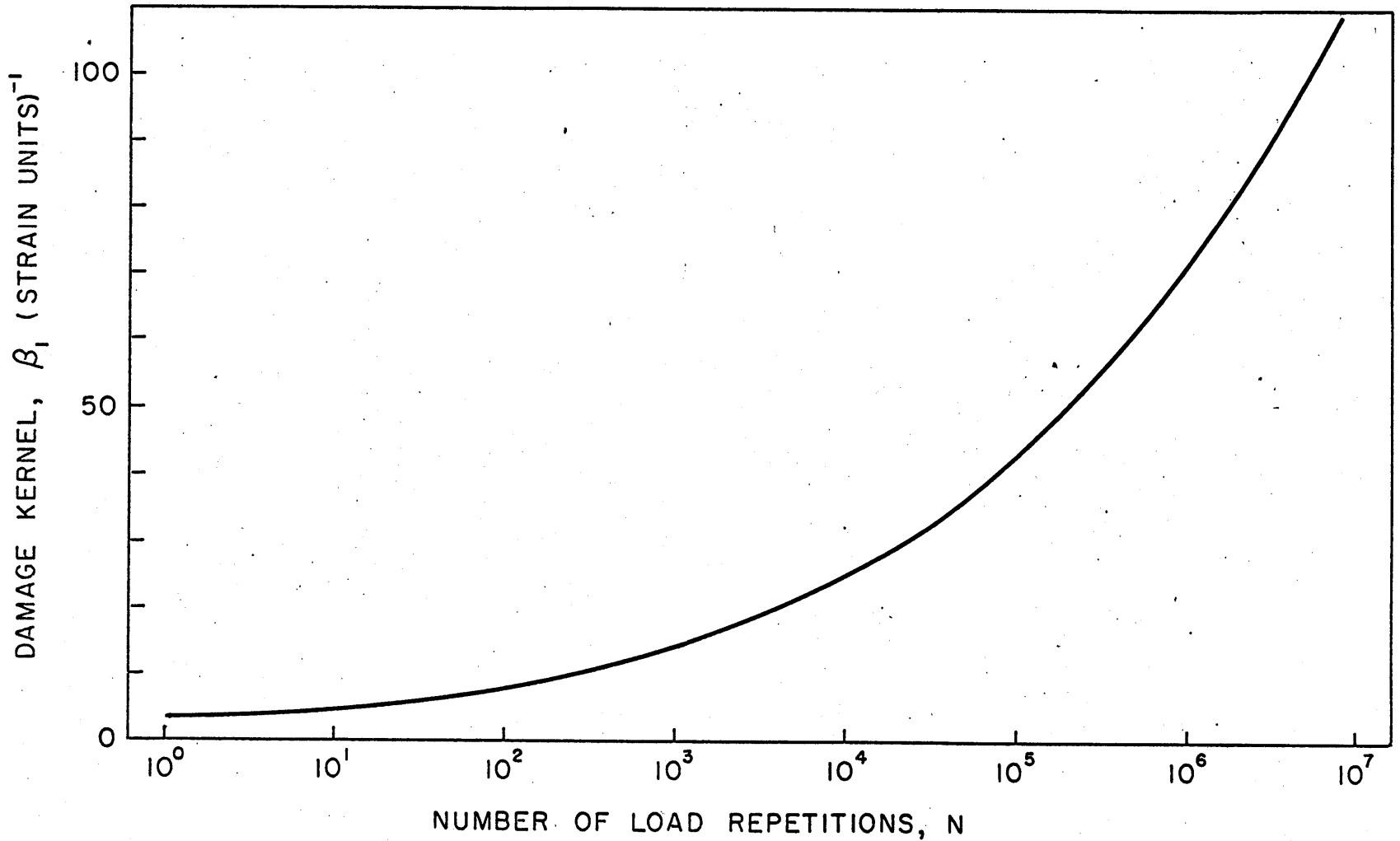


FIGURE 46. THE LINEAR KERNEL FUNCTION OBTAINED FROM THE FATIGUE EQUATION GIVEN IN THE TEXT.

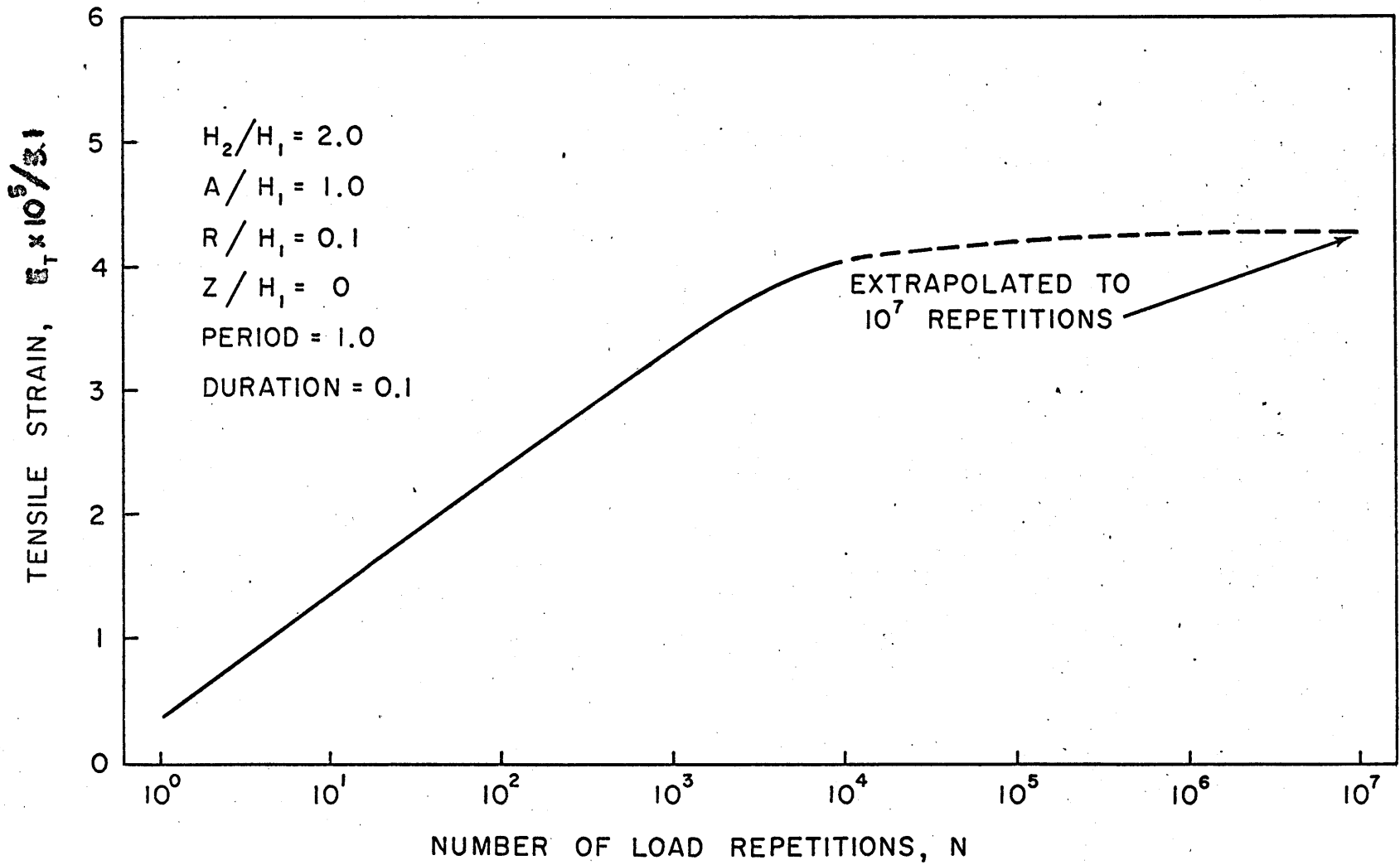


FIGURE 47. ACTUAL MANNER OF BUILD-UP OF TENSILE STRAIN AT THE BOTTOM OF THE SURFACE LAYER.

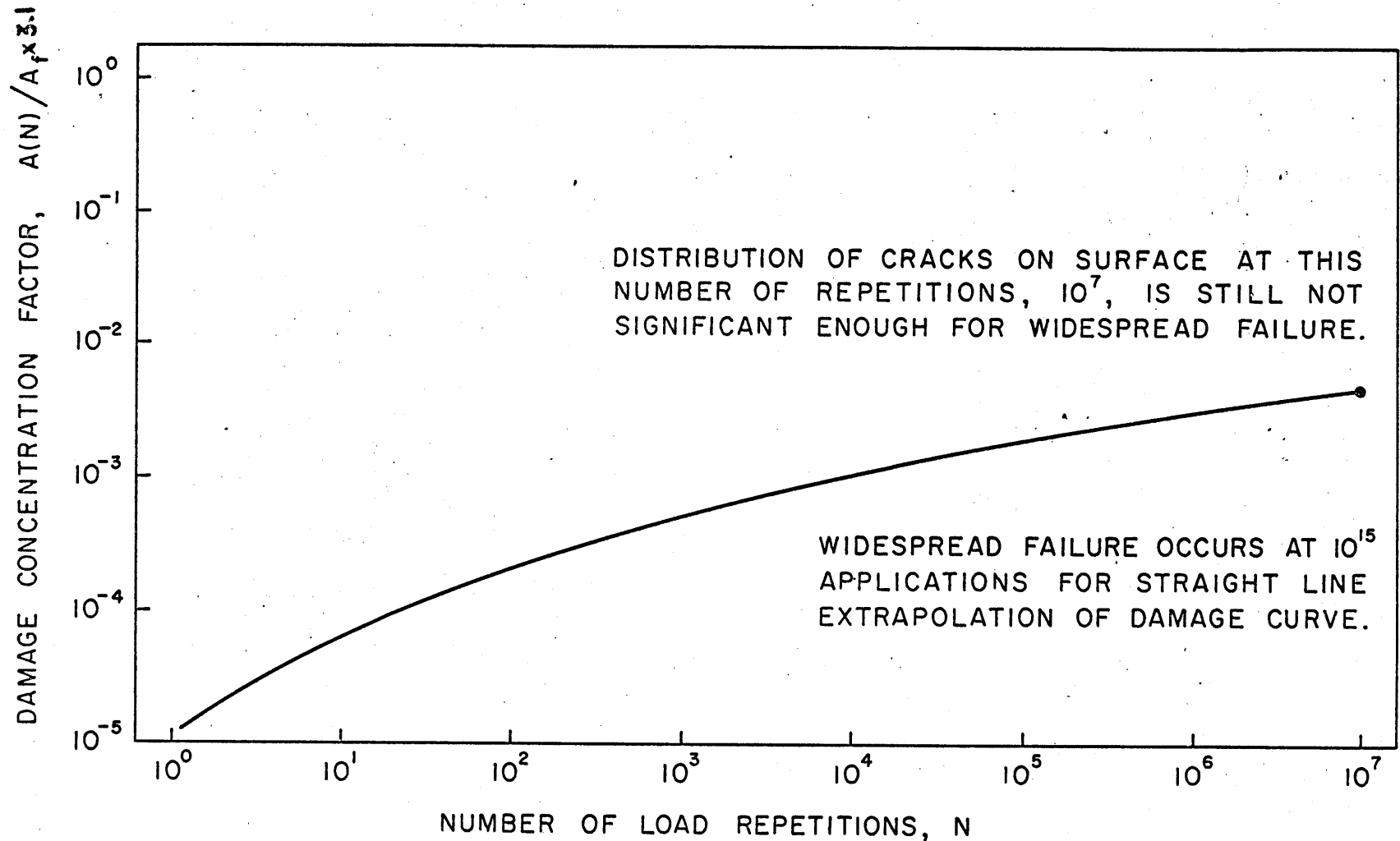


FIGURE 48. PREDICTION OF DAMAGE PROGRESSION IN ASPHALTIC CONCRETE IN SURFACE LAYER WHEN TENSILE STRAIN OBTAINED FROM MODEL I IS AS SHOWN IN FIGURE 47.

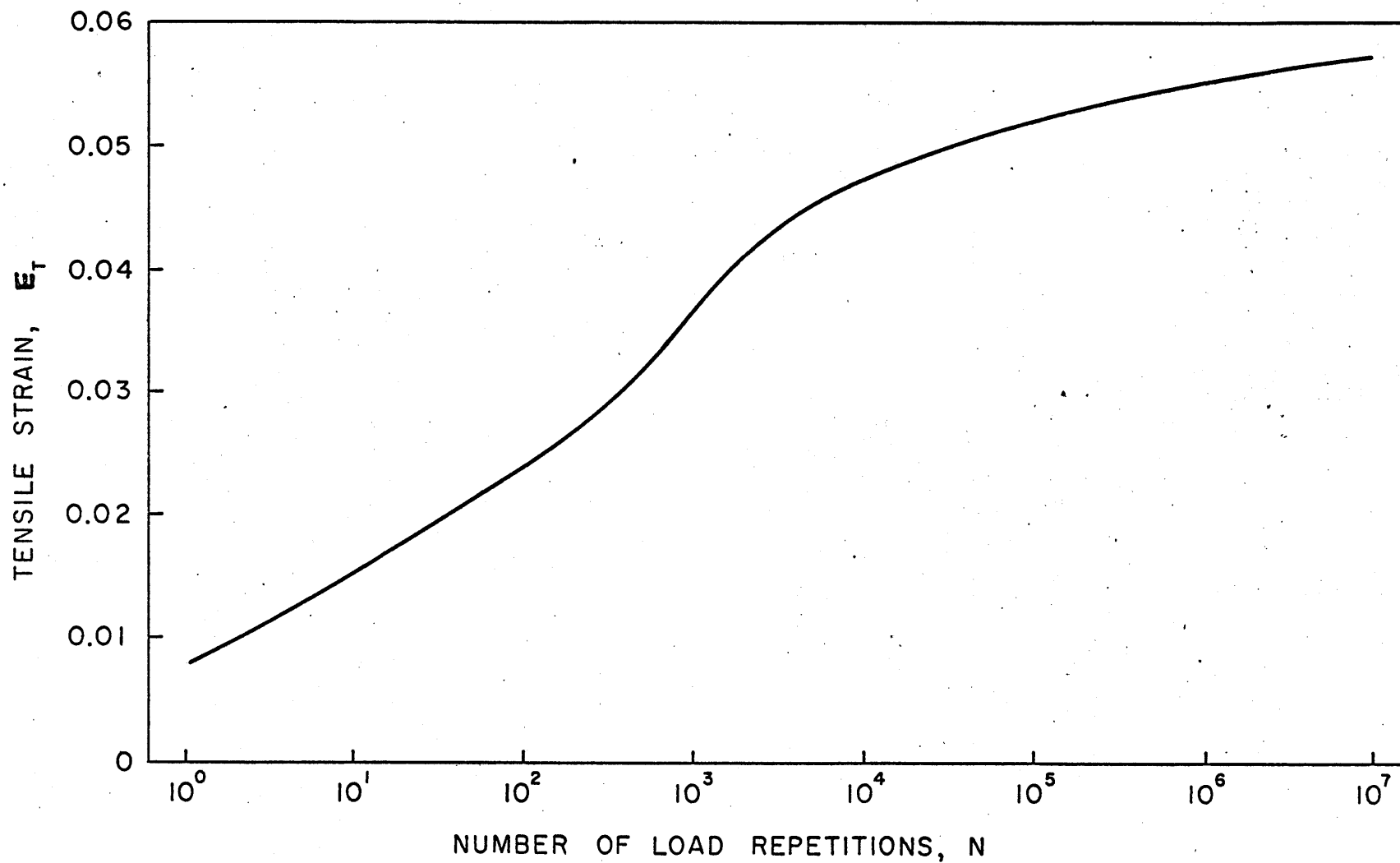


FIGURE 49. ASSUMED MANNER OF BUILD-UP OF TENSILE STRAIN AT THE BOTTOM OF THE SURFACE LAYER.

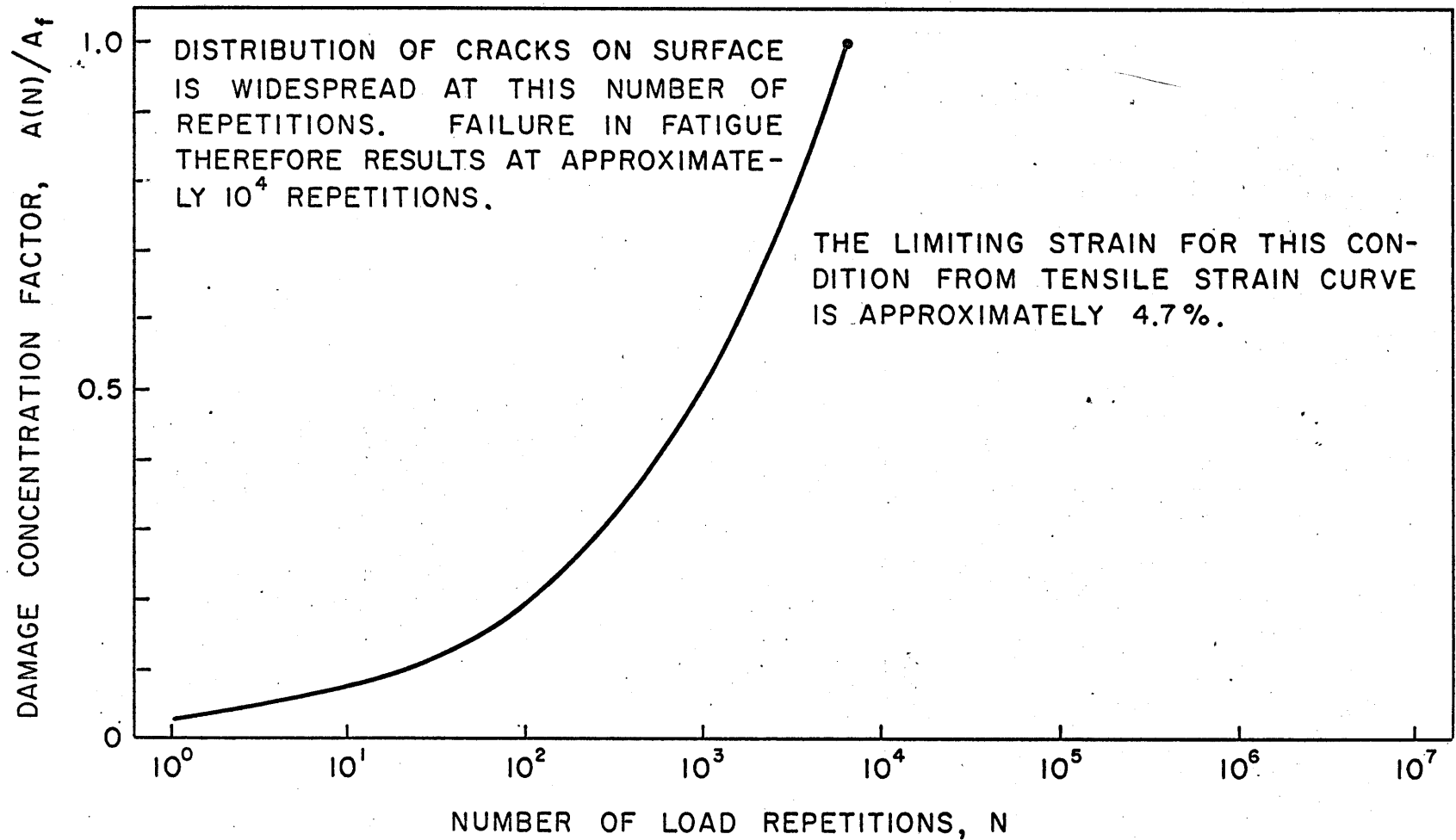


FIGURE 50. PREDICTION OF DAMAGE PROGRESSION IN ASPHALTIC CONCRETE IN SURFACE LAYER WHEN TENSILE STRAIN OBTAINED FROM MODEL I IS AS SHOWN IN FIGURE 49.

VII - CONCLUSIONS

In this study, two models have been presented to account for the primary and ultimate response behavior of a three layer linear viscoelastic system which can be considered as representative of a pavement structure in a given traffic and climatic environment.

The models can be used as a first approximation to rationally account for two of the currently observable factors responsible for the physical distress of such structures. On the one hand, the primary model may be employed to estimate the permanent deformation resulting from repetitions of load at a specified frequency; on the other hand, with the damage model, the fatigue life of the structure may be predicted.

The primary model is capable of identifying the indicators of structural inadequacy by predicting the magnitudes of the stresses and displacements induced at any point in the system due to load applications of the type considered in the study. When these magnitudes exceed allowable values set by experimental observation for the layer materials, macroscopic distress in the form of extensive cracking, and disintegration will result. The analysis can be made for different system geometries, different load characteristics, and different material properties which may be functions of both time and fixed

121

temperature. Consequently, it is possible to account for the influences of parameters such as the radius of the loaded area, the system geometry, the system properties, and the load configuration on the mechanical response of the system.

The systems framework within which this work has been undertaken is significant and points a direction in which future research and developmental plans in pavement technology should proceed. As suggested in the first chapter, a significant effort should be undertaken to develop reliable models for the assessment of the appropriate maintainability, reliability, and serviceability requirements of a particular pavement structure. To this end, some of the initial considerations in the development of such a program have been satisfied by the models presented.

VIII - SUGGESTIONS FOR FUTURE WORK

The models which have been utilised to analyse the response behavior of pavement systems are linear and deterministic in nature. In the development of the primary model, for instance, inertia and edge effects are neglected. It is assumed that the layer materials are linear, homogeneous, and isotropic, etc. For the damage model, only the linear aspects of damage behavior have been considered. The validity of such assumptions must, therefore, be further investigated. In this respect, two major areas of investigation seem to suggest themselves.

First, research must be conducted to develop realistic characterization methods for the materials employed in the building of pavement structures. Environmental actions have varying degrees of effect, some of which have already been discussed, depending on their history, distribution, and variation. A thorough study of environmental effects on roadway performance should, therefore, yield valuable information on the degree of linearity and uniformity of layer materials. From such studies, appropriate non-linear and stochastic models can be postulated. In addition, the need for laboratory testing of the paving materials under compound loading programs of the type encountered in the field cannot be over-emphasised. The results of such tests will aid in the development of damage kernels other than the linear

13)

type for distress under repeated loading. Methods of extrapolations to field conditions can then be postulated and tried out.

A second major area for further investigation is the determination of realistic inputs other than material properties into a suitable model for the stress and deformation analysis. This would require a proper identification of the space and time characteristics of the applied loads, and appropriate failure criteria for existing pavement structures. The model used should, therefore, incorporate layers that are finite and not infinite in horizontal extents.

With such an approach, edge effects can be accounted for. The model, as was mentioned before, should also possess realistic material properties. To this end, the viscoelastic analysis presented in this study is an improvement over currently used elastic ones, i.e., rate and accumulation effects have been accounted for, the rut depth can also be estimated. However, only distress in the form of fatigue has been considered. The other types of distress can be approached in a similar manner once they have been identified. Finally, the effects of inertia should also be investigated.

The above observations indicate that the actual model would be complex, since the interaction of all the aforementioned effects, some independent and some not so, must be accounted for. Similar techniques as the one used

in this study to connect a degree of cracking to a level of strain will have to be instituted to get a more realistic picture of performance. After all this is done, the problem can be attacked using the systems analysis approach discussed in Chapter I.

To conclude this section, it may be worthwhile to mention that the damage-model as presented is one dimensional. However, the possibility of multi-stress or strain behavior during damage propagation does exist, as borne out by the discussions on failure in Chapter II.

It may be true in the case of damage propagation under fatigue that a single one-dimensional stress or strain, rather than a tensorial quantity, governs the propagation. The only way to verify such suspicions will be to judiciously observe damage progression in real pavement structures so as to define a critical energy, stress or strain combination at failure. Once this has been done, the model can be modified accordingly. The next phase of the work should consider the application of stochastic methods to the present analysis so as to achieve more realistic response predictions.

IX-BIBLIOGRAPHY

1. Hudson, W.R., Finn, F.N., McCullough, B.F., Nair, K. and Vellerga, B.A., Systems Approach to Pavement Design, Final Report, NCHRP Project 1-10, Highway Research Board, March 1968.
2. von Karman, T., Mitt.Forch.Ver.Deut.Ing., pt. 118, 37-68 (1912)
3. Orowan, E., "Fracture and Strength of Solids, The Physical Society, Reports on Progress in Physics, Vol.XII, p. 185, 1949.
4. Hirata, M., Scientific Paper, Institute-Phys.Chem. Research, 16 (1931)187.
5. Joffe, A., International Conference of Physics II, the Solid State of Matter Phys.Soc.London(1934)72.
6. Yokobori, T., Journal of the Physics Society, Japan, 7(1951)44.
7. _____, Journal of the Physics Society, Japan 6(1951)81
8. _____, Journal of the Physics Society, Japan 7(1952)48
9. _____, Journal of the Physics Society, Japan 8(1953)265
10. Gladstone, S., Laidler, K.J. and Eyring, H., The Theory of Rate Processes, McGraw-Hill, New York, 1941.
11. Gnauss, W.G. "The Time Dependent Fracture of Visco-elastic Materials," Proceedings of the First International Conference on Fracture, Sendai, Japan, 1965.
12. Weibull, W., Ingen.Vetensk.Akad. (Stockholm) Proc.No. 151 (1939)a; (1939)b, Ibid., Proc. No. 153
13. Frenkel, J. and Kontorova, T.A., "A Statistical Theory of the Brittle Strength of Real Crystals," Journal of Physics U.S.S.R., 7, 108 (1943).

14. Griffith, A.A., Phil. Trans. Roy. Soc. A, 221, 163 (1920); First International Congress of Applied Mechanics (Delft) 5, (1924)
15. Nadai, A., Theory of Flow and Fracture of Solids, Vol. 1, Second Edition, McGraw-Hill Book Company, 1950.
16. Ford, H., Advanced Mechanics of Materials, Wiley, 1963.
17. Bishop, A.W., "The Strength of Soils as an Engineering Material." Geotechnique, Vol. 16, No. 2, June 1966, pp. 99-128.
18. McEvily, A.J. and Boettner, R.C. "On Fatigue Crack Propagation in F.C.C. Metals", Acta Metallurgica, Vol. 11, p. 725, 1963.
19. Grosskreut, J.C., "A Critical Review of Micro-mechanics in Fatigue," Fatigue an Interdisciplinary Approach, Proceedings of the 10th Sagamore Army Mat. Res. Conf., Syracuse University of Press, 1964.
20. McEvily, A., J., Boettner, R.C. and Johnston, T.L. "On the Formation and Growth of Fracture Cracks in Polymers," Fatigue an Interdisciplinary Approach, Proceedings of the 10th Sagamore Army Mat. Res. Conf., Syracuse University Press, 1964.
21. Erikson, William H. and Work, Clyde E., "A Study of An Accumulation of Fatigue Damage in Steel," Proceedings, ASTM, Vol. 61, 1961
22. Corten, H.T. and Dolan, T.J., "Cumulative Fatigue Damage," Proceedings, International Conference on the Fatigue of Metals. Am. Soc. Mech. Engrs., 1956.
23. de Forest, A.V., "The Rate of Growth of Fatigue Cracks" Transactions, American Society of Mechanical Engineers, Vol. 58, pp. A23-25, 1936.
24. Coleman, B.D. "Application of the Theory of Absolute Reaction Rates to the Creep Failure of Polymeric Filaments" Journal of Polymer Science, Vol. XX, 1956
25. Machlin, E.S. "Dislocation Theory of the Fatigue of Metals," National Advisory Committee for Aeronautics, Technical Notes, 1948.

26. Mott, N.F. Symposium on Dislocations in Crystals, International Conference Theoretical Physics, held at Nikko, Japan, September 1953, Abstract 56.
27. Miner, M.A., "Cumulative Damage in Fatigue," Journal of Applied Mechanics, Vol. 4, Trans. ASME Vol. 12, 1945 pp. A159-A164.
28. Valluri, S.R., "A Unified Engineering Theory of High Stress Level Fatigue," Institute of the Aeronautical Sciences Paper Number 61-149-1843, June 1961.
29. Newmark, N.M., Fatigue and Fracture of Metals, Wiley and Sons, 1952.
30. Williams, M.L., "Initiation and Growth of Visco-elastic Fracture," Proceedings of the First International Conference on Fracture, Volume 2. Sendai, Japan, 1965.
31. Frost, N.E., "The Growth of Fatigue Cracks," First International Conference on Fracture, Sendai Japan, Vol. 3, 1965.
32. Paris, P. and Erdogan, F.J. "A Critical Analysis of Crack Propagation Laws" Journal of Basic Engineering, Transaction of ASME, Series D, Vol. 85, 1963.
33. Weiss, V., "Analysis of Crack Propagation in Strain Cycling Fatigue," Fatigue an Interdisciplinary Approach, Proceedings of the 10th Sagamore Army Mat.Res.Conf., Syracuse University, 1964.
34. Liu, Discussion on article by P.C. Paris, "The Fracture Mechanics Approach to Fatigue," Fatigue as an Interdisciplinary Approach, Proceedings 10th Sagamore Army Mat.Res.Conf. Syracuse University Press, 1964.
35. Dong, R.G. "A Functional Cumulative Damage Theory and its Relation to two well-known theories," Lawrence Radiation Lab., University of California, UCRL, Jan., 1967.
36. Davis, M.M., McLeod, N.W. and Bliss, E.J. "Symposium on Pavement Design and Evaluation-Report and Discussion of Preliminary Results," Proceedings, Canadian Good Roads Association, 1960.

37. Quinn, Bayard E., and Thompson, David R., "Effect of Pavement Condition Upon Dynamic Vehicle Reactions" HRB, 1962.
38. Yoder, E.J. "Flexible Pavement Deflections - Methods of Analysis and Interpretation" Purdue University Engineering Reprints CE19A, July 1963.
39. The WASHO Road Test, HRB, Special Report 22.
40. Clegg, B. and Yoder Eldon J., "Structural Analysis and Classification of Pavements," Fourth Australia-New Zealand Conference on Soil Mechanics and Foundation Engineering.
41. Committee on Structural Design of Roadways, "Problems of Designing Roadway Structures," Transportation Engineering Journal, Proceedings ASCE, May 1969.
42. Fung, Y.C., Foundations of Solid Mechanics, Prentice-Hall, Inc.
43. Boussinesq, J., Application des Potentials, Paris, 1885.
44. Terazawa, K., Journal of the College of Sciences, Imperial University, Tokyo, December 1916.
45. Love, A.E.H., "The Stress Produced on a Semi-Infinite Body by Pressure on part of the Boundary," Philosophical Transactions of the Royal Society, Series A., Vol. 228.
46. Ahlvin, R.G. and Ulery, H.H. "Tabulated Values for Determining the Complete Pattern of Stresses, Strains and Deflections Beneath a Uniform Circular Load on a Homogeneous Half Space," Highway Research Board Bulletin, No. 342, 1962.
47. Westergaard, H.M., "Stresses in Concrete Pavements Computed by Theoretical Analysis," Public Roads, Vol. 7, No. 2, April, 1926.
48. Burmister, D.M., "The General Theory of Stresses and Displacements in Layered Soil System, I, II, III," Journal of Applied Physics, Vol. 16, No. 2, pp. 89-96; No. 3, pp. 126-127; no. 5, pp. 296-302; 1945.
49. Burmister, D.M., "The Theory of Stresses and Displacements in Layered Systems and Application to

the Design of Airport Runways," Highway Research Board Proceedings, 1954.

50. Achenbach, J. D. and Sun, C., "Dynamic Response of a Beam on a Viscoelastic Subgrade," Proceedings of the American Society of Civil Engineers, Journal of Engineering Mechanics, Vol. 91, No. EM5, October 1965.
51. Kraft, D. C. "Analysis of a Two-Layer Viscoelastic System," Proceedings of the American Society of Civil Engineers, Journal of the Engineering Mechanics Division, Vol. 91, No. EM6, Part I, December 1965.
52. Pister, K.S., "Viscoelastic Plates on Viscoelastic Foundations" Journal of the American Society of Civil Engineers pp. 43-54. February, 1961.
53. Schapery, R.A., "Approximate Methods of Transform Inversion for Viscoelastic Stress Analysis," Aeronautical Research Laboratory, Office of Aerospace Research, U. S. Air Force, Contract No. AF33(616)-8399; GALCIT 119, 1962.
54. Ashton, J. E. and Moavenzadeh, F., "The Analysis of Stresses and Displacements in a three-layered Viscoelastic System," International Conference on the Structural Design of Asphalt Pavements, 1967.
55. Porter, O.J., "Foundations for Flexible Pavements," Proceedings, Highway Research Board, Vol. 22, 1942.
56. Nijboer, L.W. and van der Poel, C., "A Study of Vibration Phenomena in Asphaltic Road Constructions," Proceedings, Association of Asphalt Paving Technology, Vol. 22, 1953, pp. 197-231.
57. Hveem, R. N., "Pavement Deflections and Fatigue Failures," Highway Research Board, Bulletin 114, 1955, pp. 43-73.
58. Seed, H.B., Chan, C.K. and Lee, C.E., "Resilience Characteristics of Subgrade Soils and Their Relation to Fatigue Failures in Asphalt Pavements," International Conference on the Structural Design of Asphalt Pavements, Ann Arbor, Michigan, 1962.
59. Hennes, R. G. and Chen, H.H., "Dynamic Design of Bituminous Pavements - the Trend in Engineering," University of Washington, 1950.

60. Monismith, C.L., "Flexibility Characteristics of Asphalt Paving Mixtures," Proceedings AAPT, Vol. 27 1958, pp. 74-106.
61. Saal, R.N.J. and Pell, P.S., "Fatigue of Bituminous Road Mixes," Kolloid Zeitschrift. Bd. 171, Heft 1, 1960, pp. 61-71.
62. Pell, P.S. "Fatigue Characterisitcs of Bitumen and Bituminous Road Mixes," Proceedings, International Conference on the Structural Design of Asphalt Pavements, Ann Arbor, Michigan (1962) pp. 310-323.
63. Monismith, C.L. "Significance of Pavement Deflection" Proceedings AAPT, Vol. 31, 1962, pp. 231-253.
64. "Three Year Evaluation of Shell Avenue Test Road," 44th Annual Meeting HRB (1965).
65. Deacon, J.A., Fatigue of Asphalt Concrete. Graduate Report Institute of Transportation and Traffic Engineering, University of California, Berkeley, 1965.
66. Larew, H.G., and Leonards, G.A., "A Strength Interior for Repeated loads," Proceedings HRB, Vol. 41 (1962) pp. 529-556.
67. Monismith, C.L., "Asphalt Mixture Behavior in Repeated Flexure," Report No. TE 65-9 Department of Civil Engineering, Institute of Transportation and Traffic Engineering, University of California, Berkeley.
68. Monismith, C.L., Kasianchuk, D.A., and Epps, J.A., "Asphalt Mixture Behavior in Repeated Flexure: A Study of an In-Service Pavement near Morro Bay, California," Report No. TE 67-4, Department of Civil Engineering, Institute of Transportation and Traffic Engineering, University of California, Berkeley.
69. Deacon, J.A., and Monismith, C.L. "Laboratory Flexural Fatigue Testing of Asphalt Concrete With Emphasis on Compound Loading Tests," HRR No. 158, HRB, Washington, D. C.
70. Herrera, I. and Gurtin, M.E., "A Correspondence Principle for Viscoelastic Wave Propagation," Quarterly of Applied Mathematics, Vol. 22, No. 4, January 1965.

71. Moavenzadeh, F., and Elliott, J.F., "Moving Loads on a Viscoelastic Layered System," Research Report R68-37, Department of Civil Engineering, Materials Research Laboratory, School of Engineering, Massachusetts Institute of Technology, Cambridge, Mass. June, 1968.
72. Moavenzadeh, F. and Ashton, J.E., "Analysis of Stresses and Displacements in a Three-Layer Viscoelastic System," Research Report, R67-31, Department of Civil Engineering, Materials Research Laboratory, Massachusetts Institute of Technology, Cambridge, Massachusetts, August, 1967.
73. Churchill, R.V., Modern Operational Mathematics In Engineering, McGraw-Hill, New York, 1944.
74. Gross, B., Mathematical Structure of the Theories of Viscoelasticity, Ed. Herman, 1953.
75. Hopkins, I.L. and Hamming, R.W., "On Creep and Relaxation" Journal of Applied Physics, Vol. 28, pp. 906-909, 1957.
76. Herrmann, C.R. and Ingram, C.E., "The Analytical Approach and Physics of Failure Technique for Large Solid Rocket Reliability," Tempo Report, General Electric, Santa Barbara, 1961.
77. Goldman, A.S. and Slattery, T.B., Maintainability, A Major Element of Systems Effectiveness, John Wiley and Sons, Inc., New York, 1964.
78. Paris, P.C. "The Fracture Mechanics Approach to Fatigue," Fatigue, An Interdisciplinary Approach, Proceedings of the 10th Sagamore Army Materials Research Conference, Syracuse University Press, 1964.
79. Tobolsky, Arthur V. "Stress Relaxation Studies of the Viscoelastic Properties of Polymers", Journal of Applied Physics, Volume 27, Number 7, July, 1956.
80. Burmister, Donald M., "Applications of Layered System Concepts and Principles to Interpretations and Evaluations of Asphalt Pavement Performances and to Design and Construction", International Conference on the Structural Design of Asphalt Pavements, University of Michigan, 1962.

81. Barksdale, Richard D. and Leonards, Gerald A.,
"Predicting the Performance of Bituminous Surfaced
Pavements". Proceedings of the Second International
Conference on the Structural Design of Asphalt
Pavements, University of Michigan, 1967.

BIOGRAPHY

John Fayi Elliott was born on July 22, 1939 in Freetown, Sierra Leone. He attended the Saint Edward Secondary School in Freetown, on a governmental scholarship and graduated with highest distinction in 1957, obtaining a first grade certificate from the West African Examinations Council.

He won a national scholarship to the University of Sierra Leone in 1958 and graduated with a Diploma in Civil Engineering in 1961. He then worked for a year in the Public Works Department, New England, Freetown as an Engineering Assistant. In this capacity he was in charge of the Soil Mechanics Laboratory and, also got involved in road surveying.

The author then entered the Ohio State University on a scholarship won in June 1961. He enrolled in the honors program of the engineering department at Ohio State University and graduated in June and September 1966 with a B.S. and an M.S. in Civil Engineering having Soil Mechanics as a major field.

He enrolled in the graduate program at M.I.T. immediately afterwards and has worked in the Materials Division, of the Civil Engineering Department as a

Research Assistant and Part-time Instructor since September, 1966. In September of 1967, he won an African Graduate Fellowship jointly sponsored by his home government and that of the United States of America.

He has co-authored a research report to the Bureau of Public Roads under the supervision of Prof. Moavenzadeh. This report is entitled "Moving Loads on a Viscoelastic Layered System".

He is a member of Chi Epsilon, the National Civil Engineering Honorary, the M.I.T. chapter of the Society of Sigma Xi, and Bellows, a Hall honorary at the Ohio State University. The author is an Associate Member of the American Society of Civil Engineers.

He expects to graduate with a Ph.D in Civil Engineering Materials in September 1969.

XI-Appendices

APPENDIX A

Definitions of Symbols

P_i	performance level at time $t=t_i$
D_i	degree of damage accumulated from zero history of load application to time $t=t_i$
γ_{ij}	a set of variables or a tensor responsible for causing damage
$l(t)$	life remaining in a material or structure (at time t) where it is under an arbitrary loading history
$\beta_i()$	linear and non-linear damage kernels
$\beta_{ij}()$	linear and non-linear damage kernels
$H_{ij}()$	a tensor responsible for causing damage
B_L	an unacceptable level of performance
M_R	Resilient Modulus
v	distortional velocity
$\sigma_r, \sigma_\theta, \sigma_z, \tau_{rz}$	stress components in cylindrical coordinates
w, u	displacement components in cylindrical coordinates
∇^2	the Laplacian Operator
$\psi(m, t)$	system function
$D_r(t)$	creep function
$E_r(t)$	relaxation modulus
$SR(t)$	response function

UF(t) input function
A(S), A_{ij}(S) damage concentration
 $\frac{A(S)}{A_f}$ damage concentration factor
l(N) life remaining after N repetition
L / full life

APPENDIX B

Definitions

- PAVEMENT:** As used in this study, it is the composite of the surface, base, and subgrade layers, i.e., the entire structure.
- SERVICEABILITY:** The ability of the pavement to serve mixed truck and automobile traffic. In practical terms, it is a subjective value determined from a user's conception or perception of the level of competence at which the pavement is executing its multi-purpose functions. (39)
- a. Spreading the wheel load to match the supporting power of the subgrade.
 - b. Providing traction and a smooth riding surface.
 - c. Protecting the subgrade from deterioration caused by the ravages of the climatic conditions.
- RELIABILITY:** The probability that the pavement will perform its stated functions satisfactorily for a given period of time under a given

set of environmental conditions. It accounts for the variability and uncertainty often encountered in nature and therefore automatically considers the role of chance in the design process (76).

MAINTAINABILITY: The characteristics (both qualitative and quantitative) of material design and installation which make it possible to meet operational objectives with an optimum expenditure of maintenance effort (manpower, personnel skill, test equipment, technical data, and maintenance support facilities under operational environmental conditions in which scheduled and unscheduled maintenance will be performed.

A More Precise Definition

Quantitative: The probability that an item will be restored to specified conditions within a given period of time when maintenance action is performed in accordance with specified procedures and available resources (77),

APPENDIX C

List of Figures

		<u>Page</u>
Figure 1.	Block Diagram of the Pavement System After Hudson, et al.	136
Figure 2.	Crack Length vs. Number of Cycles of Load, After Deforest on SAE 1020 Steel Specimens.	137
Figure 3.	Damage vs. Number of Load Cycles for Different Constant Stress Levels.	138
Figure 4.	Interaction Free Damage Law.	138
Figure 5.	Non-Interaction Free Damage Law.	138
Figure 6.	Two-Dimensional Simulation of the Performance of a Pavement Structure.	139
Figure 7.	Typical Fatigue Tests Results Illustrating Strain Failure Criteria -- Asphalt Mixtures.	140
Figure 8.	Typical Repeated Load Test Results Illustrating Critical Stress Failure Criteria -- Residual Clay.	141
Figure 9.	Crack Patterns on Bottom of Slabs Obtained in Vicinity of STA.625 + 00.	142
Figure 10.	Cross-Section of Three Layer System.	143
Figure 11.	Moving Load on Viscoelastic Half-Space.	144
Figure 12.	Time Varying Repeated Load Configuration.	145
Figure 13.	Assumed Fatigue Curve for the Determination of β_1 .	146

	<u>Page</u>
Figure 14. β_1 Curve Obtained from Assumed Curve.	147
Figure 15. Loading Programs.	148
Figure 16. Hypothetical $\beta(s_1s_2)$ Surface.	149
Figure 17. Dimensionless Pavement System No. 2.	150
Figure 18. Dimensionless Creep Functions - System 1.	151
Figure 19. Dimensionless Creep Functions - System 3.	152
Figure 20. Dimensionless Creep Functions - System 4.	153
Figure 21. Dimensionless Creep Functions - System 5	154
Figure 22. Influence of Material Variables on Vertical Deflection Factor - 4 Systems.	155
Figure 23. Influence of Material Variables on Vertical Deflection Factor - System 5.	156
Figure 24. Radial Deflection Factor for System 2.	157
Figure 25. Radial Stress Factor for System 2.	158
Figure 26. Influence of Material Variables on Vertical Stress Factor - 4 Systems.	159
Figure 27. Influence of Material Variables on Vertical Stress Factor - System 5.	160
Figure 28. Influence of Material Variables on Shear Stress Factor - 4 Systems.	161
Figure 29. Influence of Material Variables on Shear Stress Factor - System 5.	162
Figure 30. Influence of Duration on Vertical Deflection Factor.	163
Figure 31. Influence of Duration on Vertical Stress Factor.	164
Figure 32. Influence of Duration on Shear Stress Factor.	165
Figure 33. Moving Load -- Vertical Deflection Factor -- System 2.	166

	<u>Page</u>
Figure 34. Moving Load -- Vertical Deflection Factor Elastic System.	167
Figure 35. Moving Load Comparison -- Vertical Deflection Factor.	168
Figure 36. Moving Load Comparison -- Vertical Stress Factor.	169
Figure 37. Moving Load Comparison -- Shear Stress Factor Systems 2 and 3.	170
Figure 38. Influence of Height Factor on Vertical Deflection Factor.	171
Figure 39. Influence of Depth Factor on Vertical Deflection Factor.	172
Figure 40. Influence of Depth Factor on Vertical Stress Factor.	173
Figure 41. Influence of Depth Factor on Shear Stress Factor.	174
Figure 42. Influence of Radius Factor on Vertical Deflection Factor.	175
Figure 43. Influence of Offset Distance Factor on Vertical Deflection Factor.	176
Figure 44. Influence of Offset Distance Factor on Vertical Stress Factor.	177
Figure 45. Dimensionless Pavement System No. 6.	178
Figure 46. The Linear Kernel Function Obtained from the Fatigue Equation Given in the Text.	179
Figure 47. Actual Manner of Build-up of Tensile Strain at the Bottom of the Surface Layer.	180
Figure 48. Prediction of Damage Progression in Asphaltic Concrete in Surface Layer When Tensile Strain Obtained from Model I is As Shown in Figure 47.	181
Figure 49. Assumed Manner of Build-up of Tensile Strain at the Bottom of the Surface Layer.	182
Figure 50. Prediction of Damage Progression in Asphaltic Concrete in Surface Layer When Tensile Strain Obtained from Model I Is As Shown in Figure 49.	183

APPENDIX D

Derivation of the Moving Load Solution

The Load Application

The technique that was utilized to obtain the solution to the integral expression (65) is described below in detail. Consider a load $q(t)$ applied to the surface of a linear viscoelastic system. If the density function of the load is (\underline{X}, t) then the load will be given by

$$q(t) = \int_{\underline{X}_1}^{\underline{X}_2} \rho(\underline{X}, t) d\underline{x} \quad (\text{AI-1})$$

where

\underline{X} = coordinates referred to an arbitrarily fixed system of coordinates, as distinct from that of the linear system

t = time variable

Let response to a given density function

$$\rho(\underline{X}, t) = \delta(\underline{X} - X_0) H(t - \tau) \quad (\text{AI-1})$$

where

$\rho(\underline{X} - X_0)$ = the dirac delta function representing the spatial variation of the density function

$H(t - \tau_0)$ = the Heaviside step function representing the temporal variation of the density function

X_0 = the distance of the load from the origin
of a fixed system of coordinates as
distinct from that of the linear system*

τ_0 = the time of the application

be given by

$$y_p(X_0, t) = f(X_0)g(t-\tau_0) \quad (A1-3)$$

where

$f(x)^{**}$ = the spatial part of the response and,
 $g(t-\tau_0)$ = the temporal part of the response.

The response to the load $q(t)$ in equation (A1-1) is
then given by

$$\int_{\bar{X}_1}^{\bar{X}_2} y_p(X_0, t) d\bar{X} \quad (A1-4)$$

If the load is applied in such a way that its density
function has the following form,

* The linear system-coordinates are related to those of the
arbitrarily fixed coordinate system through the equation

$$R_i = |R_0 - X_i| \text{ where } R_0 = \text{initial distance of load from point of interest}$$

$$R_i = \text{distance from point of interest at any } X_i$$

** $f(X_0)$ can also be a function of time if $X_0 = X(\tau)$.
In that case, $y_p(X_0, t) = y_p(t)$

$$\begin{aligned}
& -\delta(\underline{X}-X_1) [H(t-\tau_1) - H(t-\tau_2)] \\
& + \delta(\underline{X}-X_2) [H(t-\tau_2) - H(t-\tau_3)] \\
& + \dots \dots \dots + \dots \dots \dots \quad (A1-5) \\
& + \delta(\underline{X}-X_{N-1}) [H(t-\tau_{N-1}) - H(t-\tau_N)] \\
& + \delta(\underline{X}-X_N) [H(t-\tau_N)]
\end{aligned}$$

then for very small values of $\Delta\tau = \tau_{i+1} - \tau_i$, the discrete application above corresponds to the continuous application of a moving load. The response for this case is given by

$$\begin{aligned}
Y_{p1}(t) = & f(X_1)[g(t-\tau_1) - g(t-\tau_2)] \\
& + f(X_2)[g(t-\tau_2) - g(t-\tau_3)] \\
& + \dots \dots \dots + \dots \dots \dots \\
& + f(X_{N-1})[g(t-\tau_{N-1}) - g(t-\tau_N)] + f(X_N)g(t-\tau_N) \quad (A1-6)
\end{aligned}$$

i.e. at any t_N ,

$$\begin{aligned}
Y_{p1}(t_N) = & \sum_{i=1}^{N-1} f(X_i) [g(t-t_i) - g(t-t_i + 1)] \quad (A1-7) \\
& + f(X_N) g(0)
\end{aligned}$$

For the total load the full response is given by

$$\int_{\underline{X}_1}^{\underline{X}_2} Y_{p1}(t_N) d\underline{X} \quad (A1-8)$$

For the problem considered in this study, $f(X_i)$ is analogous to $J_o(m_k(R-V\tau_i))$ (A1-9)

$$g(t-\tau_1) \text{ to } \psi_V(t-\tau_i, m_k) \quad (\text{AI-10})$$

and

$$y(t_N) \text{ to } \psi_{m_0}(t_N, m_k) \quad (\text{AI-11})$$

The value of the integral for $\psi_{m_0}(t, m)$, equation (64) is obtained using a finite difference technique as the one described above, for 91 values of m spaced 0.1 apart with $0 \leq m \leq 9$.

The integral for the moving load equation (65) is then evaluated using Simpson's Rule and the range 0 to 9. The rest of the integral from 9 to ∞ made a negligible contribution to the results.

In the finite difference technique, accuracy is a function of the size of the interval $\Delta\tau$ and increases with the number of time intervals in a curve whose slope decreases with time and approaches a zero value. However, the computation time increases exponentially with the number of time intervals. A compromise therefore had to be effected between the computation time and the accuracy. A value of $\Delta\tau = 0.5$ was deemed reasonable after choices $\Delta\tau = 10, 5, 2.5, 0.5$ and 0.25 .